AIRS/AMSU/HSB Version 6
Level 2 Product User Guide

Edited by:
Edward T. Olsen

Contributions by:
Eric Fetzer, Glynn Hulley, Peter Kalmus, Evan Manning, and Sun Wong
Jet Propulsion Laboratory, California Institute of Technology
John Blaisdell, Lena Iredell, SAIC/GSFC, Joel Susskind, GSFC
Juying Warner, Zigang Wei, UMCP
William Blackwell, MIT
Eric Maddy, STC, Inc. at NOAA/NESDIS/STAR

27 November 2017
Version 1.7.2

Jet Propulsion Laboratory
California Institute of Technology
Pasadena, CA

Submit Questions to:
http://airs.jpl.nasa.gov/ask_airs

Table of Contents

Table of Figures

1 Introduction

The purpose of the document is to give users of the V6 Level 2 products a summary of the key information they require to properly use the products in their research. This is not a complete characterization of the L2 products.

The format of these Level 2 product files is HDF-EOS Swath Version 4, rather than the current Version 5.

Each class of Level 2 product is presented. A user pursuing research on the distribution and transport of carbon monoxide will find much of interest in that section and can ignore most of the other sections. **All users, however, must read the sections describing the *Air Temperature Retrievals* and the *Water Vapor Retrievals*. Information appearing in these two sections is critically important to proper understanding and use of the other Level 2 products in research.**

The AIRS Level 2 retrieval uses layer mean quantities for water vapor, ozone, carbon monoxide, and methane. Previous versions of AIRS products reported only column totals and layer quantities for these gases. The primary products in V6 Level 2 Standard and Support Products for all gases are now level products (values at the specific pressure level upon which they are reported) instead of layer products (slab values reported on the bounding pressure level nearest to the surface). The level quantities are derived from the internal 100-layer quantities by a smoothing spline, tuned to reflect information content and atmospheric variability.

Level quantities are calculated from layer quantities by the procedure described in the Algorithm Theoretical Basis Document

AIRS_Layers_to_Levels_Theoretical_Basis_Document.pdf

The derivation of level quantities from layer quantities is essentially done by interpolation with smoothing kernels. This mathematical transformation leads to occasional strange results for water vapor profiles with inversions, typically near the surface.

We include the Level 2 Support Products in this document, but they are not recommended to the casual user. Profiles contained within the Level 2 Support Product are of higher vertical resolution (100 levels), but do not provide increased profile information content. Their major utility is for forward calculation of radiances via the AIRS rapid transmission algorithm (RTA), the calculation of level quantities from layer quantities, beta testing future products and for investigating the operation of the retrieval algorithm. The averaging kernel matrices for various products are stored here as well to avoid swelling the size of the Level 2 Standard Product files to a point that would be inconvenient for most users. Values appearing in the Support Product for interrupted or failed retrievals are likely to be the result of intermediate calculations. They might look physical, but they are not. In the words describing unknowns on ancient maritime maps: "Here there be dragons."

Users who do access the Level 2 Support Products should take note that the indices of the levels and layers of profiles are reversed from those in the Level 2 Standard Products. Thus index 20 is at a lower altitude than index 21 in the Level 2 Standard Product but index 20 is at a higher altitude than index 21 in the Level 2 Support Product. The Level 2 Standard Product pressure levels and Level 2 Support Product pressure levels are given in the documents:

V6_L2_Standard_Pressure_Levels.pdf
V6_L2_Support_Pressure_Levels.pdf

We will refer to the product files by their "shortnames" in this document when necessary to avoid confusion. There are two major versions of the Level 2 retrieval product files: one resulting from the retrieval using the combined AIRS infrared and AMSU microwave radiances and one resulting from the retrieval using only the AIRS infrared radiances. The combined AMSU+AIRS Level 2 Standard Product Physical Retrieval has shortname "**AIRX2RET**". The AIRS-Only Level 2 Standard Product Physical Retrieval has shortname "**AIRS2RET**". The corresponding Level 2 Support Product Physical Retrievals have shortnames "**AIRX2SUP**" and "**AIRS2SUP**". The corresponding shortnames for the Level 2 Cloud Cleared Products are "**AIRI2CCF**" and "**AIRS2CCF**".

A second combined IR/MW Level 2 retrieval product spans the period from beginning of mission to February 5, 2003. On that date, the Humidity Sounder for Brazil (HSB) failed. Level 2 Standard Product files resulting from the retrieval using AIRS infrared, microwave and HSB microwave radiances (AMSU+HSB+AIRS) have shortname "**AIRH2RET**". The corresponding shortnames for the Level 2 Support Product and Level 2 Cloud Cleared Product are "**AIRH2SUP**" and "**AIRH2CCF**".

1.1 Example: Level 2 Physical Retrieval Product File Names

The following are examples of Level 2 physical retrieval product files for granule 156 for the date, January 5, 2003. Recall that there are 240 daily data granules for each Level 2 product:

Standard Physical Product processed using AIRS and AMSU radiances:
Name: AIRS.2003.01.05.156.L2.RetStd.v6.0.7.0.G12335203331.hdf
Shortname: AIRX2RET

Standard Physical Product processed using AIRS, AMSU and HSB radiances:
Name: AIRS.2003.01.05.156.L2.RetStd_H.v6.0.7.0.G12335203331.hdf
Shorthame: AIRH2RET

Standard Physical Product processed using only AIRS radiances:
Name: AIRS.2003.01.05.156.L2.RetStd_IR.v6.0.7.0.G12335203331.hdf
Shortname: AIRS2RET

Support Physical Product processed using AIRS and AMSU radiances:
Name: AIRS.2003.01.05.156.L2.RetSup.v6.0.7.0.G12335203331.hdf
Shortname: AIRX2SUP

Support Physical Product processed using AIRS, AMSU and HSB radiances:
Name: AIRS.2003.01.05.156.L2.RetSup_H.v6.0.7.0.G12335203331.hdf
Shortname: AIRH2SUP

Support Physical Product processed using only AIRS radiances:
Name: AIRS.2003.01.05.156.L2.RetSup_IR.v6.0.7.0.G12335203331.hdf
Shortname: AIRS2SUP

1.2 Example: Level 2 Cloud-Cleared Radiance Product File Names

The cloud-cleared radiance file shortnames for AIRS/AMSU, AIRS-only and AIRS/AMSU/HSB retrievals are **AIRI2CCF**, **AIRS2CCF** and **AIRH2CCF**.

Example granule names of the AIRS Cloud-Cleared Radiances product files for the 3 different processing options:

Product File Name	Shortname
AIRS.2003.01.05.156.L2.CC.V6.0.7.0.G2002123120634.hdf	AIRI2CCF
AIRS.2003.01.05.156.L2.CC_H.V6.0.7.0.G2002123120634.hdf	AIRH2CCF
AIRS.2003.01.05.156.L2.CC_IR.V6.0.7.0.G2002123120634.hdf	AIRS2CCF

2 Level 2 Cloud Cleared Radiances Dimension Fields

These fields provide the dimensions of the various arrays in the Level 2 Cloud Cleared Radiances Standard Product data files (**AIRI2CCF**, **AIRS2CCF**, **AIRH2CCF**).

Field Name	Value	Description
GeoXTrack	30	Dimension across track for footprint positions. Same as number of footprints per scanline. Index starts at the left and increases toward the right as you look along the satellite's path
GeoTrack	# of scan lines in swath	Dimension along track for footprint positions. Same as number of scanlines in granule. Parallel to the satellite's path, increasing with time. (Nominally 45)
Channel	2378	Dimension of channel array (Channels are generally in order of increasing wavenumber, but because frequencies can vary and because all detectors from a physical array of detector elements (a "module") are always grouped together there are sometimes small reversals in frequency order where modules overlap.)
AIRSXTrack	3	The number of AIRS cross-track spots per AMSU-A spot. Direction is the same as GeoXTrack. Index starts at the left and increases toward the right as you look along the satellite's path
AIRSTrack	3	The number of AIRS along-track spots per AMSU-A spot. Direction is the same as GeoTrack. Parallel to the satellite's path, increasing with time
Module	17	Number of modules on the focal plane in which airs channels are grouped. The order is M-01a, M-02a, M-01b, M-02b, M-04d, M-04c, M-03, M-04b, M-04a, M-05, M-06, M-07, M-08, M-09, M-10, M-11, M-12.

3 Level 2 Cloud Cleared Radiances Geolocation Fields

These fields are provided for each AMSU FOV (i.e., retrieval footprint), but are not retrieved quantities.

Field Name	Dimension per FOV	Description
Latitude	1	FOV boresight geodetic latitude in degrees North (-90.0 → 90.0)
Longitude	1	FOV boresight geodetic longitude in degrees East (-180.0 →180.0)
Time	1	TAI time: floating-point elapsed seconds since Jan 1, 1993

4 Level 2 Cloud Cleared Radiances Channel Information Fields

These fields are provided for granule (there are 240 per day), but are not retrieved quantities.

Field Name	Number	Description
nominal_freq	Channel =2378	Nominal frequencies (in cm^{-1}) of each channel
CalChanSummary	Channel =2378	Bit field. Bitwise OR of CalFlag, by channel, over all scanlines. Noise threshold and spectral quality added.; Zero means the channel was well calibrated for all scanlines; Bit 7 (MSB): scene over/underflow; Bit 6: (value 64) anomaly in offset calculation; Bit 5: (value 32) anomaly in gain calculation; Bit 4: (value 16) pop detected with no offset anomaly; Bit 3: (value 8) noise out of bounds; Bit 2: (value 4) anomaly in spectral calibration; Bit 1: (value 2) Telemetry; Bit 0: (LSB, value 1) unused (reserved);
ExcludedChans	Channel =2378	An integer 0-6, indicating A/B detector weights. Used in L1B processing.;

Field Name	Number	Description
		0 - A weight = B weight. Probably better than channels with state > 2; 1 - A-side only. Probably better than channels with state > 2; 2 - B-side only. Probably better than channels with state > 2; 3 - A weight = B weight. Probably better than channels with state = 6; 4 - A-side only. Probably better than channels with state = 6; 5 - B-side only. Probably better than channels with state = 6; 6 - Has anomalous gain performance. Probably not usable.
NeN_L1B	Channel =2378	Level-1B Noise-equivalent Radiance (radiance units) for an assumed 250K scene. Note that effective noise on cloud-cleared radiances will be modified.
NeN_L1B_Static	Channel =2378	Expected Noise-equivalent Radiance (radiance units) for an assumed 250K scene. This static estimate comes from a channel properties file and reflects nominal conditions for an epoch of months. It is a more stable value than NeN_L1B but does not reflect recent or transient changes to noise levels.

5 Level 2 Cloud Cleared Radiances Product

There are three Level 2 Cloud-Cleared Radiance Product data streams:

- **AIRICCF** produced by AIRS+AMSU retrieval processing
- **AIRHCCF** produced by AIRS+AMSU+HSB retrieval processing
- **AIRSCCF** produced by AIRS retrieval processing

These fields are provided for each AMSU FOV (i.e., retrieval footprint). We include in this table available informative fields, for example viewing geometry, so that it will not be necessary for users to open the associated Level 2 Physical Retrieval product granules to access that information. All data are available in the Level 2 Standard Cloud-Cleared Radiance Product, a series of HDF-EOS Swath format files for each 6 minute AIRS retrieval granule similar to the Level 2 Standard Product and Level 2 Support Product.

Researchers using the cloud cleared radiance product should read the document

V6_Level_2_Cloud_Cleared_Radiances.pdf

In all QC fields: 0→Highest Quality, 1→Good Quality, 2→ Do Not Use

Field Name	Dimension per FOV	Description
radiances	Channel = 2378	Cloud-cleared radiances for each channel (milliWatts/m^2/cm^{-1}/steradian)
radiances_QC	Channel = 2378	Quality flag array (0,1,2)
radiance_err	Channel = 2378	Error estimate for radiances (milliWatts/m^2/cm^{-1}/steradian)
CldClearParam	AIRTrack *AIRSXTrack =3x3	Cloud clearing parameter Eta. Positive values are cloudier than average for the FOR, negative values are clearer.
scanang	1	Scanning angle of the central AIRS instrument field-of-view with respect to the spacecraft (-180.0 → 180.0, negative at start of scan, 0 at nadir)

Field Name	Dimension per FOV	Description
satzen	1	Spacecraft zenith angle (0.0 → 180.0) degrees from zenith (measured relative to the geodetic vertical on the reference (WGS84) spheroid and including corrections outlined in EOS SDP toolkit for normal accuracy.)
satazi	1	Spacecraft azimuth angle (-180.0 → 180.0) degrees E of N GEO)
solzen	1	Solar zenith angle (0.0 → 180.0) degrees from zenith (measured relative to the geodetic vertical on the reference (WGS84) spheroid and including corrections outlined in EOS SDP toolkit for normal accuracy.)
solazi	1	Solar azimuth angle (-180.0 → 180.0) degrees E of N GEO)
sun_glint_distance	1	Distance (km) from footprint center to location of the sun glint (-9999 for unknown, 30000 for no glint visible because spacecraft is in Earth's shadow)
topog	1	Mean topography in meters above reference ellipsoid
topog_err	1	Error estimate for topog
landFrac	1	Fraction of spot that is land (0.0 → 1.0)
landFrac_err	1	Error estimate for landFrac
Doppler_shift_ppm	1	Doppler shift for this footprint in parts per million.

Field Name	Dimension per FOV	Description
dust_flag	1	Flag telling whether dust was detected in any of the 9 Level-1B IR fields of view that make up this scene; 1: Dust detected in at least one contributing FOV; 0: Dust test valid in at least one contributing IR FOV but dust not detected in any of the valid contributing IR FOVs; -1: Dust test not valid for any contributing IR FOV (land, poles, cloud, problem with inputs)
CC_noise_eff_amp_factor	1	Effective amplification of noise in IR window channels due to extrapolation in cloud clearing and uncertainty of clear state. (< 1.0 for noise reduction, >1.0 for noise amplification, -9999.0 for unknown)
CC1_noise_eff_amp_factor	1	Equivalent of CC_noise_eff_amp_factor but from the first attempt at cloud clearing
CC1_Resid	1	Internal retrieval quality indicator -- residual between the first cloud cleared radiances for channels used in the determination and the radiances calculated from the best estimate of clear, in K
CCfinal_Resid	1	Internal retrieval quality indicator -- residual between the final cloud cleared radiances for channels used in the determination and the radiances calculated from the best estimate of clear, in K
TotCld_4_CCfinal	1	Internal retrieval quality indicator -- total cloud fraction estimated before final cloud clearing (as seen from above), dimensionless between zero and one

Field Name	Dimension per FOV	Description
CCfinal_Noise_Amp	1	Internal retrieval quality indicator -- noise amplification factor from cloud clearing because of extrapolation, dimensionless. Note: the name is misleading: this is the value after the second cloud clearing iteration, not the last.
invalid	1	Profile is not valid
all_spots_avg	1	1: the cloud clearing step judged the scene to be clear enough that it averaged all spots' radiances; 0: cloud clearing was applied to the radiances; -1/255: cloud clearing not attempted
MW_ret_used	1	MW-only final retrieval used
bad_clouds	1	invalid cloud parameters
retrieval_type	1	**DEPRECATED** -- use Xxx_QC flags. Retrieval type:; 0 for full retrieval; 10 for MW + final succeeded, initial retrieval failed; 20 for MW + initial succeeded, final failed; 30 for only MW stage succeeded, initial + final retrieval failed; 40 for MW + initial succeeded, final cloud-clearing failed; 50 for only MW stage succeeded, initial + final cloud-clearing failed; 100 for no retrieval;

5.1 Description

The AIRS Level 2 Cloud Cleared Radiances are the clear column radiances due to the atmospheric column resulting from the physical retrieval, i.e. the radiances that the instrument would have observed in the absence of clouds.

5.2 Type of Product

The radiances are reported for all 2378 AIRS infrared channels for each AMSU FOV retrieval footprint (50km spatial resolution at nadir) in the units of W/m^2-sr-cm^{-1}. There are 1350 possible retrievals in each AIRS 6-minute granule. The AIRS Level 2 Cloud Cleared Radiance Product is reported in the same HDF-EOS swath format as the accompanying AIRS Level 2 Standard Product and AIRS Level 2 Support Product.

5.3 Quality Indicators

The channel-by-channel quality flags are new in V6. The error estimates for each channel (**radiance_err**) are converted to brightness temperature error estimates (ΔT), and **radiances_QC** values are then set as follows:

= 0 if $\Delta T < 1.0$ K
= 1 if $1.0 <= \Delta T < 2.5$ K
= 2 otherwise

Initial studies of V6 test data have identified retrievals for which the cloud cleared radiances in the window regions

750 cm^{-1} to 1137 cm^{-1} and 2400 cm^{-1} to 2665 cm^{-1}

exhibit large biases and standard deviations while thought to be clear scenes. It was found that under some conditions with extensive stratus cloud cover, window channel observations “thought to be clear” were awarded very low noise amplification factors. Users can remove these cases by applying the additional filter:

Do not use (i.e., set radiances_QC = 2) for channels in the window regions if:

0.3333 < **CCfinal_Noise_Amp** < 0.3334

and

TSurfStd_QC = 2

Please study the last several pages discussing Figures 4 and 5 of

V6_Level_2_Cloud_Cleared_Radiances.pdf

5.4 Validation

A Validation Report for V6 data is currently under preparation and will be published after the V6 data products become publicly available. A V5 Validation Report, summarizing relevant publications, is also being prepared. Early V6 validation results are partially summarized in

V6_L2 Performance_and_Test_Report.pdf

5.5 Caveats

This section will be updated over time as V6 data products are analyzed and validated.

5.6 Suggestions for Researchers

This section will be updated over time as V6 data products are analyzed and validated.

5.7 Recommended Papers

This section will be updated over time as research with V6 data products are published.

Chahine, M.T. (1977), Remote Sounding of cloudy atmospheres. II. Multiple cloud formations, J. Atmos Sci, 34, 744-757.

Susskind, J, C.D. Barnet, and J. Blaisdell (1998), Determination of atmospheric and surface parameters from simulated AIRS/AMSU sounding data: Retrieval methodology and cloud clearing methodology, Adv. Space Res, 21, 369-384.

Susskind, J., C.D. Barnet, J.M. Blaisdell (2003), Retrieval of Atmospheric and Surface Parameters from AIRS/AMSU/HSB Data in the Presence of Clouds, IEEE Trans. Geoscience and Remote Sensing, 41, 390-409, doi:10.1109/TGRS.2002.808236.

Susskind J,. C. Barnet, J. Blaisdell, L. Iredell, F. Keita, L. Kouvaris, G. Molnar, M. Chahine (2006), Accuracy of geophysical parameters derived from Atmospheric Infrared Sounder/Advanced Microwave Sounding Unit as a function of fractional cloud cover, J. Geophys, Res,. 111, D09S17, doi:10.1029/02005JD006272.

Susskind, Joel, John M. Blaisdell, and Lena Iredell. "Improved methodology for surface and atmospheric soundings, error estimates, and quality control procedures: the atmospheric infrared sounder science team version-6 retrieval algorithm." Journal of Applied Remote Sensing 8, no. 1 (2014): 084994-084994.

5.8 Recommended Supplemental User Documentation

V6_Data_Release_User_Guide.pdf
V6_Data_Disclaimer.pdf
V6_Level_2_Cloud_Cleared_Radiances.pdf
V6_L2_Performance_and_Test_Report.pdf
V6_L2_Quality_Control_and_Error_Estimation.pdf
V6_Released_Processing_File_Description.pdf
V6_Retrieval_Channel_Sets.pdf
V6_Retrieval_Flow.pdf
V6_L1B_QA_QuickStart
V6_L1B_Calibration_Properties_Files (series of ASCII files)
V6_L2_Channel_Properties_Files (series of ASCII files)

6 Level 2 Physical Retrieval Dimension Fields

These fields provide the dimensions of the various arrays in the Physical Retrieval Level 2 Standard Product data files (**AIRX2RET**, **AIRS2RET**, **AIRH2RET**).

Field Name	Value	Description
GeoXTrack	30	Dimension across track for footprint positions. Same as number of footprints per scanline. -- starting at the left and increasing towards the right as you look along the satellite's path
GeoTrack	# of scan lines in swath	Dimension along track for footprint positions. Same as number of scanlines in granule. Parallel to the satellite's path, increasing with time. (Nominally 45)
StdPressureLev	28	Number of standard pressure altitude levels (from bottom of the atmosphere to the top). IMPORTANT NOTE: the 100 levels in the support file are ordered from top of atmosphere down.
StdPressureLay	28	Number of standard pressure altitude layers (Always equal to StdPressureLev: last layer goes to the top of the atmosphere, 0.005 hPa).
AIRSXTrack	3	The number of AIRS cross-track spots per AMSU-A spot. Direction is the same as GeoXTrack -- starting at the left and increasing towards the right as you look along the satellite's path
AIRSTrack	3	The number of AIRS along-track spots per AMSU-A spot. Direction is the same as GeoTrack -- parallel to the satellite's path, increasing with time
Cloud	2	Cloud layer dimension in order of increasing pressure. Only first nCld or numCloud elements are valid
MWHingeSurf	7	Number of standard frequency hinge points in Microwave surface emissivity and surface brightness. Frequencies are 23.8, 31.4, 50.3, 52.8, 89.0, 150.0, 183.31 GHz respectively. Values are also found in field MWHingeSurfFreqGHz.
H2OFunc	11	Functions on which water vapor retrieval is calculated
O3Func	9	Functions on which ozone retrieval is calculated

Field Name	Value	Description
COFunc	9	Functions on which carbon monoxide retrieval is calculated
CH4Func	10	Functions on which methane retrieval is calculated
HingeSurf	100	Maximum number of frequency hinge points in IR surface emissivity
H2OPressureLev	15	Number of water vapor pressure altitude levels (from bottom of the atmosphere up).
H2OPressureLay	14	Number of standard pressure altitude layers (Always one less than H2OPressureLev).

7 Level 2 Physical Retrieval Pressure and Microwave Hinge Frequency Fields

These fields are provided once per granule.

Field Name	Dimension per FOV	Description
pressStd	StdPressureLev =28	Standard pressure array, bottom of atmosphere first (hPa)
pressH2O	H2OPressureLev =15	Water vapor pressure array, bottom of atmosphere first (hPa)
MWHingeSurfFreqGHz	MWHingeSurf =7	Frequencies at which MW surface parameters (SfcTbMWStd, EmisMWStd, etc) are reported, (GHz)

Note: the **pressH2O** are identical to the first 15 entries in **pressStd**.

7.1 Recommended Supplemental User Documentation

V6_Data_Release_User_Guide.pdf
V6_Data_Disclaimer.pdf
V6_L2_Standard_Pressure_Levels.pdf
V6_L2_Support_Pressure_Levels.pdf

8 Level 2 Physical Retrieval Geolocation and Surface Ancillary Fields

These fields are provided for all retrievals, but are not retrieved quantities.

Field Name	Dimension per FOV	Description
Latitude	1	FOV boresight geodetic latitude in degrees North (-90.0 → 90.0)
Longitude	1	FOV boresight geodetic longitude in degrees East (-180.0 →180.0)
Time	1	TAI time: floating-point elapsed seconds since Jan 1, 1993
satzen	1	Spacecraft zenith angle (0.0 ... 180.0) degrees from zenith (measured relative to the geodetic vertical on the reference (WGS84) spheroid and including corrections outlined in EOS SDP toolkit for normal accuracy.)
satazi	1	Spacecraft azimuth angle (-180.0 ... 180.0) degrees E of N GEO)
solzen	1	Solar zenith angle (0.0 ... 180.0) degrees from zenith (measured relative to the geodetic vertical on the reference (WGS84) spheroid and including corrections outlined in EOS SDP toolkit for normal accuracy.)
solazi	1	Solar azimuth angle (-180.0 → 180.0) degrees E of N GEO)
sun_glint_distance	1	Distance (km) from footprint center to location of the sun glint (-9999 for unknown, 30000 for no glint visible because spacecraft is in Earth's shadow)
topog	1	Mean topography above reference ellipsoid (m)
topog_err	1	Error estimate for topog (m)
landFrac	1	Fraction of spot that is land (0.0 → 1.0)
landFrac_err	1	Error estimate for landFrac
latAIRS	AIRTrack *AIRSXTrack =3x3	Geodetic center latitude of AIRS spots in degrees North (-90.0 → 90.0)

Field Name	Dimension per FOV	Description
lonAIRS	AIRTrack *AIRSXTrack =3x3	Geodetic center longitude of AIRS spots in degrees East (-180.0 →180.0)
PSurfStd	1	Surface pressure first guess, interpolated from the NCEP GFS forecasts and local DEM topography (hPa)
pressStd	StdPressureLev =28	Pressure levels upon which temperature profiles and geopotential heights are reported (hPa)
PSurfStd_QC	1	Quality flag for surface pressure guess input; 0: Highest Quality - from timely forecast (normal case) 1: Good Quality - from climatology/topography 2: Do Not Use - guess not available (occurs only if satellite is not in normal operational mode)
nSurfStd	1	Standard level index (1-based) of lowest altitude pressStd element which is above the mean surface (unitless)

9 Level 2 Physical Retrieval Quality Indicator Pressure Boundaries

These overall QA fields are provided for all retrievals, and are set as a result of QA determinations in the retrieval algorithm. They are very useful for deciding which retrievals should be excluded from a sample. For example, a study of the lower troposphere should not use retrievals for which **PBest** < 700 hPa.

Field Name	Dimension per FOV	Description
PBest	1	Maximum value of pressure for which atmospheric temperature profile QC=0 (hPa)
PGood	1	Maximum value of pressure for which atmospheric temperature profile QC=0 or 1 (hPa)
nBestStd	1	Standard level index (1-based) of highest pressure (i.e., lowest altitude) for which atmospheric temperature profile QC=0. A value of 29 (there are only 28 standard pressure levels) indicates that no part of the profile satisfies QC=0 (1 → 29)
nGoodStd	1	Standard level index (1-based) of highest pressure (i.e., lowest altitude) for which atmospheric temperature profile QC=0 or 1. A value of 29 (there are only 28 standard pressure levels) indicates that no part of the profile satisfies QC=0 or 1 (1 → 29)

9.1 Level Indices Are 1-Based

All parameters that are level numbers, such as **nSurfStd, nBestStd and nGoodStd** are 1-based. Those who work in FORTRAN and MATLAB will be unaffected. However, those who work in C and IDL must take care when using **nSurfStd** and other parameters that are level numbers. The following two expressions yield the same value for mypress:

FORTRAN and MATLAB: mypress = **pressStd**(**nBestStd**)

C and IDL: mypress = **pressStd**[**nBestStd**-1]

10 Level 2 Physical Retrieval Microwave-Only Standard Products

The Microwave-Only (MW-Only) standard products are retrieved by the MW retrieval stage of the AIRS algorithm using AMSU radiances in the **AIRX2RET** product and AMSU+HSB radiances in the **AIRH2RET** product. No IR data are used to retrieve these products. All other products described later in this document are retrieved employing the AMSU+AIRS (**AIRX2RET**) or AIRS-Only (**AIRS2RET**) retrieval stages of the AIRS algorithm, providing greater vertical resolution of temperature and water vapor fields, improved surface emissivity and retrievals of atmospheric constituents. The spatial footprint for all retrievals is the field-of-view (FOV) of the Advanced Microwave Sounding Unit (AMSU), which is 40.5 km at nadir. Note that MW-Only products are absent from the AIRS-Only (**AIRS2RET**) products.

The **AIRH2RET** Microwave-Only Support Products contain useful (at altitudes below the 300 hPa level) retrieved moisture profiles as well as rain rate, cloud liquid water and a cloud/ice flag. This is not the case for the **AIRX2RET** Microwave-Only Support Products.

In all QC fields: 0→Highest Quality, 1→Good Quality, 2→ Do Not Use

Standard Product

Field Name	Dimension per FOV	Description
TAirMWOnlyStd	StdPressureLev =28	Retrieved Atmospheric Temperature Profile. Value below index nSurfStd may be an unphysical extrapolated value for a pressure level below the surface (K)
TAirMWOnlyErr	StdPressureLev =28	Error estimate (K), only located in the Level 2 Support Product
TAirMWOnlyStd_QC	StdPressureLev =28	Quality flag profile for TAirMWOnlyStd (0,1,2)
GP_Height_MWOnly	StdPressureLev =28	Geopotential height (above mean sea level) for each pressStd (m)
GP_Height_MWOnly_QC	StdPressureLev =28	Quality flag array (0,1,2)
MW_ret_used	1	MW-Only final retrieval used

Field Name	Dimension per FOV	Description
GP_Height_MWOnly_QC	StdPressureLev =28	Quality flag array (0,1,2)
MWSurfClass	1	Surface class from microwave (MW) information:; 0 → coastline (Liquid water covers 50-99% of area); 1 → land (Liquid water covers < 50% of area); 2 → ocean (Liquid water covers > 99% of area); 3 → sea ice (High MW emissivity); 4 → sea ice (Low MW emissivity); 5 → snow (Higher-frequency MW scattering); 6 → glacier/snow (Very low-frequency MW scattering); 7 → snow (Lower-frequency MW scattering); -1 → unknown (not attempted) (unitless)
sfcTbMWStd	MWHingeSurf =7	Microwave surface brightness. Includes only emitted radiance, i.e. no reflected radiance, at the 7 MW frequencies stored in attribute MWHingeSurfFreqGHz (K)
sfcTbMWStd_QC	MWHingeSurf =7	Quality flag array (0,1,2)
EmisMWStd	MWHingeSurf =7	Spectral MW emissivity at the 7 MW frequencies (unitless)
EmisMWStdErr	MWHingeSurf =7	Error estimate (unitless)
EmisMWStd_QC	MWHingeSurf =7	Quality flag array (0,1,2)
totH2OMWOnlyStd	1	Total precipitable water vapor (kg/m^2)
totH2OMWOnlyStd_QC	1	Quality flag (0,1,2)
totCldH2OStd	1	Total cloud liquid water (kg/m^2)
totCldH2OStdErr	1	Error estimate (kg/m^2)
totCldH2OStd_QC	1	Quality flag (0,1,2)

Support Product

Field Name	Dimension per FOV	Description
H2OCDMYOnly	XtraPressureLay=100	Layer column water vapor (molecules/cm^2)
H2OCDMYOnly_QC	XtraPressureLay=100	Quality flag (0,1,2)

Parameters in Support Product if HSB Radiances Available (AIRH2SUP)

Field Name	Dimension per FOV	Description
rain_rate_50km	1	Rain rate (mm/hr)
rain_rate_15km	AIRSTrack*AIRSXTrack =3x3	Rain rate for HSB 15km spots (mm/hr)
lwCDSup	XtraPressureLay=100	Layer molecular column density of cloud liquid water (molecules/cm^2)
lwCDSup_QC	XtraPressureLay=100	Quality flag (0,1,2)
lwCDSupErr	XtraPressureLay=100	Error estimate (molecules/cm^2)
cIWSup	XtraPressureLay=100	Cloud Ice/Water flag liquid = 0 ice = 1

10.1 Description

The 28 Level 2 Standard pressure levels (**pressStd**) are arranged in order of decreasing pressure, from 1100 hPa to 0.1 hPa. The document, **V6_L2_Standard_Pressure_Levels.pdf**, provides a table of their values. The index of the lowest altitude pressure level for which a reported **TAirMWOnlyStd** is valid is **nSurfStd**, which may be 1→15 depending upon topography. The surface pressure, interpolated from the NCEP GFS forecast and the local DEM topography, is **PSurfStd**.

totCldH2OStd is the integral of the cloud liquid water profile. The estimated error, **totCldH2OStdErr**, is set according to surface type with values ranging from 0.02 kg/m^2 to 0.15 kg/m^2 if **totH2OMWOnlyStd_QC** = 0 or 1. In the event that **totH2OMWOnlyStd_QC** = 2, it is set to 1.00 kg/m^2.

MWSurfClass is produced by a classification algorithm employing AMSU-A data and the **landFrac** parameter (i.e., the fraction of the surface of the FOV covered by land). The possible values are:

MWSurfClass	Description
-1	unknown (not attempted)
0	coastline (liquid water covers 50% to 99% of FOV)
1	land (liquid water covers less than 50% of FOV)
2	ocean (liquid water covers more than 99% of FOV)
3	sea ice (high MW emissivity)
4	sea ice (low MW emissivity)
5	snow (higher-frequency MW scattering)
6	glacier/snow (very low-frequency MW scattering)
7	snow (lower-frequency MW scattering)

The difference between **MWSurfClass** = 3 and 4, or among **MWSurfClass** = 5, 6, 7 is in the microwave signature of the ice and/or snow. There are complex physical reasons for the differences, including age. Users may collapse the **MWSurfClass** values present here into NOAA's AMSU-product classes by combining 3 and 4 for sea ice and 5, 6 and 7 for land snow/ice.

sfcTbMWStd is the surface brightness temperature retrieved at the seven frequencies: 23.8, 31.4, 50.3, 52.8, 89.0, 150.0, 183.31 GHz. **EmisMWStd** is derived as the ratio of **sfcTbMWStd** to an estimated MW-Only surface skin temperature. The estimated error, **EmisMWStdErr**, is frequency dependent and varies between 0.015 and 0.034, based on simulations. If the retrieved values are rejected, **EmisMWStdErr** values are set ≥ 1.0 and **EmisMWStd_QC** values are set to 2. The effective MW-Only surface skin temperature may be calculated by dividing an element of **sfcTbMWStd** by the corresponding element of **EmisMWStd**, but we advise users doing so that the values resulting from this calculation are not supported and are not validated as a product.

10.2 Type of Product

All MW-Only Standard Product profiles are **level** quantities, i.e. the values are reported at fixed pressure levels. This differs from layer quantities (in the Support Product), which are reported on the fixed pressure levels but represent the layer bounded by the level on which they are reported and the next higher (in altitude) level. Users may calculate the approximate effective layer pressure by taking the geometric mean of the level pressures bounding the layer. Thus the effective layer pressure for a layer quantity reported on the 700 hPa level is SQRT(600.0*700.0) = 648 hPa.

For more detail, see **V6_L2_Levels_Layers_Trapezoids.pdf** for a full discussion of level and layer quantities. See also **V6_L2_Standard_Pressure_Levels.pdf**.

10.3 Quality Indicators

The user is encouraged to read the QC and error estimation document:

V6_L2_Quality_Control_and_Error_Estimation.pdf

The MW-Only retrieval stage sets bits in **MW_ret_code** (located in the Level 2 Support Product) upon encountering errors:

MW_ret_code	Explanation
1	moisture variables rejected by residual test
2	tropospheric temperature profile rejected by residual test
4	excessive liquid water (> 0.5 kg/m^2)
8	insufficient valid channels
16	numerical error
32	emissivity > 1 for any AMSU-A channel
64	stratospheric temperature profile rejected by residual test
128 or -128	microwave retrieval not attempted

The part of the **TAirMWOnlyStd** profile at pressures equal to or greater than 201 hPa is set by examining the bits in **MW_ret_code** corresponding to microwave retrieval in that portion of the atmospheric column.

If any of the first six bits (bits 1→6) are set, then **TAirMWOnlyStd_QC** for those levels is set to Quality = 2; otherwise it is set to Quality = 0. **sfcTbMWStd_QC** and **EmisMWStd_QC** are also set by this check.

The part of the **TAirMWOnlyStd** profile at pressures less than 201 hPa is set by examining the bits in **MW_ret_code** corresponding to microwave retrieval in that portion of the atmospheric column.

If any of three bits (bits 4, 5 or 7) are set, then **TAirMWOnlyStd_QC** for those levels is set to 2; otherwise it is set to 0.

The failure of HSB on February 5, 2003 degraded various moisture research products, and the quality flags **totH2OMWOnlyStd_QC** and **totcldH2OStd_QC** are set in part by the availability of HSB data. If any of the first six bits (bits 1→6) of **MW_ret_code** are set then these two quality flags are set to Quality = 2. If the test on **MW_ret_code** yields no fault, an additional test is performed. If HSB data are present these quality flags are set to 0. If HSB data are not present and **MWSurfClass** = 0 or 2, these quality flags are set to Quality = 1, and they are set to Quality = 2 for all other surface types. **Note that Quality = 1 constitutes the best level of quality that can be achieved for totH2OMWOnlyStd and totcldH2OStd when HSB data are not available (i.e., the AIRX2RET product).**

The failure of HSB also impacts **sfcTbMWStd** and **EmisMWStd**. In the absence of HSB, array elements 6 and 7 (corresponding to 150 GHz and 183.31 GHz) are marked Quality = 2 and contain fill values (-9999).

The degradation and ultimate failure of AMSU channels 4 and 5, impacts array element 4 (corresponding to 52.8 GHz) of **sfcTbMWStd, EmisMWStd, sfcTbMWStd_QC** and **EmisMWStd_QC**. Array element 4 of **sfcTbMWStd** and **EmisMWStd** contain values derived by regression, but array element 4 of **sfcTbMWStd_QC** and **EmisMWStd_QC** are set to Quality = 2 to reflect the absence of an actual measurement.

To ensure continuity throughout the entire mission, the V6 retrieval algorithm for MW-Only products provided by the AMSU+AIRS processing does not use AMSU channels 4 and 5, even in the earlier stage of the mission when those channels were good.

To maximize the quality of the retrieval (of moisture product in particular), the V6 retrieval algorithm for MW-Only products provided by the AMSU+HSB+AIRS processing does use AMSU channels 4 and 5.

The quantity **GP_Height_MWOnly** depends on both temperature and moisture, working upward from the surface. **GP_Height_MWOnly_QC** for the entire profile is set to the higher value of **TAirMWOnly_QC** (at the surface, i.e. first array element) or **H2OCDMWOnly_QC** (at the surface).

10.4 Validation

A Validation Report for V6 data is currently under preparation and will be published after the V6 data products become publicly available. A V5 Validation Report, summarizing relevant publications, is also being prepared. Early V6 validation results are partially summarized in

V6_L2 Performance_and_Test_Report.pdf

10.5 Caveats

This section will be updated over time as V6 data products are analyzed and validated.

There is no retrieval of MW-Only water vapor for altitudes above the 300 hPa pressure level in the AIRS+AMSU+HSB (**AIRH2RET**) product. There is no retrieval of MW-Only water vapor profile at any altitude in the AIRS+AMSU (**AIRX2RET**) product; there is only a constraint on the total burden of moisture for the **AIRX2RET** product. We do not recommend the use of the MW-Only water vapor profile in the **AIRX2RET** product.

Note that there are values for **EmisMWStd** and **sfcTbMWStd** for the 150 GHz and 183 GHz channels only if HSB data are available, otherwise the values will be set to -9999.0. The AIRS Level 2 Standard Product in which HSB data are available is the **AIRH2RET** version. The **AIRX2RET** version does not ingest HSB data.

Note also that with the failure of AMSU channels 4 and 5 and thus their exclusion in V6 AMSU+AIRS processing, we have no independent value for **sfcTbMWStd** and **EmisMWStd** at 52.8 GHz.

In brief, the user should filter MW-Only moisture retrievals as follows:

If HSB data are used in the retrieval (**AIRH2RET**), then users may use both the column totals and profiles of the MW-Only moisture products, subject to their individual QC values.

If HSB data are not used in the retrieval (**AIRX2RET**), then users may only use the column totals of the MW-Only moisture products, subject to their individual QC values.

Rejected moisture retrievals (Quality = 2) should be avoided.

All parameters that are level numbers, such as **nSurfStd**, are 1-based. Those who work in FORTRAN and MATLAB will be unaffected. However, those who work in C and IDL must take care when using nSurfStd and other parameters that are level numbers. The following two expressions yield the same value:

FORTRAN and MATLAB: **TAirMWOnlyStd**(**nSurfStd**)

C and IDL: **TAirMWOnlyStd**[nsurfStd-1]

The value of **TAirMWOnlyStd** at index **nSurfStd** (in FORTRAN and MATLAB) or index **nSurfStd**-1 (in C and IDL) may be an unphysical extrapolated value for a pressure level below the surface. The user must also compare **PSurfStd** to the associated **pressStd** element. If (for IDL) **PSurfStd** < **pressStd**[**nSurfStd**-1] then the level falls below the local surface and **TAirMWOnlyStd**[**nsurfStd**-1] is not physical.

10.6 Suggestions for Researchers

This section will be updated over time as V6 data products are analyzed and validated.

We caution users to avoid combining MW-only retrieval products with products retrieved via the combined IR/MW algorithm (AMSU+AIRS or AMSU+HSB+AIRS) or the AIRS-Only algorithm in their analyses. The three products are quite different in character, sampling and quality.

10.7 Recommended Papers

This section will be updated over time as research with V6 data products are published.

Cadeddu et al, 2007, “Measurements and retrievals from a new 183 GHz water vapor radiometer in the Arctic, IEEE Trans. Geosci. Rem. Sens. v.45, pp.2207-2215, doi: 10.1109/TGRS.2006.888970

Fetzer, E.; McMillin, L.M.; Tobin, D.; Aumann, H.H.; Gunson, M.R.; McMillan, W.W.; Hagan, D.E.; Hofstadter, M.D.; Yoe, J.; Whiteman, D.N.; Barnes, J.E.; Bennartz, R.; Vomel, H.; Walden, V.; Newchurch, M.; Minnett, P.J.; Atlas, R.; Schmidlin, F.; Olsen, E.T.; Goldberg, M.D.; Sisong Zhou; HanJung Ding; Smith, W.L.; Revercomb, H., "AIRS/AMSU/HSB validation," Geoscience and Remote Sensing, IEEE Transactions on , vol.41, no.2, pp. 418-431, Feb. 2003

Fetzer, E. J., W. G. Read, D. Waliser, B. H. Kahn, B. Tian, H. Vömel, F. W. Irion, H. Su, A. Eldering, M. de la Torre Juarez, J. Jiang and V. Dang (2008), Comparison of upper tropospheric water vapor observations from the Microwave Limb Sounder and Atmospheric Infrared Sounder, J. Geophys. Res., 113, D22110, doi:10.1029/2008JD010000.

Gettelman,A., Weinstock,E. M., Fetzer,E. J., Irion,F. W., Eldering,A., Richard,E. C., Rosenlof,K. H., Thompson,T. L., Pittman,J. V., Webster,C. R., Herman,R. L. (2004), Validation of Aqua satellite data in the upper troposphere and lower stratosphere with in situ aircraft instruments, Geophys. Res. Lett., 31, L22107, doi:10.1029/2004GL020730.

Grody, F.Weng, and R. Ferraro (2000), “Application of AMSU for obtaining hydrological parameters,” in Microwave Radiometry and Remote Sensing of the Earth’s Surface and Atmosphere, edited by P. Pampaloni and S. Paloscia, pp. 339–352, Brill Acad., Leiden, Netherlands.

Hagan D. E., C. R. Webster, C. B. Farmer, R. D. May, R. L. Herman, E. M. Weinstock, L. E. Christensen, L. R. Lait, P. A. Newman (2004), Validating AIRS upper atmosphere water vapor retrievals using aircraft and balloon in situ measurements, Geophys. Res. Lett., 31, L21103, doi:10.1029/2004GL020302.N.

Lambrigtsen, B.H., "Calibration of the AIRS microwave instruments," Geoscience and Remote Sensing, IEEE Transactions on , vol.41, no.2, pp. 369-378, Feb. 2003.

Lambrigtsen, B.H.; Calheiros, R.V., "The Humidity Sounder for Brazil - an international partnership," Geoscience and Remote Sensing, IEEE Transactions on , vol.41, no.2, pp. 352-361, Feb. 2003.

Read, W. G., A. Lambert, J. Bacmeister, R. E. Cofield, L. E. Christensen, D. T. Cuddy, W. H. Daffer, B. J. Drouin, E. Fetzer, L. Froidevaux, R. Fuller, R. Herman, R. F. Jarnot, J. H. Jiang, Y. B. Jiang, K. Kelly, B. W. Knosp, L. J. Kovalenko, N. J.

Livesey, H.-C. Liu, G. L. Manney, H. M. Pickett, H. C. Pumphrey, K. H. Rosenlof, X. Sabounchi, M. L. Santee, M. J. Schwartz, W. V. Snyder, P. C. Stek, H. Su, L. L. Takacs, R. P. Thurstans, H. Voemel, P. A. Wagner, J. W. Waters, C. R. Webster, E. M. Weinstock and D. L. Wu (2007), Aura Microwave Limb Sounder upper tropospheric and lower stratospheric H2O and relative humidity with respect to ice validation, J. Geophys. Res., 112, D24S35, doi:10.1029/2007JD008752.

Rosenkranz, P.W. (2001), “Retrieval of temperature and moisture profiles from AMSU-A and AMSU-B measurements”, IEEE Trans. Geosci. Rem. Sens. v.39, pp.2429-2435.

Rosenkranz, P.W. (2003), “Rapid radiative transfer model for AMSU/HSB channels,” IEEE Trans. Geosci. Rem. Sens., v.41, pp.362-368.

Rosenkranz, P.W. (2006), “Cloud liquid-water profile retrieval algorithm and validation,” J. Geophys. Res., v.111, D09S08, doi:10.1029/2005JD00583.

Rosenkranz, P.W. and C. D. Barnet (2006), “Microwave radiative transfer model validation,” J. Geophys. Res., v.111, D09S07, doi:10.1029/2005JD006008.

Tretyakov et al., 2005, “60 GHz Oxygen Band: precise broadening and central frequencies of fine structure lines, absolute absorption profile at atmospheric pressure and revision of mixing coefficients,” J. Mol. Spectros. v.231, pp.1-14, doi: 10.1016/j.j,s.2004.11.011

10.8 Recommended Supplemental User Documentation

V6_Data_Release_User_Guide.pdf
V6_Data_Disclaimer.pdf
V6_L2_Performance_and_Test_Report.pdf
V6_L2_Quality_Control_and_Error_Estimation.pdf
V6_Released_Processing_File_Description.pdf
V6_L2_Standard_Pressure_Levels.pdf
V6_Retrieval_Flow.pdf

11 Level 2 Physical Retrieval Surface Property Retrievals

Field Name	Dimension per FOV	Description
TSurfStd	1	Surface skin temperature (K)
TSurfStdErr	1	Error estimate for TSurfStd (K)
TSurfStd_QC	1	Quality flag (0,1,2)
TSurfAir	1	Retrieved Surface Air Temperature (K)
TSurfAirErr	1	Error Estimate for TSurfAir (K)
numHingeSurf	1	Number of IR hinge points for surface emissivity and reflectance, (unitless)
freqEmis	HingeSurf =100	Frequencies for surface emissivity and reflectance in order of increasing frequency. Only the first numHingeSurf elements are valid. (cm^{-1})
emisIRStd	HingeSurf =100	Spectral IR surface emissivities in order of increasing frequency from 649 to 2666 cm^{-1} by a series of “hinge points” that differ between land and ocean. Only the first numHingeSurf elements are valid. (unitless)
emisIRStdErr	HingeSurf =100	Error estimate (unitless)
emisIRStd_QC	HingeSurf =100	Quality flag array (0,1,2)

PSurfStd is not an AIRS product. It is interpolated from the Global Forecast System (GFS) forecasts and corrected using the local digital elevation model (DEM) topography of the retrieval field-of-view (FOV) and is used as an input to the AIRS processing.

11.1 Description

The AIRS standard surface product is the result of the combined IR/MW retrieval or of the IR-Only retrieval (AIRS-Only) when AMSU is not used. The AIRS+AMSU Level 2 Standard Product has shortname **AIRX2RET**; the AIRS+AMSU+HSB Level 2 Standard Product has shortname **AIRH2RET**. The AIRS-Only Level 2 Standard Product has shortname **AIRS2RET**. See the MW-Only product (above) for surface products derived solely from the microwave radiance data, which is absent from **AIRS2RET**.

The initial surface emissivity over non-frozen ocean (**landFrac** < 0.01, **MWSurfClass** = 2) follows the shape of the Masuda model as updated by Wu and Smith (1997) as recomputed at higher spectral resolution by van Delst and Wu (http://airs2.ssec.wisc.edu/~paulv/#IRsse) monthly for the year 2008. Their adjustable parameter set for a wind speed of 5 meters/sec.

In V5 the initial surface emissivity over all other surface classes (e.g., land and ice), was set using a NOAA surface regression. In V6, the first guess emissivity is set using the UW-Madison global MODIS IR baseline-fit emissivity product (**UWIREMIS**) (http://cimss.ssec.wisc.edu/iremis/). The **UWIREMIS** is based on the MODIS **MYD11C3** v4.1 product and extends the original 6 MODIS IR emissivity bands to 10 'hinge-points' in the infrared domain (3.6-12 μm). The MODIS-derived starting emissivity is available in support product fields as **MODIS_emis**, **MODIS_emis_spots** (6 hinge points, AMSU and AIRS spot size respectively), and **MODIS_emis_10hinge** (10 hinge points, AMSU spots size). This makes **UWIREMIS** applicable to any given sensor's spectral resolution (e.g. AIRS, IASI). Using **UWIREMIS** greatly improves shortwave emissivity spectral shape compared to V5, where shortwave emissivity was regressed from the longwave emissivity shape. Once the LST has been solved for, the longwave spectral emissivity is solved for in a separate step, assuming that values of Ts, T(p) an q(p) are already known. The logic for the emissivity guess based on **UWIREMIS** for different surface classes (Table 1) is shown in Table 2.

Table 1. Surface class type and associated logic

n	Surface Class	Logic
0	Coastline	Liquid water covers 50-99% of area
1	Land	Liquid water covers <50% of area
2	Ocean	Liquid water covers >99% of area
3	Sea ice	High microwave emissivity
4	Sea ice	Low microwave emissivity
5	Snow	Higher-frequency microwave scattering
6	Glacier/snow	Very low-frequency microwave scattering
7	Snow	Lower-frequency microwave scattering

The AIRS V6 surface retrieval includes three major changes from V5 discussed in detail in Susskind et al. (2008) and summarized in Table 3. These include: (1) changes in the form of the emissivity and reflectance perturbation functions, (2) a modification to the reflectance initial guess, and (3) a modified channel set for the surface retrieval. The perturbation functions (Table 3) are now defined so that unphysical values (ε>1) often seen in V5 will not occur, resulting in a more stable retrieval. The channel selection for V6 differs substantially from V5 in that only shortwave channels are used for retrieval of LST (see Susskind et al. 2008 for details). The new methodology for V6 uses 57 shortwave window channels to determine the LST, T(p), and q(p) along with coefficients of 2 shortwave spectral emissivity perturbation functions, and then assumes these parameters are known and held fixed in determination of the longwave spectral emissivity. The motivation behind this change was the same as when only shortwave CO_2 absorption channels were used to retrieving tropospheric T(p) in V5. Cloud clearing errors now have less effect on LST errors allowing retrievals under more challenging cloud conditions. Improvement in emissivity spectral shape is clearly seen in Figure 1, which shows mean emissivity spectra for the V5 and V6 retrieval over the Grand Erg Oriental desert in Algeria from 2003-2006.

Table 2. MODIS emissivity first guess logic based on surface type and topography

Surface Type	Logic	Emissivity Guess	Reasoning
Ocean	(n=2) and (topog=0) and no MODIS guess	Masuda water	Definitely Ocean
	(n=2) and MODIS provides guess	(MODIS + Masuda water)/2	MODIS provides guess indicating land or inland water possible
	(n=2) and topog>0 and no MODIS guess	Masuda water	Probably Ocean
Sea ice	(n=3) or (n=4)	MODIS ice (UCSB Library spectra from Mammoth Lakes)	Definitely sea ice
Non-frozen land	(m=0) or (m=1)	f*MODIS + (f-1)*Masuda f = land fraction	Mixed land and water based on land fraction
Frozen land	(n=5, 6, 7) and MODIS provides guess	(MODIS + MODIS ice)/2	Could be bare or frozen surface
	(n=5, 6, 7) and no MODIS guess	MODIS ice	Sea ice or glacier most likely

There has been considerable confusion over the years about the use of "hinge points" to define the emissivity and reflectance spectrum. Different retrievals may use different sets of hinge points. There is no physical meaning to the choice of hinge points. They are purely a method of describing a piecewise linear (in frequency) curve in spectral space. To compute a surface emissivity at a particular frequency, the researcher should interpolate in frequency between the emissivities provided at adjacent hinge points. Nothing philosophical should be read into the choice of hinge points or why they vary among profiles.

For modeling the upwelling radiance surfaces are assumed Lambertian, except for the short wave component of the reflected solar component. In this case, the reflectance is modeled to take into account the reflected incoming solar component that may not be Lambertian.

Table 3. AIRS V6 major surface retrieval modifications from V5 (from Susskind et al. 2008)			
Modification	**Version 5**	**Version 6**	**Justification**
Emissivity Perturbation Function	$\varepsilon_\nu = \varepsilon_{o,\upsilon} \sum_i A_i F_i(\upsilon)$	$(1 - \varepsilon_\nu) = (1 - \varepsilon_{o,\upsilon})[1 + \sum_i A_i F_i(\upsilon)]$	Eliminates unphysical Values with $\varepsilon_\upsilon > 1$ $\varepsilon_\nu > 1$
Reflectance Perturbation Function	$\rho_\nu = \rho_{o,\upsilon} \sum_i B_i G_i(\upsilon)$	$\rho_\nu = \rho_{o,\upsilon}[1 + \sum_i B_i G_i(\upsilon)]$	Eliminates unphysical values with $\rho_\nu < 0$
Initial Reflectance Guess	$\rho_{o,\upsilon} = \frac{1-\varepsilon_{o,\upsilon}}{\pi}$	$\rho_{o,\upsilon} = d\left(\frac{1-\varepsilon_{o,\upsilon}}{\pi}\right)$	Accounts for attenuation of solar radiation by clouds from sun to observation point.
Channels used for LST	15 longwave: (758-1228 cm^{-1}) 10 shortwave: (2456-2658 cm^{-1})	57 shortwave: (2396 - 2660 cm^{-1})	Reduced cloud clearing errors, minimizes day/night emissivity differences, shortwave independent of incorrect longwave emissivity.
Emissivity first guess	NOAA surface regression	MODIS Baseline-Fit Emissivity	Using a physical-based, coincident emissivity retrieved from MODIS improves shortwave spectral shape and LST accuracy

The surface air temperature (**TSurfAir**) is obtained from the 100-level support product air temperature profile (**TAirSup**) using interpolation that is linear in the logarithm of the support pressure (**pressSup**).

Note that **TSurfAir** will equal **TAirStd**(**nSurfStd**) only if **pressStd**(**nSurfStd**) is equal to **PSurfStd**. This will seldom be the case.

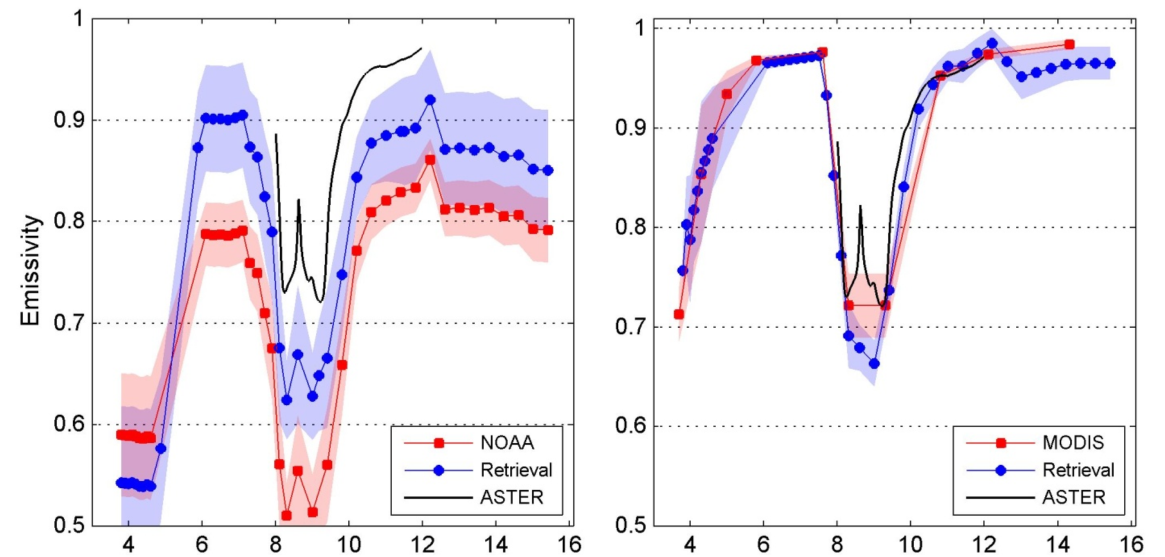

Figure 1: AIRS mean emissivity spectra from 2003-2006 over the Grand Erg Oriental validation site in Algeria

Left Panel: V5 using the NOAA surface regression first guess
Right Panel: V6 using the UW-Madison MODIS baseline-fit emissivity database

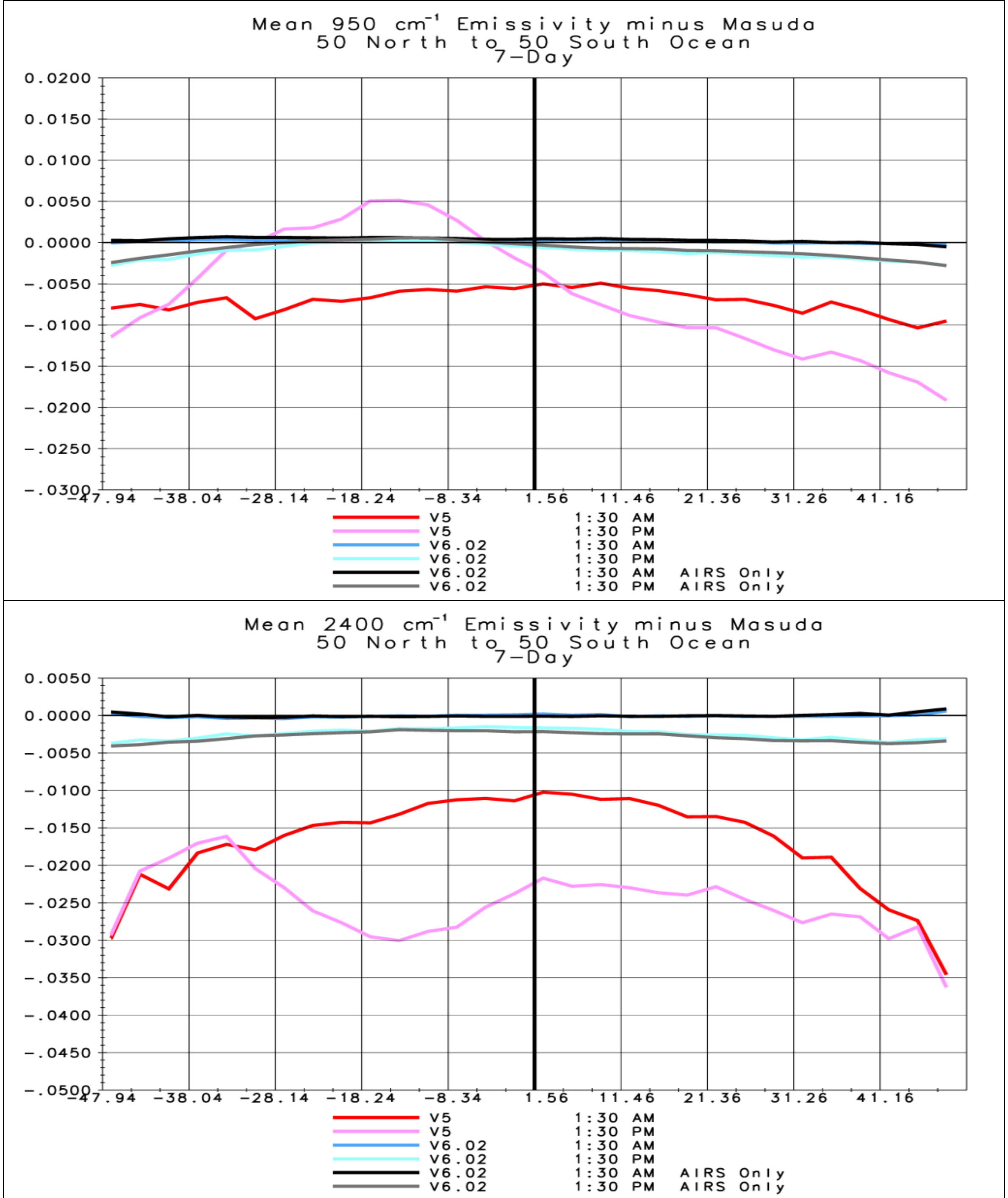

Figure 2: Mean difference between AIRS and Masuda emissivity
Top Panel: Comparison of V5 and V6 differences with Masuda at 950 cm^{-1}
Bottom Panel: Comparison of V5 and V6 differences with Masuda at 2400 cm^{-1}

11.2 Type of Product

The AIRS surface products are all level quantities, describing the state at **PSurfStd**.

11.3 Quality Indicators

The user is encouraged to read the QC and error estimation document:

V6_L2_Quality_Control_and_Error_Estimation.pdf

The surface quality **Qual_Surf** is set by testing the surface temperature error estimate, **TSurfStdErr** against a threshold.

Over Ocean:
Qual_Surf = 0 if **TSurfStdErr** < 1.1 K (1.2 K in AIRS-only)
Qual_Surf = 1
    if Lat > -40° and **TSurfStdErr** < 1.4 K
    if Lat < -60° and **TSurfStdErr** < 2.0 K
    if -60° ≤ Lat ≤ -40°
        and **TSurfStdErr** < 2.0 – (0.3)(60+Lat)
Qual_Surf = 2 if TSurfStdErr fails test

Over Land and Frozen Cases:
Qual_Surf = 1 if PGood = PSurfStd and TSurfStdErr < 7 K
Qual_Surf = 2 otherwise

Qual_Surf is not reported separately, but is used to set **TSurfStd_QC** and the other surface QC flags.

The philosophy for quality control over ocean differs from that of all other cases. Over ocean the quality control attempts to identify quite good cases because we think that is what researchers require. If the yield is not appropriate for a particular application, users are encouraged to use **TSurfStdErr** as a more precise filter. Over land, other data sources are not as readily available and we have chosen to mark few cases as "best" pending further refinement and validation of the emissivity products, but mark a large selection of cases as "good" to ensure adequate coverage for production of 8-day and monthly means for climate studies.

11.4 Validation

Validation of the V6 surface products is currently underway.
A brief summary of early testing is provided in

V6_L2 Performance_and_Test_Report.pdf

The AIRS V5 IR emissivity product has been validated using a combination of ASTER and field emissivity data at two sites over large sand dune seas of the Namib and Kalahari deserts in southern Africa. Details of the validation are discussed in Hulley et al. (2009). The AIRS V5 LST product has also been validated using a Radiance-based method over two desert sites (Gran Desierto, Namib) and a vegetated site (Redwood forest). Details of this validation are discussed by Hulley and Hook (2012).

11.5 Caveats

This section will be updated over time as V6 data products are analyzed and validated.

The AIRS surface emissivity/reflectance products are still being refined.

emisIRstd represents the emissivity from 649 cm^{-1} to 2666 cm^{-1} by a series of "hinge points" which may differ between land and ocean because of the internal processing paths and assumptions. The user must read **freqEmis** to know the values of the **numHingeSurf** hinge points for each profile, and then interpolate linearly in wavelength to find the emissivity at a particular frequency. In V6, all profiles define the same 39 hinge points. However, this is not guaranteed for future versions if we develop better land spectra, so the user is well-advised to continue to read **numHingeSurf** and **freqEmis** for each profile to be certain of consistency.

TSurfAir sometimes differs by more than 2.5 K from the interval defined by the values of **TAirStd** for the levels immediately above and below the surface.

11.6 Suggestions for Researchers

This section will be updated over time as V6 data products are analyzed and validated.

The surface emissivity retrieval is set to have minimum limits of 0.65 (shortwave band 2564 cm^{-1}) and 0.92 (longwave band 909 cm^{-1}). Emissivity retrievals with values that fall below these limits are generally considered unphysical at AIRS spatial resolution (50km). However, on occasion emissivity values below these limits will be reported for Q0 (best) and Q1 (good) quality flags when there is a valid first guess emissivity (from MODIS **MYD11C3** climatology) that is unusually low, most likely due to cloud contamination. **TSurfStd** values should be used with due caution for these causes.

11.7 Recommended Papers

This section will be updated over time as research with V6 data products are published.

Chen, Francis, Miller (2002), Surface temperature of the Arctic: Comparison of TOVS satellite retrievals with surface observations, J. Climate, 15, 3698–3708. DOI: 10.1175/1520-0442(2002)015<3698:STOTAC>2.0.CH4;2

Ferguson, Craig R., Eric F. Wood, 2010: An Evaluation of Satellite Remote Sensing Data Products for Land Surface Hydrology: Atmospheric Infrared Sounder*. J. Hydrometeor, 11, 1234–1262. doi: 10.1175/2010JHM1217.

Gao, W.H., Zhao, F.S., Xu, Y.F., Feng, X., "Validation of the Surface Air Temperature Products Retrieved From the Atmospheric Infrared Sounder Over China," Geoscience and Remote Sensing, IEEE Transactions on Geoscience and Remote Sensing, vol.46, no.6, pp.1783-1789, June 2008

Hulley, G. C., S. J. Hook, E. Manning, S-Y Lee, and E. Fetzer, 2009. Validation of the Atmospheric Infrared Sounder (AIRS) Version 5 Land Surface Emissivity Product over the Namib and Kalahari Deserts, J. Geophys. Res, 114, D19104

Hulley, G. C., and S. J. Hook (2012), A radiance-based method for estimating uncertainties in the Atmospheric Infrared Sounder (AIRS) land surface temperature product, J. Geophys. Res., 117, D20117, doi:10.1029/2012JD018102.

Heilliette,S., Chedin,A., Scott,N. A., Armante,R. (2004), Parametrization of the effect of surface reflection on spectral infrared radiance measurements. Application to IASI, Journal of Quantitative Spectroscopy & Radiative Transfer, 86, 201-214. doi:10.1016/j.jqsrt.2003.08.002

Knuteson et al (2003), Aircraft measurements for validation of AIRS land surface temperature and emissivity products at the Southern Great Plains validation site, Fourier Transform Spectroscopy (Trends in Optics and Photonics Series Vol.84). 138.

Maddy, E. S. and C. D. Barnet (2008), Vertical Resolution Estimates in Version 5 of AIRS Operational Retrievals, IEEE Trans. Geosci. Remote Sens., 46(8), 2375-2384.

Nalli,N. R. and Smith,W. L. (2003), Retrieval of ocean and lake surface temperatures from hyperspectral radiance observations, Journal of Atmospheric and Oceanic Technology, 20, 810-1825. doi: 10.1175/1520-0426(2003)020<1810:ROOALS>2.0.CH4;2

Seemann, Suzanne W., Eva E. Borbas, Robert O. Knuteson, Gordon R. Stephenson, Hung-Lung Huang, 2008: Development of a Global Infrared Land Surface Emissivity Database for Application to Clear Sky Sounding Retrievals from Multispectral Satellite Radiance Measurements. J. Appl. Meteor. Climatol., 47, 108–123, doi: http://dx.doi.org/10.1175/2007JAMC1590.1

Susskind, J., C. D. Barnet, and J. Blaisdell (2003), Retrieval of atmospheric and surface parameters from AIRS/AMSU/HSB data in the presence of clouds, IEEE Trans. Geosci. Remote Sens., 41(2), 390–409.

Susskind, J., and J. Blaisdell (2008), Improved surface parameter retrievals using AIRS/AMSU data, Proc. SPIE Int. Soc. Opt. Eng., 6966, 696610, doi:10.1117/12.774759.

Wu and Smith (1997), Emissivity of rough sea surface for 8-13 mm: modeling and verification," Appl. Opt. 36, 2609-2619

Yao, Zhigang, Jun Li, Jinlong Li, Hong Zhang, 2011: Surface Emissivity Impact on Temperature and Moisture Soundings from Hyperspectral Infrared Radiance Measurements. J. Appl. Meteor. Climatol., 50, 1225–1235. doi: 10.1175/2010JAMC2587.

Zhou, L., M. Goldberg, C. Barnet, Z. Cheng, F. Sun, W. Wolf, T. King, X. Liu, H. Sun, and M. Divakarla (2008), Regression of surface spectral emissivity from hyperspectural instruments, IEEE Trans. Geosci. Remote Sens., 46(2), 328–333, doi:10.1109/TGRS.2007.912712

11.8 Recommended Supplemental User Documentation

V6_Data_Release_User_Guide.pdf

V6_Data_Disclaimer.pdf

V6_L2_Performance_and_Test_Report.pdf

V6_L2_Quality_Control_and_Error_Estimation.pdf

V6_Retrieval_Channel_Sets.pdf

V6_Retrieval_Flow.pdf

12 Level 2 Physical Retrieval Air Temperature Retrievals

Standard Product

Field Name	Dimension per FOV	Description
TAirStd	StdPressureLev =28	Retrieved Atmospheric Temperature Profile (K)
TAirStdErr	StdPressureLev =28	Error estimate for TAIRStd (K)
TAirStd_QC	StdPressureLev =28	Quality flag array (0,1,2)
Temp_Resid_Ratio	1	Internal retrieval quality indicator; residuals of temperature channels compared to predicted uncertainty (unitless)
TSurfAir	1	Retrieved Surface Air Temperature (K)
TSurfAirErr	1	Error Estimate for TSurfAir (K)
TSurfAir_QC	1	Quality flag (0,1,2)
Temp_dof	1	Degrees of freedom, a measure of the amount of information in temperature profile retrieval (dimensionless)

Support Product

Field Name	Dimension per FOV	Description
TAirSup	XtraPressureLev=100	Atmospheric Temperature at XtraPressLev in Kelvins. Value at 1-based index of nSurfSup may be an unphysical extrapolated value for a pressure level below the surface. Use TSurfAir for the surface air temperature
TAirSup_QC	XtraPressureLev=100	Quality flag array (0,1,2)
TAirSupErr	XtraPressureLev=100	Error estimate for TAIRSup (K)

Field Name	Dimension per FOV	Description
num_Temp_Func	1	Number of valid entries in each dimension of Temp_ave_kern
Temp_ave_kern	TempFunc*TempFunc =23x23	Averaging kernel for temperature retrieval
Temp_verticality	TempFunc = 23	Sum of the rows of Temp_Ave_kern

12.1 Description

The AIRS standard temperature product is the result of the combined IR/MW retrieval. See the MW-Only product (above) for temperature products derived solely from the microwave data. The atmospheric temperature profile (**TAirStd**) is reported on the standard pressure levels (**pressStd**) that are above the altitude of the highest topography in the retrieval field-of-view (FOV).

The surface air temperature (**TSurfAir**) and **TAirStd** are obtained from the 100-level support product air temperature profile (**TAirSup**) using interpolation that is linear in the logarithm of the support pressure (**pressSup**).

Note that **TSurfAir** will equal **TAirStd**(**nSurfStd**) only if **pressStd**(**nSurfStd**) is equal to **PSurfStd**. This will seldom be the case.

The 28 Level 2 Standard pressure levels (**pressStd**) are arranged in order of decreasing pressure. The highest altitude pressure level is pressStd(28) = 0.1 hPa. The index of the lowest altitude pressure level for which a reported **TAirStd** is valid is **nSurfStd**, which may be 1, 2, …, 15 depending upon topography. The surface pressure, **PSurfStd**, is interpolated from the NCEP GFS forecast and the local DEM topography.

The 100 Level 2 Support pressure levels (**pressSup**) are arranged in order of increasing pressure. The highest altitude pressure level is pressSup(1) = 0.0161 hPa. Use **TSurfAir** for the surface air temperature at the index of the surface pressure level **nSurfSup**.

Temp_verticality is a 23 point vector computed by summing the rows of the 23x23 Temperature averaging kernel, **Temp_avg_kern**, stored in the AIRS Level 2 Support Product. The associated 23 point pressure array is NOT provided in **Temp_eff_press** (UNDEFINED AND NOT IN PRODUCT FILE, SEE TABLE 1 BELOW). The peak value of **Temp_verticality** indicates the vertical location of the maximum sensitivity of the Temperature product and the width of this peaked function qualitatively describes the vertical resolution of the retrieval. The magnitudes of **Temp_verticality** are a rough measure of the fraction of the retrieval determined from the data as opposed to the first guess. A value near unity indicates the retrieval is highly determined by the radiance measurements and thus has high information content. A smaller value indicates the retrieval contains a large fraction of the first guess. **Temp_dof** is the number of degrees of freedom (a measure of the amount of information in the retrieval), and is the trace of **Temp_avg_kern**.

NOTE: **num_Temp_Func** provides the number of valid entries in each dimension of **Temp_ave_kern**. Topography limits the number of valid temperature averaging kernel trapezoids.

The effective pressures of the temperature trapezoids may be calculated from the minimum pressure level boundaries and maximum pressure level boundaries tabulated in Section 3.3 of **V6_L2_Levels_Layers_Trapezoids.pdf**. But there are two modifications to the pressures in that table. The first is that the minimum pressure level for the top of the atmosphere is 0.005 hPa, because the RTA assumes that as the TOA minimum pressure. The second is that the maximum pressure level can be no greater than **PSurfStd**. This will reduce the number of trapezoids over land due to topography. The algorithm to calculate the **Temp_eff_press** array is:

Temp_eff_press(1) = (press(2) – 0.005)/log(press(2)/0.005)

Temp_eff_press(i) = (press(i+1)-press(i))/log(press(i+1)/press(i))

For first occurrence of press(i+1) > PSurfStd,
Temp_eff_press(i_last) = (PSurfStd-press(i_last))/log(PSurfStd/press(i_last))

And all trapezoids below this one are null and void.

The result of this calculation is shown in the following Table 1:

TABLE 1 – 23 effective pressures for temperature trapezoidal averaging kernels

Trapezoid Number	Temp_eff_press (hPa)
1	0.14290
2	0.97675
3	1.9140
4	3.3419
5	5.8865
6	11.821
7	19.734
8	30.679
9	47.190
10	63.522
11	83.223
12	110.22
13	142.36
14	185.07
15	241.19
16	306.91
17	382.62
18	*459.61
19	*544.95
20	*628.19
21	*706.40
22	*814.53
23	*variable

*Over land, may be variable or null and void
(pressure at summit of Mt Everest is approximately 300 hPa)

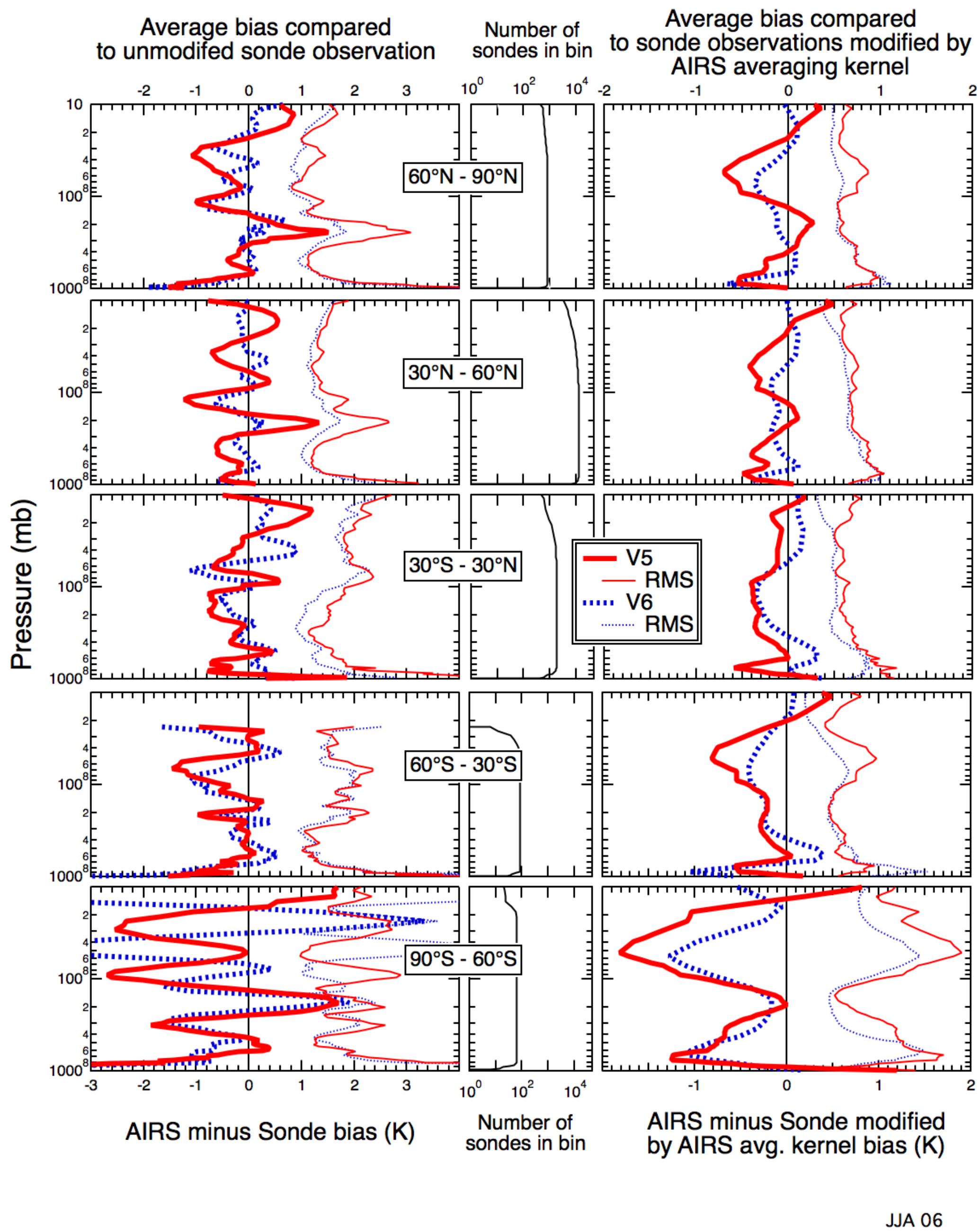

Figure 3: Zonally-averaged comparisons of V5 and V6 temperature product to operational radiosondes for JJA of 2006 (TAirSup_Qual = 0).
(AIRS-Sonde) and RMS as a function of latitude, raw (left) and kerned (right). Center panel shows number of samples averaged as a function of altitude.

Fraction of All Cases Accepted (%)	1 km Layer Mean RMS Differences from ECMWF (K)	1 km Layer Mean Bias differences from ECMWF (K)

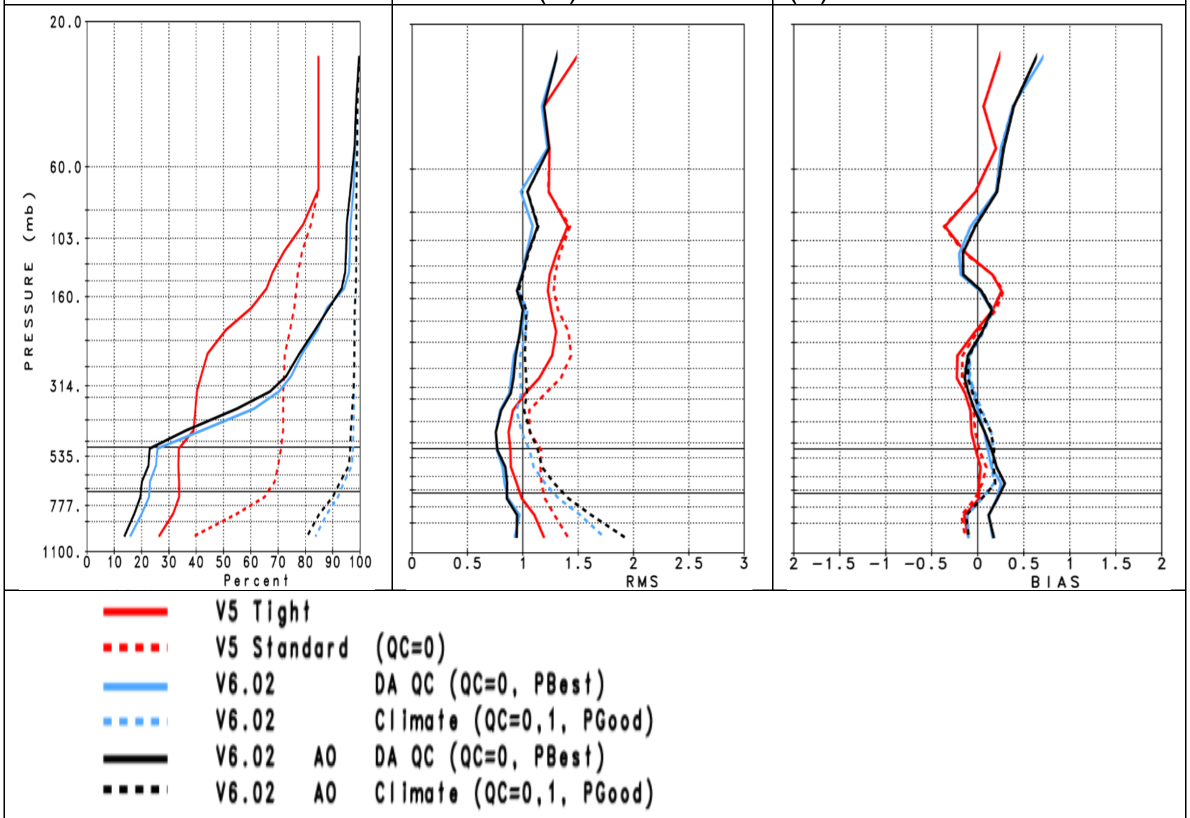

Figure 4: Global temperature statistics of AIRS retrievals compared to collocated ECMWF for seven study days.

Left panel shows % of QC'd retrievals accepted as a function of altitude; Central panel shows the RMS differences of 1 km mean temperatures wrt ECMWF; Right panel shows the biases of 1 km mean temperatures wrt ECMWF

Study Days: 20020906, 20030125, 20040929, 20050805, 20070224, 20070810, 20100530

12.2 Type of Product

All standard temperature products are level quantities, which means that the values are reported at fixed pressure levels. This differs from layer quantities, which are reported on the fixed pressure levels but represent the layer bounded by the level on which they are reported and the next higher level (in altitude).

For more detail, see **V6_L2_Levels_Layers_Trapezoids.pdf** for a full discussion of level and layer quantities.

12.3 Quality Indicators

The user is encouraged to read the QC and error estimation document:

V6_L2_Quality_Control_and_Error_Estimation.pdf

The temperature profile (**TAirStd**) has associated error and QC profiles (**TAirStdErr** and **TAirStd_QC**), providing estimates of error and the QC at each pressure level. The users will find that the parameters **PBest** and **PGood** will facilitate their filtering of data.

The V4 legacy quality factors that were carried forward in V5 have been removed from the V6 products as they are no longer consistent with the current complexity of quality flagging.

12.3.1 PBest and nBestStd

PBest indicates **TAirStd** is "best" from the top of the atmosphere (TOA) downward to the level of **PBest**, i.e. **TAIRStd_QC** = 0 for the profile for levels at altitudes above and including **PBest**. "Best" data products individually meet our accuracy requirements and may be used for comparison with in situ measurements, data assimilation and statistical climate studies

nBestStd is the index of the lowest altitude level of the **pressStd** and **TAirStd** profiles for which the quality is "best". Levels whose indices are in the range i = **nBestStd**, **nBestStd** + 1, …, 28 are therefore marked quality = 0. It is set to a value of 29 to indicate that none are "best". Take note that **nBestStd** is 1-based (as are arrays in FORTRAN and MATLAB) rather than 0-based (as are arrays in C and IDL).

12.3.2 PGood and nGoodStd

PGood indicates **TAirStd** is "good" from the level below **PBest** to the level of **PGood**, i.e. **TAIRStd_QC** ≤ 1 for the portion of the **TAirStd** profile above and including the level of **PGood**. If **PBest** is less than **PGood**, then the levels below that of **PBest** and above and including that of **PGood** are flagged as quality = 1 ("good"). If **PBest** = **PGood**, then all levels above and including the common pressure level are flagged quality = 0. "Good" data products may be used for statistical climate studies, as they meet the accuracy requirements only when temporally and/or spatially averaged.

nGoodStd is the index of the lowest altitude level of the **pressStd** and **TAirStd** profiles for which the quality is "good". Levels whose indices are in the range i = **nGoodStd**., **nGoodStd** + 1, …, **nBestStd**-1 are therefore marked quality = 1. It is set to a value of 29 to indicate that none are "good". Take note that **nGoodStd** is 1-based (as are arrays in FORTRAN and MATLAB) rather than 0-based (as are arrays in C and IDL).

Note that it is possible that **PBest** = **PGood** and **nBestStd** = **nGoodStd**. The **TAirStd** profile below **PGood** is rejected and its quality set = 2 ("do not use").

If the entire temperature profile is rejected, **PBest** = **PGood** = 0 and **nBestStd** = **nGoodStd** = 29. There may, however, still be values in the **TAirStd** profile if some stage of the retrieval was successful. The flagged profile may be an excessively noisy full retrieval or the output from an intermediate stage of the retrieval process.

12.4 Validation

A Validation Report for V6 data is currently under preparation and will be published after the V6 data products become publicly available. A V5 Validation Report, summarizing relevant publications, is also being prepared. Early V6 validation results are partially summarized in

V6_L2 Performance_and_Test_Report.pdf

12.5 Caveats

This section will be updated over time as V6 data products are analyzed and validated.

All parameters that are level numbers, such as **nSurfStd, nBestStd and nGoodStd** are 1-based. Those who work in FORTRAN and MATLAB will be unaffected. However, those who work in C and IDL must take care when using **nSurfStd** and other parameters that are level numbers. The following two expressions yield the same value:

FORTRAN and MATLAB: **pressStd**(**nBestStd**)

C and IDL: **pressStd**[**nBestStd**-1]

The quality indicator is based on the empirical error estimate **TAirStdErr.** The output error estimate may not be consistent with the atmospheric temperature error estimate used by the physical retrieval algorithm. The latter is not written to the output.

Our analysis of V5 retrievals showed that data assimilation applications profited from tighter quality control than that given in V5. The neural network first guess provides a much better first guess in difficult cases for V6 when compared with V5. Accordingly, we have greatly increased the number of Quality = 1 cases and reduced the number of both Quality = 0 and Quality = 2 cases to provide better discrimination of cases.

In response to the desire of researchers to use retrievals near to tropical storms, we have revised the algorithm to report the stratospheric portion of the temperature retrieval above 30 hPa as Quality = 0 in all cases where the retrieval successfully completed. In these difficult cases, **PBest** is set to a relatively low value. At pressures greater than **PBest**, Quality = 1. This continues toward the surface until the pressure **PGood**. Beyond that pressure Quality = 2. In these cases, retrieval values are provided where possible. Less than 1 % of cases are now marked Quality = 2 for the entire profile, and these rare cases indicate difficulties in the IR/MW retrieval that makes them very suspect.

12.6 Suggestions for Researchers

This section will be updated over time as V6 data products are analyzed and validated.

We strongly recommend using the **PBest** and **PGood** quality indicators. The values that are set for subsetting data should be carefully chosen, and depend upon how the data are to be used. At the very least, **PGood** should exceed the maximum pressure of interest. If the thrust of the research is comparison with in situ measurements (e.g., radiosondes), then **PBest** should exceed the maximum pressure of interest. The portions of profiles nearer to the surface than PGood should be discarded and those at pressures greater than **PSurfStd** are invalid.

The level-by-level quality factors are consistent with the definitions of **PGood** and **PBest**.

12.7 Recommended Papers

This section will be updated over time as research with V6 data products are published.

Behrangi, A., E. J. Fetzer, and S. L. Granger (2016), Early detection of drought onset using near surface temperature and humidity observed from space, Int.J.Remote Sens., 37(16), 3911-3923. https://dx.doi.org/10.1080/01431161.2016.1204478

Bisht, Jagat Singh Heet, Pradeep Kumar Thapliyal, Munn Vinayak Shukla, and Raj Kumar. "A comparative study of different AIRS products for the detection of near-surface temperature inversion: a case study over New Delhi." Remote Sensing Letters 4, no. 1 (2013): 94-103.

Boisvert, L. N., J. N. Lee, J. T. M. Lenaerts, B. Noël, M. R. van den Broeke, and A. W. Nolin (2016), Using remotely sensed data from AIRS to estimate the vapor flux on the Greenland ice sheet: Comparisons with observations and a regional climate model, J. Geophys. Res. Atmos., 122, doi:10.1002/2016JD025674.

Divakarla, M., C. D. Barnet, M. D. Goldberg, L. M. McMillin, E. Maddy, W. Wolf and L. Zhow (2006), Validation of AIRS temperature and water vapor retrievals with matched radiosonde measurements and forecasts, J. Geophys. Res., 111, D09S15, doi:10.1029/2005JD006116

Devasthale, A., J. Sedlar, T. Koenigk, and E. J. Fetzer. "The thermodynamic state of the Arctic atmosphere observed by AIRS: comparisons during the record minimum sea ice extents of 2007 and 2012." Atmospheric Chemistry and Physics 13, no. 15 (2013): 7441-7450.

Dwivedi, S., Narayanan, M. S., Venkat Ratnam, M., and Narayana Rao, D.: Characteristics of monsoon inversions over the Arabian Sea observed by satellite sounder and reanalysis data sets, Atmos. Chem. Phys., 16, 4497-4509, doi:10.5194/acp-16-4497-2016, 2016

Fetzer E. J., J. Teixeira, E. T. Olsen, E. F. Fishbein (2004), Satellite remote sounding of atmospheric boundary layer temperature inversions over the subtropical eastern Pacific, Geophys. Res. Lett., 31, L17102, doi:10.1029/2004GL020174.

Gao, W., Zhao, F. Gai, C. (2006), Validation of AIRS retrieval temperature and moisture products and their application in numerical models, Acta Metorol. Sinica, Acta Meteorologica Sinica, 64, 271-280.

Guan, B., D. E. Waliser, F. M. Ralph, E. J. Fetzer, and P. J. Neiman (2016), Hydrometeorological characteristics of rain-on-snow events associated with atmospheric rivers, Geophys. Res. Lett., 43, 2964–2973, doi:10.1002/2016GL067978.

Gupta, A., S. K. Dhaka, V. Panwar, R. Bhatnagar, V. Kumar, Savita M. Datta, and S. K. Dash. "AIRS observations of seasonal variability in meridional temperature gradient over Indian region at 100 hPa." Journal of Earth System Science 122, no. 1 (2013): 201-213.

Hearty, T. J., A. Savtchenko, B. Tian, E. Fetzer, Y. L. Yung, M. Theobald, B. Vollmer, E. Fishbein, and Y.-I. Won (2014), Estimating sampling biases and measurement uncertainties of AIRS/AMSU-A temperature and water vapor observations using MERRA reanalysis, J. Geophys. Res. Atmos., 119, 2725–2741, doi:10.1002/2013JD021205.

Kalmus, P., S. Wong, and J. Teixeira (2015), The Pacific Subtropical Cloud Transition: A MAGIC Assessment of AIRS and ECMWF Thermodynamic Structure, IEEE Geoscience and Remote Sensing Letters, Article in Press, doi: http://dx.doi.org/10.1109/LGRS.2015.2413771.

Milstein, A. B., and W. J. Blackwell (2016), Neural network temperature and moisture retrieval algorithm validation for AIRS/AMSU and CrIS/ATMS, J. Geophys. Res. Atmos., 121, 1414–1430, doi:10.1002/2015JD024008.

Naud, C. M., J. F. Booth, and A. D. Del Genio (2016), The Relationship between Boundary Layer Stability and Cloud Cover in the Post-Cold-Frontal Region, Journal of Climate, 29(22), 8129-8149. http://dx.doi.org/10.1175/jcli-d-15-0700.1

Ricaud, P., F. Carminati, Y. Courcoux, A. Pellegrini, J.-L. Attié, L. El Amraoui, R. Abida, C. Genthon, T. August and J. Warner (2014). Statistical analyses and correlation between tropospheric temperature and humidity at Dome C, Antarctica . Antarctic Science, 26, pp 290-308. doi:10.1017/S0954102013000564.

Susskind, J., J. Blaisdell, L. Iredell, and F. Keita (2011), "Improved Temperature Sounding and Quality Control Methodology Using AIRS/AMSU Data: The AIRS Science Team Version-5 Retrieval Algorithm," IEEE Transactions on Geoscience and Remote Sensing, 49, 3, doi:10.1109/TGRS.2010.2070508.

Susskind J., C. Barnet, J. Blaisdell, L. Iredell, F. Keita, L. Kouvaris, G. Molnar, M. Chahine (2006), Accuracy of geophysical parameters derived from Atmospheric Infrared Sounder/Advanced Microwave Sounding Unit as a function of fractional cloud cover, J. Geophys. Res., 111, D09S17, doi:10.1029/2005JD006272.

Tobin D. C., H. E. Revercomb, R. O. Knuteson, B. M. Lesht, L. L. Strow, S. E. Hannon, W. F. Feltz, L. A. Moy, E. J. Fetzer, T. S. Cress (2006), Atmospheric Radiation Measurement site atmospheric state best estimates for Atmospheric Infrared Sounder temperature and water vapor retrieval validation, J. Geophys. Res., 111, D09S14, doi:10.1029/2005JD006103.

Wong, Sun, Eric J. Fetzer, Mathias Schreier, Gerald Manipon, Evan F. Fishbein, Brian H. Kahn, Qing Yue, and Fredrick W. Irion. "Cloud-induced uncertainties in AIRS and ECMWF temperature and specific humidity." Journal of Geophysical Research: Atmospheres (2015).

Wu,X. B., Li,J., Zhang,W. J., Wang,F. (2005), Atmospheric profile retrieval with AIRS data and validation at the ARM CART site.

Zhang, J., Z. Li, J. Li, and J. Li (2014), Ensemble retrieval of atmospheric temperature profiles from AIRS, Adv. Atmos. Sci., 31(3), 559-569, doi:http://dx.doi.org/10.1007/s00376-013-3094-z.

12.8 Recommended Supplemental User Documentation

V6_Data_Release_User_Guide.pdf

V6_Data_Disclaimer.pdf

V6_L2_Performance_and_Test_Report.pdf

V6_L2_Quality_Control_and_Error_Estimation.pdf

V6_Released_Processing_File_Description.pdf

V6_L2_Standard_Pressure_Levels.pdf

V6_L2_Support_Pressure_Levels.pdf

V6_L2_Levels_Layers_Trapezoids.pdf

V6_Retrieval_Channel_Sets.pdf

V6_Retrieval_Flow.pdf

13 Level 2 Physical Retrieval Water Vapor Saturation Quantities Derived from Temperature

13.1 Description

Users found the layer quantities in earlier releases confusing, so V6 introduces **level** quantities, **H2OMMRSatLev_liquid** and **H2OMMRSatLevStd**, which of the integrated mass of water vapor in saturated equilibrium divided by the mass of dry air at the **pressH2O** pressure levels upon which they are reported. The surface saturation equilibrium specific humidity at **PSurfStd** is provided by **H2OMMRSatSurf**. **H2OMMRSatLev_liquid** assumes equilibrium with liquid water. **H2OMMRSatLevStd** is in equilibrium with liquid so long as the **TAirSup** (100 level profile) exceeds 273.15 K. If **TAirSup** drops below that threshold, the saturation calculation shifts to that over water ice. Near the surface the two saturation profiles are identical, but they will diverge in the case that the temperature profile crosses the threshold. The constituent relationship employed is that of Murphy and Koop (2005).

Level quantities are calculated from layer quantities by the procedure described in the Algorithm Theoretical Document

AIRS_Layers_to_Levels_Theoretical_Basis_Document.pdf

The derivation of level quantities from layer quantities is essentially done by interpolation with smoothing kernels. This mathematical transformation leads to occasional strange results for water vapor profiles with inversions, typically near the surface.

For backward compatibility, we retain the **layer** profiles, **H2OMMRSat_liquid** and **H2OMMRSat**. Both provide profiles of the integrated mass of water vapor in saturated equilibrium between **pressH2O** levels divided by the integrated mass of dry air in layers. **H2OMMRSat_liquid** assumes equilibrium with liquid water. **H2OMMRSat** is in equilibrium with liquid so long as the **TAirSup** (100 level profile) exceeds 273.15 K. If **TAirSup** drops below that threshold, the saturation calculation shifts to that over water ice. Thus within a layer in which the temperature crosses 273.15 K, the calculation will shift between saturation over liquid to that over ice to derive its integrated mass of water vapor. Near the surface the two saturation profiles are identical, but they will diverge in the case that the temperature profile crosses the threshold. The constituent relationship employed is that of Murphy and Koop (2005).

Standard Product

Field Name	Dimension per FOV	Description
H2OMMRSat	H2OPressureLay =14	Layer Water vapor saturation mass mixing ratio (gm/kg dry air) over equilibrium phase (set to -9999 when saturation pressure exceeds 1% of ambient pressure.)
H2OMMRSat_QC	H2OPressureLay =14	Quality flag array (0,1,2)
H2OMMRSatLevStd	H2OPressureLev =15	Level Water vapor saturation mass mixing ratio (gm/kg dry air) over equilibrium phase (set to -9999 when saturation pressure exceeds 1% of ambient pressure.)
H2OMMRSatLevStd_QC	H2OPressureLev =15	Quality flag array (0,1,2)
H2OMMRSatSurf	1	Water Vapor saturation Mass Mixing Ratio at the surface (gm/kg dry air) over equilibrium phase
H2OMMRSatSurf_QC	1	Quality flag (0,1,2)
H2OMMRSat_liquid	H2OPressureLay =14	Layer Water vapor saturation mass mixing ratio (gm/kg dry air) over liquid phase (set to -9999 when saturation pressure exceeds 1% of ambient pressure.)
H2OMMRSat_liquid_QC	H2OPressureLay =14	Quality flag array (0,1,2)

Field Name	Dimension per FOV	Description
H2OMMRSatLevStd_liquid	H2OPressureLev =15	Level Water vapor saturation mass mixing ratio (gm/kg dry air) over liquid phase (set to -9999 when saturation pressure exceeds 1% of ambient pressure.)
H2OMMRSatLevStd_liquid_QC	H2OPressureLev =15	Quality flag array (0,1,2)
H2OMMRSatSurf_liquid	1	Water Vapor saturation Mass Mixing Ratio at the surface (gm/kg dry air) over liquid phase
H2OMMRSatSurf_liquid_QC	1	Quality flag (0,1,2)

Support Product

Field Name	Dimension per FOV	Description
H2OMMRSatLevSup	XtraPressureLev =100	Level Water vapor saturation mass mixing ratio (gm/kg dry air) over equilibrium phase (set to -9999 when saturation pressure exceeds 1% of ambient pressure.)
H2OMMRSatLevSup_QC	XtraPressureLev =100	Quality flag array (0,1,2)
H2OMMRSatLevSup_liquid	XtraPressureLev =100	Level Water vapor saturation mass mixing ratio (gm/kg dry air) over liquid phase (set to -9999 when saturation pressure exceeds 1% of ambient pressure.)
H2OMMRSatLevSup_liquid_QC	XtraPressureLev =100	Quality flag array (0,1,2)

13.2 Type of Product

The equilibrium saturation specific moisture is provided both as **layer** profiles and as **level** profiles. Layer quantities are reported on the fixed pressure levels but represent the layer bounded by the level on which they are reported and the next higher level (in altitude). Level quantities are values reported at fixed pressure levels and represent the product at each level. For more detail, see

V6_L2_Levels_Layers_Trapezoids.pdf
AIRS_Layers_to_Levels_Theoretical_Basis_Document.pdf

for a full discussion of level and layer quantities.

13.3 Quality Indicators

The user is encouraged to read the QC and error estimation document:

V6_L2_Quality_Control_and_Error_Estimation.pdf

The temperature profile (**TAirStd**) has associated error and QC profiles (**TAirStdErr** and **TAirStd_QC**), providing estimates of error and the QC at each pressure level. The users will find that the parameters **PBest** and **PGood** will facilitate their filtering of data.

13.4 Caveats

This section will be updated over time as V6 data products are analyzed and validated.

To ensure continuity throughout the entire mission, the V6 retrieval algorithm for products provided by the AMSU+AIRS processing does not use AMSU channels 4 and 5, even in the earlier stage of the mission when those channels were good.

To maximize the quality of the retrieval (of moisture product in particular), the V6 retrieval algorithm for products provided by the AMSU+HSB+AIRS processing does use AMSU channels 4 and 5.

H2OMMRSatLevStd and **H2OMMRSatLevStd_liquid** both provide level profiles of the integrated mass of water vapor in saturated equilibrium at the **pressH2O** levels on which they are reported. **H2OMMRSatSurf** provides a level quantity at the surface pressure, **PSurfStd**. The constituent relationship employed for these level quantities is also that of Murphy and Koop (2005).

H2OMMRSat_liquid and **H2OMMRSat** both provide layer profiles of the integrated mass of water vapor in saturated equilibrium between **pressH2O** levels divided by the integrated mass of dry air. **H2OMMRSat_liquid** assumes equilibrium with liquid water. **H2OMMRSat** is in equilibrium with the physically correct equilibrium phase: liquid or ice. The physically correct equilibrium phase is ice from the point at which **TAirSup** (100 level profile) falls below 273.15 K; otherwise the equilibrium phase is liquid water. Thus within a layer in which the **TAirSup** crosses 273.15 K, the saturation calculation will shift between saturation over ice and that over liquid water. Near the surface the two saturation profiles are identical, but they will diverge in the case that the temperature profile crosses the threshold. The constituent relationship employed is that of Murphy and Koop (2005).

13.5 Recommended Papers

Buck, A. L. (1981), New equations for computing vapor pressure and enhancement factor, J. Appl. Meteorol., 20, 1527-1532.

Murphy, D. M. and T. Koop (2005), Review of the vapour pressures of ice and supercooled water for atmospheric applications, Quart. J. Royal Met. Soc, 608 Part B, 1539-1565.

14 Level 2 Physical Retrieval Tropopause Derived from Temperature

Field Name	Dimension per FOV	Description
PTropopause	1	Tropopause height (hPa)
PTropopause_QC	1	Quality flag (0,1,2)
T_Tropopause	1	Tropopause temperature (K)
T_Tropopause_QC	1	Quality flag (0,1,2)

PTropopause is determined by testing the lapse rate of the higher vertical resolution air temperature profile (**TAirSup**) against the WMO (1992) criteria:

1. The first tropopause (i.e., the conventional tropopause) is defined as the lowest level at which
    a. the lapse rate decreases to 2 K/km or less, and
    b. the average lapse rate from this level to any level within the next higher 2 km does not exceed 2 K/km.
2. If above the first tropopause the average lapse rate between any level and all higher levels within 1 km exceed 3 K/km, then a second tropopause is defined by the same criterion as under the statement above. This tropopause may be either within or above the 1 km layer.
3. A level otherwise satisfying the definition of tropopause, but occurring at an altitude below that of the 500 hPa level will not be designated a tropopause unless it is the only level satisfying the definition and the average lapse rate fails to exceed 3 K/km over at least 1 km in any higher layer.

The V6 code evaluates the lapse rate by taking the derivative of the cubic spline interpolation of the Level 2 Support Product profiles of **TAirSup** versus **pressSup**. Between the 100 support levels, the lapse rate is linearly interpolated between values at the support levels to determine where condition (1a) is satisfied. Linearly interpolation is used rather than evaluating the derivative of the spline (a quadratic function) to filter oscillation from the interpolation. Average lapse rates to test against conditions (1b), (2), and (3) are evaluated in the same fashion, except that the averages are evaluated over the thickness obtained by approximating altitude thicknesses by the first term of the Taylor series expansion of altitude in temperature:

$$\Delta\,\text{Altitude} = \Delta\,\text{Pressure} \times \frac{T}{T_0}$$

T_Tropopause is thus determined as well. The V6 algorithm interpolates between the levels of the support profile in order to obtain a better estimate of the temperature minimum and a continuous range of pressure.

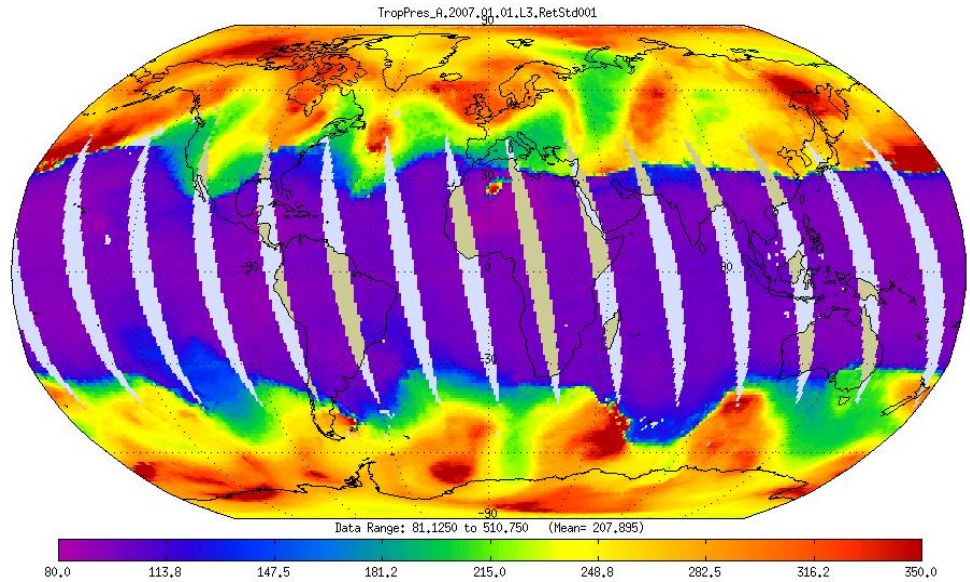

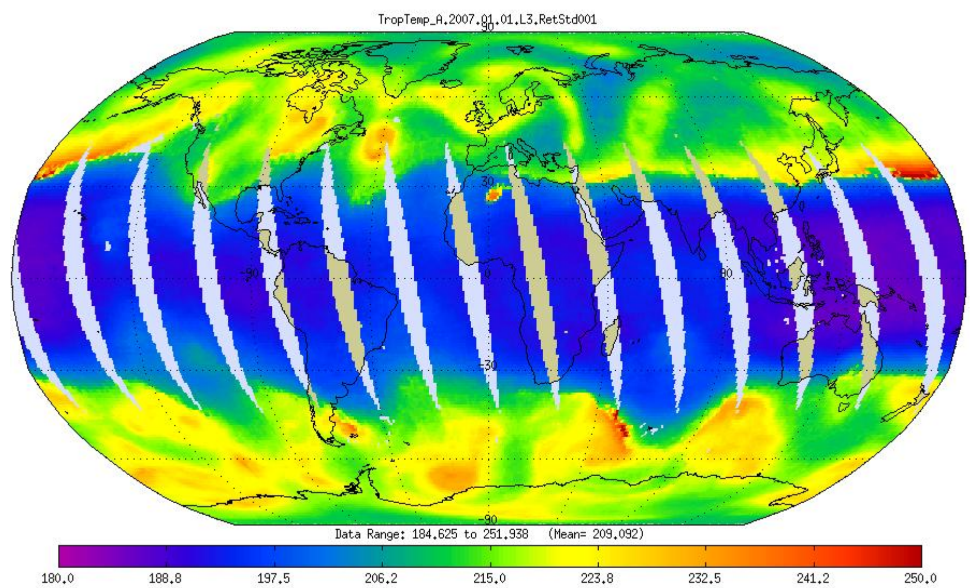

Figure 5: AIRS V6 tropopause product for ascending node of 1 January 2007 for JJA of 2006 (Qual_* = 0).
Top Panel: PTropopause (hPa)
Bottom Panel: T_Tropopause (K)

15 Level 2 Physical Retrieval Water Vapor Retrievals

The AIRS water vapor retrievals are the result of the combined IR/MW retrieval algorithm. See the MW-Only product (above) for moisture products derived solely from the microwave data.

Note that V6 reports **level** profiles in addition to the layer profiles common to V5. A **layer** profile value is the mass mixing ratio (integrated over log of pressure) of a layer bounded by the pressure level on which it is reported and the next higher (in altitude) pressure level. A level profile value is the mass mixing ratio at the pressure level upon which it is reported.

Level quantities are calculated from layer quantities by the procedure described in the Algorithm Theoretical Document

AIRS_Layers_to_Levels_Theoretical_Basis_Document.pdf

The derivation of level quantities from layer quantities is essentially done by interpolation with smoothing kernels. This mathematical transformation leads to occasional strange results for water vapor profiles with inversions, typically near the surface. Be sure to filter the level profile by means of **H2OMMRLevStd_QC**.

Standard Product

Field Name	Dimension per FOV	Description
totH2OStd	1	Total precipitable water vapor (kg/m^2)
totH2OStd_QC	1	Quality flag (0,1,2)
totH2OStdErr	1	Error estimate for totH2OStd (kg/m^2)
H2OMMRStd	H2OPressureLay =14	Layer water Vapor Mass Mixing Ratio (gm/kg dry air)
H2OMMRStd_QC	H2OPressureLay =14	Quality flag array (0,1,2)
H2OMMRStdErr	H2OPressureLay =14	Error estimate for H2OMMRStd (gm/kg dry air)
H2OMMRLevStd	H2OPressureLev =15	Level water Vapor Mass Mixing Ratio (gm/kg dry air)
H2OMMRLevStd_QC	H2OPressureLev =15	Quality flag array (0,1,2)
H2OMMRLevStdErr	H2OPressureLev =15	Error estimate for H2OMMRLevStd (gm/kg dry air)

Field Name	Dimension per FOV	Description
H2OMMRSurf	1	Water Vapor Mass Mixing Ratio at the surface (gm/kg dry air)
H2OMMRSurf_QC	1	Quality flag (0,1,2)
H2OMMRSurfErr	1	Error estimate for H2OMMRSurf
num_H2O_Func	1	Number of valid entries in each dimension of H2O_ave_kern.
H2O_verticality	H2OFunc=11	Sum of the rows of H2O_ave_kern.
H2O_dof	1	Measure of the amount of information in H2O retrieval (degrees of freedom).
H2O_ave_kern	H2OFunc *H2OFunc =11x11	Averaging kernel for water vapor retrieval, located in the support product
Water_Resid_Ratio	1	Internal retrieval quality indicator; residuals of moisture channels compared to predicted uncertainty, located in the support product (unitless)

Support Product

Field Name	Dimension per FOV	Description
H2OCDSup	XtraPressureLay =100	Layer column water vapor (molecules/cm^2)
H2OCDSup_QC	XtraPressureLay =100	Quality flag array (0,1,2)
H2OCDSupErr	XtraPressureLay =100	Error estimate for H2OCDSup (molecules/cm^2)
H2OMMRLevSup	XtraPressureLay =100	Level water Vapor Mass Mixing Ratio (gm/kg dry air)
H2OMMRLevSup_QC	XtraPressureLay =100	Quality flag array (0,1,2)
H2OMMRLevSupErr	XtraPressureLay =100	Error estimate for H2OMMRLevSup (gm/kg dry air)
H2O_eff_press	H2OFunc=11	Effective pressure for the center of each H2O trapezoid (hPa)
H2O_VMR_eff	H2OFunc=11	Effective H2O volume mixing ratio for each trapezoid (vmr) (unitless)

Field Name	Dimension per FOV	Description
H2O_VMR_eff_QC	H2OFunc=11	Quality flag array (0,1,2)
H2O_VMR_eff_err	H2OFunc=11	Error estimate for H2O_VMR_eff (unitless)
H2O_ave_kern	H2OFunc *H2OFunc =11x11	Averaging kernel for water vapor retrieval (unitless)

15.1 Description

The **level** atmospheric precipitable water vapor profile (**H2OMMRLevStd**) is the retrieved mean mass mixing ratio at the pressure level upon which it is reported; the **layer** atmospheric precipitable water vapor profile (**H2OMMRStd**) is the retrieved mean mass mixing ratio between two **pressH2O** levels and is reported on the lower altitude bounding pressure level bounding the layer. Standard pressure levels are arranged in order of decreasing pressure. The pressure levels on which moisture products are reported, **pressH2O**, are the same as the first 15 levels of the 28 available (i.e. for **PressStd** ≥ 50mb). The **H2OMMRStd** quoted on the lowest altitude pressure level above the surface (index = **nSurfStd**, which may be 1, 2, …, 15) is the mean mass mixing ratio in the layer bounded by the next higher level and the surface, i.e. the pressure of the lower boundary of that layer is actually **PSurfStd**.

totH2OStd is the total column moisture burden from top of atmosphere (TOA) to the surface. It is impossible for a user to integrate **H2OMMRStd** to compare the result to **totH2OStd**. The standard product moisture profile does not have sufficient vertical resolution, and the intrusion of topography into the final layer over land further complicates the calculation.

H2O_verticality is an 11 point vector computed by summing the rows of the 11x11 H_2O averaging kernel, **H2O_avg_kern**, stored in the AIRS Level 2 Support Product. The associated 11 point pressure array is provided in **H2O_eff_press**. The peak value of **H2O_verticality** indicates the vertical location of the maximum sensitivity of the H_2O product and the width of this peaked function qualitatively describes the vertical resolution of the retrieval. The magnitudes of **H2O_verticality** are a rough measure of the fraction of the retrieval determined from the data as opposed to the first guess. A value near unity indicates the retrieval is highly determined by the radiance measurements and thus has high information content. A smaller value indicates the retrieval contains a large fraction of the first guess. **H2O_dof** is the number of degrees of freedom (a measure of the amount of information in the retrieval), and is the trace of **H2O_avg_kern**.

NOTE: **num_H2O_Func** provides the number of valid entries in each dimension of **H2O_ave_kern**. Topography limits the number of valid H_2O averaging kernel trapezoids.

NOTE: the problem with associating the verticality with a total column averaging kernel is that it neglects the fact that the retrieval can only move as superpositions of the trapezoids. Convolution using the verticality alone will not account for the possibility that the “independent H_2O profile” contains structure that the trapezoids can or cannot resolve.

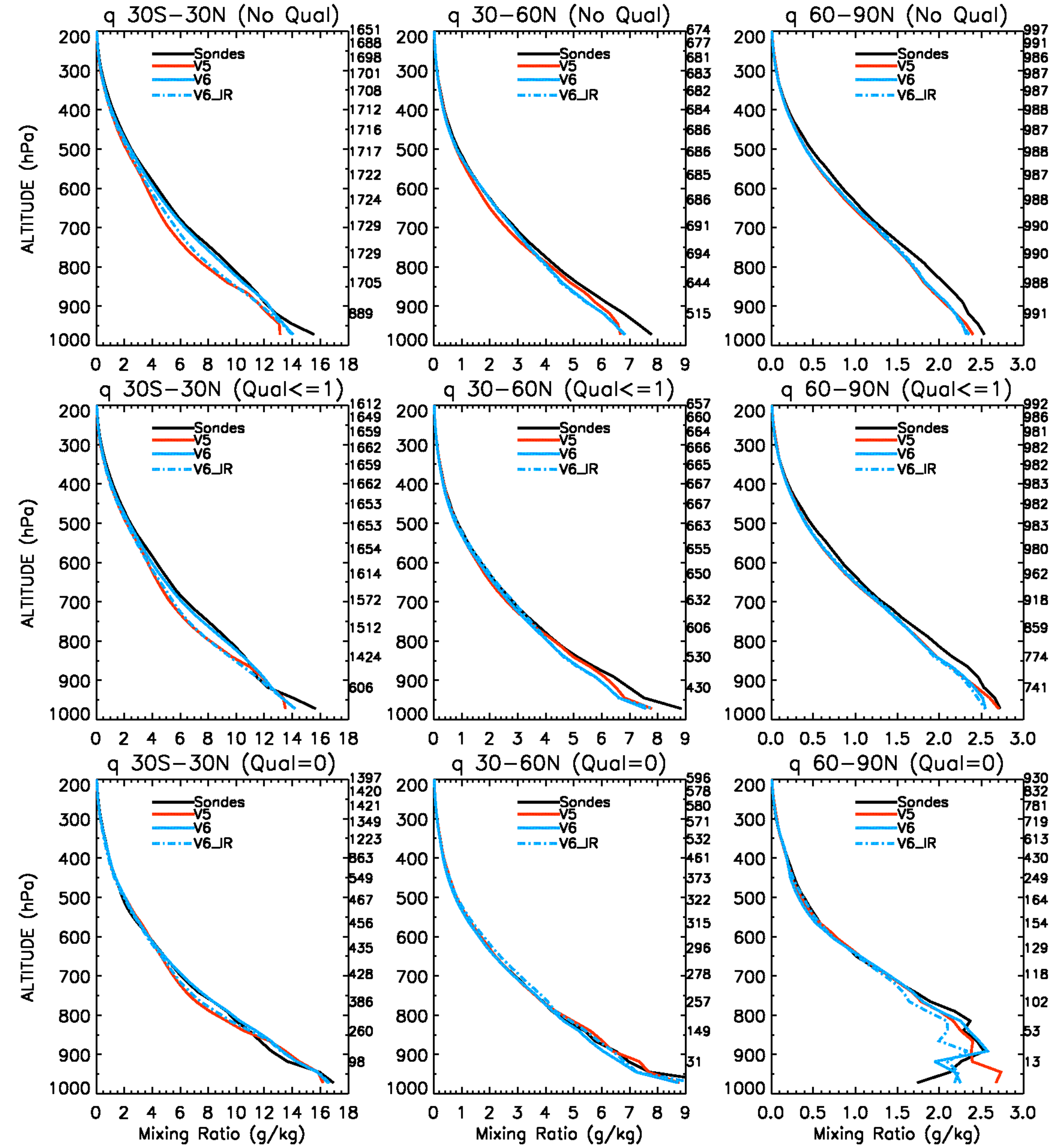

Figure 6: Comparison of AIRS Level 2 specific humidity vertical profiles to collocated dedicated sondes (2002 through 2007).

Columns (Left to Right): 30S→30N; 30N→60N; 60N→90N

Rows (Top to Bottom): No QC; Qual ≤ 1; Qual = 0 (i.e., "best")

Right hand vertical scale is number of samples as a function of altitude

Fraction of All Cases Accepted (%)	1 km Layer Mean Precipitable Water RMS Differences from ECMWF (%)	1 km Layer Mean Bias differences from ECMWF (K)

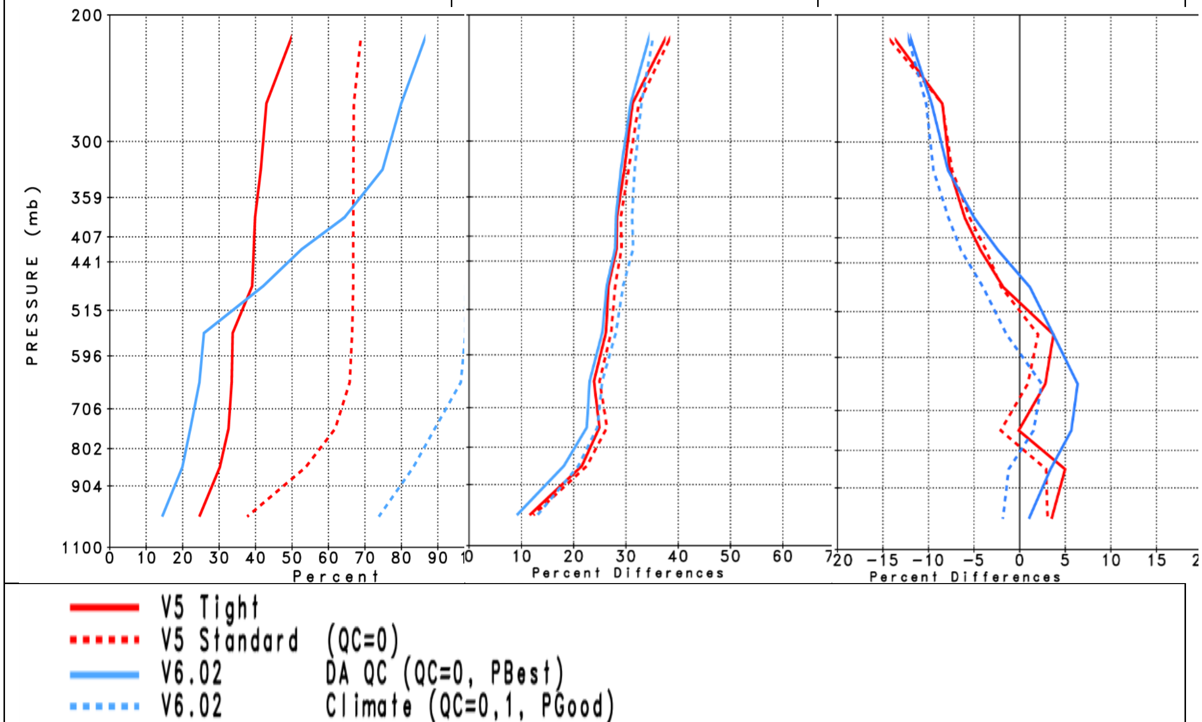

Figure 7: Global water vapor statistics of AIRS retrievals compared to collocated ECMWF for seven study days.

Left panel shows % of QC'd retrievals accepted as a function of altitude; Central panel shows the % RMS difference of 1 km mean precipitable water wrt ECMWF; Right panel shows the % bias of 1 km mean precipitable water wrt ECMWF Study Days: 20020906, 20030125, 20040929, 20050805, 20070224, 20070810, 20100530

15.2 Type of Product

V6 provides standard moisture product profiles as layer quantities and level quantities. See

V6_L2_Levels_Layers_Trapezoids.pdf
AIRS_Layers_to_Levels_Theoretical_Basis_Document.pdf

for a full discussion of level and layer quantities.

15.3 Quality Indicators

The user is encouraged to read the QC and error estimation document:

V6_L2_Quality_Control_and_Error_Estimation.pdf

The quality flags for profile values (**H2OMMRStd_QC** and **H2OMMRLevStd_QC**) should be used as filters for inclusion/exclusion of moisture profiles. These profile QC arrays are set according to **PBest** and **PGood**, with the exception that **H2OMMRLevStd_QC** may differ if the algorithm that derived the level quantity from the layer quantity encountered difficulty. The safest path is to use the two moisture QC arrays. **TOTH2OStd_QC** and **H2OMMRSurf_QC** depend on the entire water profile being of acceptable quality, since a large fraction of the water is near the surface. This represents a change and simplification from the V5 quality control and is now more consistent among profile quantities.

15.4 Validation

A Validation Report for V6 data is currently under preparation and will be published after the V6 data products become publicly available. A V5 Validation Report, summarizing relevant publications, is also being prepared. Early V6 validation results are partially summarized in

V6_L2 Performance_and_Test_Report.pdf

15.5 Caveats

This section will be updated over time as V6 data products are analyzed and validated.

There is no retrieval of water vapor for altitudes at or above the 100 hPa pressure level. The profile of water vapor at 100 hPa and higher altitudes is set equal to the first guess. The quality of AIRS+AMSU (**AIRX2RET**) and AIRS_AMSU+HSB (**AIRH2RET**) and AIRS-Only (**AIRS2RET**) water vapor retrievals begins to degrade for altitudes above the 300 hPa pressure level. AIRS is insensitive to water vapor at mixing ratios of less than 15-20 ppm. This is extensively documented against in situ data by Gettelman et al (2004) and against MLS in Read et al (2007) and Fetzer et al (2008).

We have found a spurious ~7% negative (day-night) difference in global mean total precipitable water in Version 6. The bias is primarily due to low daytime values of total precipitable water vapor in regions with large amounts of mid- to high-level cloud cover. The source is felt to be sunlight reflected from clouds contaminating shortwave channels used by the retrieval algorithm.

Users can avoid this daytime dry bias by using total column water vapor data for which QC=0.

There is no dry bias in nighttime total column water vapor data, so users may continue to use these data if QC=0 or 1.

One of the new features in V6 is that parameters that have previously been provided as layer averages are now also provided at pressure levels. This is essentially done by interpolation with smoothing kernels. This mathematical transformation leads to occasional strange results for water vapor profiles with inversions, typically near the surface. Be sure to filter the level profile by means of **H2OMMRLevStd_QC**.

15.6 Suggestions for Researchers

This section will be updated over time as V6 data products are analyzed and validated.

Researchers must use the values of **PBest** and **PGood** to identify the portion of the moisture profile which is suitable for assimilation and which is of somewhat lesser quality but is suitable for statistical climate studies.

- **pressH2O** ≤ **PBest** is suitable for assimilation
- **pressH2O** ≤ **Good** is suitable for statistical climate studies
- **pressH2O** > **Good** must be discarded

These pressure values are reflected in the level-by-level quality flags for the water vapor variables. The levels and/or layers whose *_QC values equal 0 are suitable for assimilation, whereas those whose *_QC values equal 1 are suitable for statistical climate studies. Do not use levels/layers whose *_QC values equal 2.

We recommend that researchers also employ the estimated error, **H2OMMRStdErr**, as an additional filter to excise those profiles in which the estimated error is negative or greater than 50% of **H2OMMRStd**.

15.7 Recommended Papers

This section will be updated over time as research with V6 data products are published.

Behrangi, Ali, Sun Wong, Kaniska Mallick, and Joshua B. Fisher (2014), "On the net surface water exchange rate estimated from remote-sensing observation and reanalysis." International Journal of Remote Sensing 35, no. 6: 2170-2185.

Behrangi, A., E. J. Fetzer, and S. L. Granger (2016), Early detection of drought onset using near surface temperature and humidity observed from space, Int.J.Remote Sens., 37(16), 3911-3923. https://dx.doi.org/10.1080/01431161.2016.1204478

Bloch, Magdalena, and Grzegorz Karasiński. "Water vapour mixing ratio profiles over Hornsund, Arctic. Intercomparison of lidar and AIRS results." Acta Geophysica 62, no. 2 (2014): 290-301.

Boisvert, L. N., J. N. Lee, J. T. M. Lenaerts, B. Noël, M. R. van den Broeke, and A. W. Nolin (2016), Using remotely sensed data from AIRS to estimate the vapor flux on the Greenland ice sheet: Comparisons with observations and a regional climate model, J. Geophys. Res. Atmos., 122, doi:10.1002/2016JD025674.

Buck, A. L. (1981), New equations for computing vapor pressure and enhancement factor, J. Appl. Meteorol., 20, 1527-1532.

Chung, E.-S., B. J. Soden, X. Huang, L. Shi, and V. O. John (2016), An assessment of the consistency between satellite measurements of upper tropospheric water vapor, J. Geophys. Res. Atmos., 121, doi:10.1002/2015JD024496

Divakarla, M., C. D. Barnet, M. D. Goldberg, L. M. McMillin, E. Maddy, W. Wolf and L. Zhow (2006), Validation of AIRS temperature and water vapor retrievals with matched radiosonde measurements and forecasts, J. Geophys. Res., 111, D09S15, doi:10.1029/2005JD006116

Du, J., F. Cooper, and S. Fueglistaler (2012), Statistical analysis of global variations of atmospheric relative humidity as observed by AIRS, J. Geophys. Res., 117, D12315, doi:10.1029/2012JD017550

Dwivedi, S., Narayanan, M. S., Venkat Ratnam, M., and Narayana Rao, D.: Characteristics of monsoon inversions over the Arabian Sea observed by satellite sounder and reanalysis data sets, Atmos. Chem. Phys., 16, 4497-4509, doi:10.5194/acp-16-4497-2016, 2016

Fetzer E. J., B. H. Lambrigtsen, A. Eldering, H. H. Aumann, M. T. Chahine (2006), Biases in total precipitable water vapor climatologies from Atmospheric Infrared Sounder and Advanced Microwave Scanning Radiometer, J. Geophys. Res., 111, D09S16, doi:10.1029/2005JD006598.

Fetzer, E. J., W. G. Read, D. Waliser, B. H. Kahn, B. Tian, H. Vömel, F. W. Irion, H. Su, A. Eldering, M. de la Torre Juarez, J. Jiang and V. Dang (2008), Comparison of upper tropospheric water vapor observations from the Microwave Limb Sounder and Atmospheric Infrared Sounder, J. Geophys. Res., 113, D22110, doi:10.1029/2008JD010000.

Froidevaux, L, N. J., Livesey, W. G. Read, Y. B. Jiang, C C. Jimenez, M. J. Filipiak, M. J. Schwartz, M. L. Santee, H. C. Pumphrey, J. H. Jiang, D. L. Wu, G. L. Manney, B. J. Drouin, J. W. Waters, E. J. Fetzer, P. F. Bernath, C. D. Boone, K. A. Walker, K. W. Jucks, G. C. Toon, J. J. Margitan, B. Sen, C. R. Webster, L. E. Christensen, J. W. Elkins, E. Atlas, R. A. Lueb, and R. Hendershot (2006), Early validation analyses of atmospheric profiles from EOS MLS on the Aura satellite, IEEE Transactions Geosciences and Remote Sensing, 44(5), 1106-1121.

Fu X., B. Wang, L. Tao (2006), Satellite data reveal the 3-D moisture structure of Tropical Intraseasonal Oscillation and its coupling with underlying ocean, Geophys. Res. Lett., 33, L03705, doi:10.1029/2005GL025074.

Gettelman,A., Weinstock,E. M., Fetzer,E. J., Irion,F. W., Eldering,A., Richard,E. C., Rosenlof,K. H., Thompson,T. L., Pittman,J. V., Webster,C. R., Herman,R. L. (2004), Validation of Aqua satellite data in the upper troposphere and lower stratosphere with in situ aircraft instruments, Geophys. Res. Lett., 31, L22107, doi:10.1029/2004GL020730.

Gettelman A., V. P. Walden, L. M. Miloshevich, W. L. Roth, B. Halter (2006), Relative humidity over Antarctica from radiosondes, satellites, and a general circulation model, J. Geophys. Res., 111, D09S13, doi:10.1029/2005JD006636.

Gettleman, A., E.J. Fetzer, A. Eldering, W.F. Irion (2006), “The Global Distribution of Supersaturation in the Upper Troposphere from the Atmospheric Infrared Sounder”, J. Climate, 19, 6089-6103. DOI: 10.1175/JCLI3955.1

Gettleman, A., W.D. Collins, E.J. Fetzer, A. Eldering, W.F. Irion, P.B. Duffy, G. Bala (2006), Climatology of Upper-Tropospheric Relative Humidity from the Atmospheric Infrared Sounder and Implications for Climate, J. Climate, 19, 6104-6121. DOI: 10.1175/JCLI3956.1

Guan, B., D. E. Waliser, F. M. Ralph, E. J. Fetzer, and P. J. Neiman (2016), Hydrometeorological characteristics of rain-on-snow events associated with atmospheric rivers, Geophys. Res. Lett., 43, 2964–2973, doi:10.1002/2016GL067978.

Hagan D. E., C. R. Webster, C. B. Farmer, R. D. May, R. L. Herman, E. M. Weinstock, L. E. Christensen, L. R. Lait, P. A. Newman (2004), Validating AIRS upper atmosphere water vapor retrievals using aircraft and balloon in situ measurements, Geophys. Res. Lett., 31, L21103, doi:10.1029/2004GL020302.

Hearty, T. J., A. Savtchenko, B. Tian, E. Fetzer, Y. L. Yung, M. Theobald, B. Vollmer, E. Fishbein, and Y.-I. Won (2014), Estimating sampling biases and measurement uncertainties of AIRS/AMSU-A temperature and water vapor observations using MERRA reanalysis, J. Geophys. Res. Atmos., 119, 2725–2741, doi:10.1002/2013JD021205.

Kalmus, P., S. Wong, and J. Teixeira (2015), The Pacific Subtropical Cloud Transition: A MAGIC Assessment of AIRS and ECMWF Thermodynamic Structure, IEEE Geoscience and Remote Sensing Letters, Article in Press, doi: http://dx.doi.org/10.1109/LGRS.2015.2413771.

Livingston, J., E.J. Fetzer et al. (2007), Comparison of water vapor measurements by airborne Sun photometer and near-coincident in situ and satellite sensors during INTEX/ITCT 2004, J. Geophys. Res., 112, D12S16, doi:10.1029/2006JD007733.

Miloshevich L. M., H. Vömel, D. N. Whiteman, B. M. Lesht, F. J. Schmidlin, F. Russo (2006), Absolute accuracy of water vapor measurements from six operational radiosonde types launched during AWEX-G and implications for AIRS validation, J. Geophys. Res., 111, D09S10, doi:10.1029/2005JD006083.

Moradizadeh, M., M. Momeni, and M. R. Saradjian (2014), Estimation and validation of atmospheric water vapor content using a MODIS NIR band ratio technique based on AIRS water vapor products, Arabian Journal of Geosciences, 7(5), 1891-1897, doi:http://dx.doi.org/10.1007/s12517-013-0828-2.

Murphy, D. M. and T. Koop (2005), Review of the vapour pressures of ice and supercooled water for atmospheric applications, Quart. J. Royal Met. Soc, 608 Part B, 1539-1565.

Milstein, A. B., and W. J. Blackwell (2016), Neural network temperature and moisture retrieval algorithm validation for AIRS/AMSU and CrIS/ATMS, J. Geophys. Res. Atmos., 121, 1414–1430, doi:10.1002/2015JD024008.

Pierce D. W., T. P. Barnett, E. J. Fetzer, P. J. Gleckler (2006), Three-dimensional tropospheric water vapor in coupled climate models compared with observations from the AIRS satellite system, Geophys. Res. Lett., 33, L21701, doi:10.1029/2006GL027060.

Pressel, Kyle G., William D. Collins, 2012: First-Order Structure Function Analysis of Statistical Scale Invariance in the AIRS-Observed Water Vapor Field. J. Climate, 25, 5538â€“5555. doi: http://dx.doi.org/10.1175/JCLI-D-11-00374.1

Qin, J., K. Yang, T. Koike, H. Lu, Y. Ma, and X. Xu (2012), Evaluation of AIRS Precipitable Water Vapor against Ground-based GPS Measurements over the Tibetan Plateau and Its Surroundings, Journal of the Meteorological Society of Japan, 90C, 87-98, doi:http://dx.doi.org/10.2151/jmsj.2012-C06.

Read, W.G., A. Lambert, J. Backmeister, R.E. Cofield, L.E. Christensen, D.T. Cuddy, W.H. Daffer, B.J. Drouin, E. Fetzer, L. Froidevaux, R. Fuller, R. Herman, R.F. Jarnot, J.H. Jiang, Y.B. Jiang, K. Kelly, B.W. Knosp, H.C. Pumphrey, K.H. Rosenlof, X. Sabounchi, M.L. Santee, M.J. Schwartz, W.V. Snyder, P.C. Stek, H. Su, L.L. Takacs, R.P. Thurstans, H. Vomel, P.A. Wagner, J.W. Waters, C.R. Webster, E.M. Weinstock, and D.L. Wu, "Aura Microwave Limb Sounder Upper Tropospheric and Lower Stratospheric H2O and RHi Validation," J. Geophys. Res., in review (preprint available at http://mls.jpl.nasa.gov/publications.php)

Ricaud, P., F. Carminati, Y. Courcoux, A. Pellegrini, J.-L. Attié, L. El Amraoui, R. Abida, C. Genthon, T. August and J. Warner (2014). Statistical analyses and correlation between tropospheric temperature and humidity at Dome C, Antarctica . Antarctic Science, 26, pp 290-308. doi:10.1017/S0954102013000564.

Roman, J., R. Knuteson, T. August, T. Hultberg, S. Ackerman, and H. Revercomb (2016), A global assessment of NASA AIRS v6 and EUMETSAT IASI v6 precipitable water vapor using ground-based GPS SuomiNet stations, J. Geophys. Res. Atmos., 121, 8925–8948, doi:10.1002/2016JD024806.

Ruzmaikin, Alexander, Hartmut H. Aumann, Evan M. Manning, 2014: Relative Humidity in the Troposphere with AIRS. J. Atmos. Sci., 71, 2516–2533. doi: http://dx.doi.org/10.1175/JAS-D-13-0363.1

Tobin D. C., H. E. Revercomb, R. O. Knuteson, B. M. Lesht, L. L. Strow, S. E. Hannon, W. F. Feltz, L. A. Moy, E. J. Fetzer, T. S. Cress (2006), Atmospheric Radiation Measurement site atmospheric state best estimates for Atmospheric Infrared Sounder temperature and water vapor retrieval validation, J. Geophys. Res., 111, D09S14, doi:10.1029/2005JD006103.

Wong, Sun, Eric J. Fetzer, Brian H. Kahn, Baijun Tian, Bjorn H. Lambrigtsen, Hengchun Ye, 2011: Closing the Global Water Vapor Budget with AIRS Water Vapor, MERRA Reanalysis, TRMM and GPCP Precipitation, and GSSTF Surface Evaporation. J. Climate, 24, 6307â€“6321. doi: http://dx.doi.org/10.1175/2011JCLI4154.1

Wong, Sun, Eric J. Fetzer, Mathias Schreier, Gerald Manipon, Evan F. Fishbein, Brian H. Kahn, Qing Yue, and Fredrick W. Irion. "Cloud‐induced uncertainties in AIRS and ECMWF temperature and specific humidity." Journal of Geophysical Research: Atmospheres (2015).

Ye, H., E. J. Fetzer, S. Wong, A. Behrangi, E. T. Olsen, J. Cohen, B. H. Lambrigtsen, and L. Chen (2014), Impact of increased water vapor on precipitation efficiency over northern Eurasia, Geophys. Res. Lett., 41, 2941–2947, doi:10.1002/2014GL059830.

Zhang, Y., D. Wang, P. Zhai, and G. Gu (2012), Applicability of AIRS Monthly Mean Atmospheric Water Vapor Profiles over the Tibetan Plateau Region, J. Atmos. Ocean. Technol., 29(11), 1617-1628, http://dx.doi.org/10.1175/JTECH-D-11-00207.1

15.8 Recommended Supplemental User Documentation

V6_Data_Release_User_Guide.pdf
V6_Data_Disclaimer.pdf
V6_L2_Performance_and_Test_Report.pdf
V6_L2_Quality_Control_and_Error_Estimation.pdf
V6_Released_Processing_File_Description.pdf
V6_L2_Standard_Pressure_Levels.pdf
V6_L2_Support_Pressure_Levels.pdf
V6_L2_Levels_Layers_Trapezoids.pdf
V6_Retrieval_Channel_Sets.pdf
V6_Retrieval_Flow.pdf

16 Level 2 Physical Retrieval Relative Humidity Derived from Temperature and Water Vapor

Field Name	Dimension per FOV	Description
RelHum	H2OPressureLev =15	Relative humidity over equilibrium phase (%)
RelHum_QC	H2OPressureLev =15	Quality flag array (0,1,2)
RelHumSurf	1	Relative humidity at the surface over equilibrium phase (%)
RelHumSurf_QC	1	Quality flag (0,1,2)
RelHum_liquid	H2OPressureLev =15	Relative humidity over liquid phase (%)
RelHum_liquid_QC	H2OPressureLev =15	Quality flag array (0,1,2)
RelHumSurf_liquid	1	Relative humidity at the surface over liquid phase (%)
RelHumSurf_liquid_QC	1	Quality flag (0,1,2)

16.1 Description

RelHum takes into account the possibility of a phase change from liquid to ice whereas **RelHumid_liquid** does not. The pressure levels on these products are reported, **pressH2O**, are the same as the first 15 levels of the 28 available (i.e. for **PressStd** ≥ 50mb). **RelHumSurf** is the relative humidity at the surface pressure, **PSurfStd**.

The relative humidity quantities are calculated as ratios of the retrieved specific humidity mixing ratios from section 15 and the temperature-dependent saturation mixing ratios in section 13.

16.2 Type of Product

The Level 2 Standard Product relative humidity products are all level quantities

16.3 Quality Indicators

The user is encouraged to read the QC and error estimation document:

V6_L2_Quality_Control_and_Error_Estimation.pdf

The QC of the relative humidity profiles is set by the QC of temperature/specific humidity profiles, and the QC of the relative humidity at the surface is set by the QC of the surface air parameters.

16.4 Validation

A Validation Report for V6 data is currently under preparation and will be published after the V6 data products become publicly available. A V5 Validation Report, summarizing relevant publications, is also being prepared. Early V6 validation results are partially summarized in

V6_L2 Performance_and_Test_Report.pdf

16.5 Caveats

This section will be updated over time as V6 data products are analyzed and validated.

There is no retrieval of water vapor for altitudes at or above the 100 hPa pressure level. The profile of water vapor at 100 hPa and higher altitudes is set equal to the first guess. The quality of AIRS water vapor retrievals begins to degrade for altitudes above the 300 hPa pressure level. AIRS is insensitive to water vapor at mixing ratios of less then 15-20 ppm.

16.6 Suggestions for Researchers

This section will be updated over time as V6 data products are analyzed and validated.

16.7 Recommended Papers

This section will be updated over time as research with V6 data products are published.

16.8 Recommended Supplemental User Documentation

V6_Data_Release_User_Guide.pdf
V6_Data_Disclaimer.pdf
V6_L2_Performance_and_Test_Report.pdf
V6_L2_Quality_Control_and_Error_Estimation.pdf
V6_Released_Processing_File_Description.pdf
V6_L2_Standard_Pressure_Levels.pdf
V6_L2_Support_Pressure_Levels.pdf
V6_L2_Levels_Layers_Trapezoids.pdf
V6_Retrieval_Channel_Sets.pdf
V6_Retrieval_Flow.pdf

17 Level 2 Physical Retrieval Geopotential Height Derived from Temperature and Water Vapor

Field Name	Dimension per FOV	Description
GP_Tropopause	1	Geopotential height at tropopause (m above mean sea level)
GP_Tropopause_QC	1	Quality flag (0,1,2)
GP_Height	StdPressureLev =28	Geopotential Heights at StdPressureLev (m above mean sea level)
GP_Height_QC	StdPressureLev =28	Quality flag array (0,1,2)
GP_Surface	1	Geopotential Height of surface (m above mean sea level)
GP_Surface_QC	1	Quality flag (0,1,2)

17.1 Description

AIRS profiles and tropopause height are generally provided on a pressure grid. Geopotential heights provide the information users need to translate between this pressure grid and physical altitude.

17.2 Type of Product

GP_Height and **GP_Height_QC** are level products.

17.3 Quality Indicators

The user is encouraged to read the QC and error estimation document:

V6_L2_Quality_Control_and_Error_Estimation.pdf

17.4 Validation

A Validation Report for V6 data is currently under preparation and will be published after the V6 data products become publicly available. A V5 Validation Report, summarizing relevant publications, is also being prepared. Early V6 validation results are partially summarized in

V6_L2 Performance_and_Test_Report.pdf

17.5 Caveats

This section will be updated over time as V6 data products are analyzed and validated.

Geopotential heights are derived by integrating up through the atmosphere from the surface therefore the quality at all levels of the atmosphere is only good when the quality of both temperature and water vapor is good near the surface.

18 Pressure at the Top of the PBL

18.1 Description

A new provisional product, **bndry_lyr_top**, the pressure at the top of the planetary boundary layer and its associated quality control are reported in the Level 2 Support Product at the resolution of the AMSU FOV, since the vertical positioning of thermodynamic profile gradients are used to locate the top of the PBL. This height is reported in units of pressure (hPa). The boundary layer top height is the pressure of the level with the largest gradient of a relative humidity (relative to liquid phase of water) layer profile calculated on the support pressure layer grid. As a result, the boundary layer top height may derive from a strong gradient in either temperature or water vapor mixing ratio. This product is considered a derived rather than a retrieved parameter, and so no error estimate is provided. See Martins et al (2010).

18.2 Type of Product

bndry_lyr_top is a level product.

18.3 Quality Indicators

The user is encouraged to read the QC and error estimation document:

V6_L2_Quality_Control_and_Error_Estimation.pdf

bndry_lyr_top_QC is set to 0 unless:

1. If **SurfClass** ≠ 2 (i.e., not nonfrozen ocean) then **bndry_lyr_top_QC** = 2
2. If a noncontiguous layer has a gradient over 97% of the value of the gradient for the chosen layer then **bndry_lyr_top_QC** = 1
3. If the relative humidity input to the calculation is < 0 or > 3 then **bndry_lyr_top_QC** = 1.
4. **bndry_lyr_top_QC** is set never to be lower (better) than **TSurfAir_QC**.
5. If RelHumSurf > 100% then **bndry_lyr_top_QC** = 2.

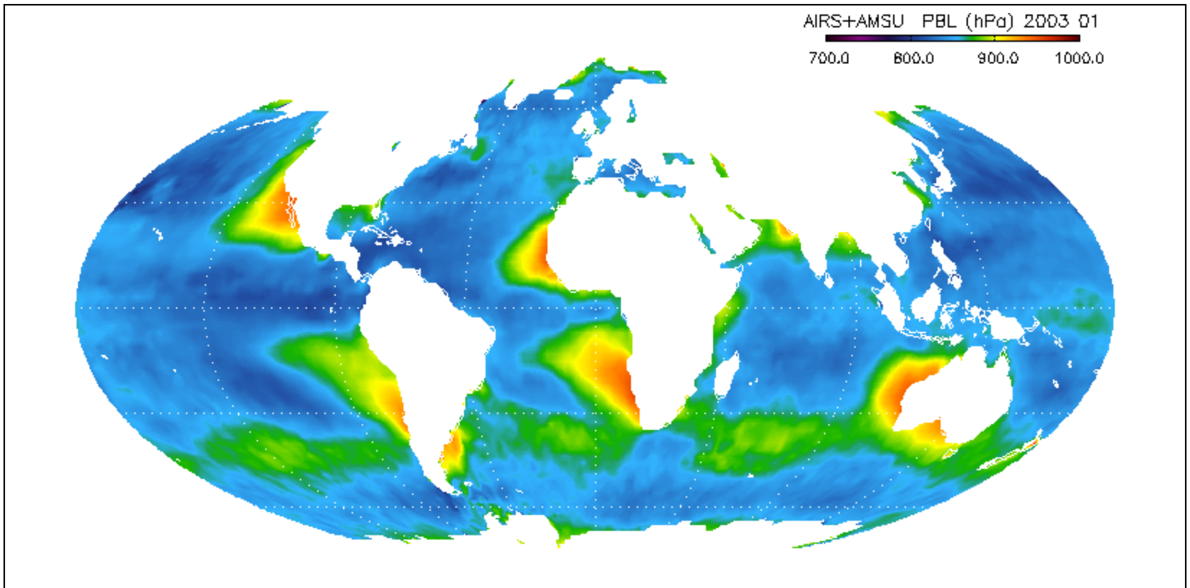

Figure 8: AIRS V6 monthly average PBL height (hPa) product (bndry_lyr_top) over ocean for January 2003 (QC = 0 or 1).
Note that the PBL is shallower in regions dominated by stratocumulus clouds and in the southern hemisphere storm track.

18.4 Suggestions for Researchers

This section will be updated over time as V6 data products are analyzed and validated.

18.5 Recommended Papers

This section will be updated over time as research with V6 data products are published.

Kahn, B. H., G. Matheou, Q. Yue, T. Fauchez, E. J. Fetzer, M. Lebsock, J. Martins, M. M. Schreier, K. Suzuki, and J. Teixeira (2017), A satellite and reanalysis view of cloud organization, thermodynamic, and dynamic variability within the subtropical marine boundary layer, Atmos. Chem. Phys. Discuss., doi:10.5194/acp-2017-59

Kalmus, P., S. Wong, and J. Teixeira (2015), The Pacific Subtropical Cloud Transition: A MAGIC Assessment of AIRS and ECMWF Thermodynamic Structure, IEEE Geoscience and Remote Sensing Letters, Article in Press, doi: http://dx.doi.org/10.1109/LGRS.2015.2413771.

Luo, T., Z. Wang, D. M. Zhang, and B. Chen (2016), Marine boundary layer structure as observed by A-train satellites, Atmospheric Chemistry and Physics, 16(9), 5891-5903. https://dx.doi.org/10.5194/acp-16-5891-2016.

Martins, J. P. A., J. Teixeira, P. M. M. Soares, P. M. A. Miranda, B. H. Kahn, V. T. Dang, F. W. Irion, E. J. Fetzer, *and* E. Fishbein (2010), Infrared sounding of the trade-wind boundary layer: AIRS and the RICO experiment, Geophys. Res. Lett., 37, *L24806, doi:*10.1029/2010GL045902

Yue, Qing, Brian H. Kahn, Eric J. Fetzer, and João Teixeira. "Relationship between marine boundary layer clouds and lower tropospheric stability observed by AIRS, CloudSat, and CALIOP." Journal of Geophysical Research: Atmospheres (1984–2012) 116, no. D18 (2011).

Yue, Qing, Brian H. Kahn, Heng Xiao, Mathias M. Schreier, Eric J. Fetzer, João Teixeira, and Kay Sušelj. "Transitions of cloud-topped marine boundary layers characterized by AIRS, MODIS, and a large eddy simulation model." Journal of Geophysical Research: Atmospheres 118, no. 15 (2013): 8598-8611.

18.6 Recommended Supplemental User Documentation

V6_Data_Release_User_Guide.pdf
V6_Data_Disclaimer.pdf
V6_L2_Performance_and_Test_Report.pdf
V6_L2_Quality_Control_and_Error_Estimation.pdf
V6_Released_Processing_File_Description.pdf
V6_L2_Standard_Pressure_Levels.pdf
V6_L2_Support_Pressure_Levels.pdf
V6_Retrieval_Flow.pdf

19 Level 2 Physical Retrieval Cloud Retrievals on 3x3 AIRS Field of View

Field Name	Dimension per FOV	Description
CldFrcTot	1	Total effective cloud fraction over all cloud layers and all 9 spots (0.0 → 1.0) assuming unit cloud top emissivity.
CldFrcTot_QC	1	Quality flag (0,1,2)
CldFrcStd	AIRSTrack *AIRSXTrack *Cloud =3x3x2	Effective cloud fraction (0.0 → 1.0) assuming unit cloud top emissivity (in order of increasing pressure. Only first nCld elements are valid).
CldFrcStd_QC	AIRSTrack *AIRSXTrack *Cloud =3x3x2	Quality flag array (0,1,2)
CldFrcStdErr	AIRSTrack *AIRSXTrack *Cloud =3x3x2	Error estimate for CldFrcStd (0.0 → 1.0)
PCldTop	AIRSTrack *AIRSXTrack *Cloud =3x3x2	Cloud top pressure in each of the 9 AIRS FOVs within the AMSU retrieval FOV. (in order of increasing pressure. Only first nCld elements are valid) (hPa)
PCldTop_QC	AIRSTrack *AIRSXTrack *Cloud =3x3x2	Quality flag array (0,1,2)
PCldTopErr	AIRSTrack *AIRSXTrack *Cloud =3x3x2	Error estimate for PCldTop.
TCldTop	AIRSTrack *AIRSXTrack *Cloud =3x3x2	Cloud top temperature (in order of increasing pressure in each of the 9 AIRS FOVs within the AMSU retrieval FOV. Only first nCld elements are valid) (K)

Field Name	Dimension per FOV	Description
TCldTop_QC	AIRSTrack *AIRSXTrack *Cloud =3x3x2	Quality flag array (0,1,2)
TCldTopErr	AIRSTrack *AIRSXTrack *Cloud =3x3x2	Error estimate for TCldTop in each of the 9 AIRS FOVs within the AMSU retrieval FOV. (K)
nCld	AIRSTrack *AIRSXTrack *Cloud =3x3x2	Number of retrieved cloud layers in each of the 9 AIRS FOVs within the AMSU retrieval FOV (can be 0,1,2)
numCloud	1	Number of cloud layers for the AMSU FOV when clouds are retrieved assuming a common set of cloud top pressures over all 9 AIRS spots. Located in Support Product. DEPRECATED—do not use. The associated coarse (one value per AMSU FOV) TCldTopStd and PCldTopStd located in the Support Product are also DEPRECATED.

19.1 Description

The V6 AIRS Level 2 Standard cloud products are significantly improved over those in V5. **PCldTop**, **TCldTop** and **nCld** are reported for the 3x3 (14 km at nadir) AIRS spots within the (50 km at nadir) AMSU FOV.

NOTE: The effective cloud fraction is given by the product of the fraction of the FOV covered by clouds and the cloud emissivity at 11 μm.

The combined IR/MW algorithm retrieves up to two amounts of clouds at distinct pressure levels, each having its own effective cloud fraction as seen from above for each AIRS FOV. (geospatial extent is ~13 km at nadir). If there are two reported layers, the first is the one at the higher altitude. AIRS radiances at a given frequency are affected by the product of the cloud fraction and the cloud emissivity as well as the geophysical state. We currently solve for the best fit cloud solution across a wide range of frequencies assuming that the cloud emissivity is frequency independent. The cloud retrieval minimizes the radiance residuals given the retrieved geophysical state. (Note: cloud formations occur in cloud clearing and are not necessarily flat. Cloud layers occur in cloud retrieval and are pancakes.)

PCldTop is the retrieved cloud top pressure for each reported cloud height at the AIRS resolution, **PCldTopStd** the retrieved cloud top pressure averaged to the AMSU resolution. Each has an associated error and quality flag at the same resolution. In addition, the cloud top temperature and its associated error and QC flag at each resolution are reported as **TCldTop** and **TCldTopStd** for the same cloud formations. These are interpolated from the AIRS **TAirSup** and **TAirSupErr** fields.

The effective cloud fraction **CldFrcStd** and its error **CldFrcStdErr** are derived from the radiances in the 9 AIRS spots (each of geospatial extent ~14 km at nadir) within the AMSU FOV. The values in both range between 0.0 and 1.0. In the event that two cloud heights are reported, the sum over both layers of **CldFrcStd** does not exceed 1.0. Under some conditions the final nine spot cloud parameter retrieval fails. If the final cloud retrieval fails, then the retrieval is marked Quality = 2 and the **CldFrcStd** array is set to the value of an earlier single FOV cloud retrieval step within the AMSU FOV which is more stable. Under this condition, we report nine sets of cloud parameters that are all identical. This occurs in less than one percent of the retrievals and we do not think these values will be useful.

Please consult the recently-published discussion paper by Kahn et al (2014), “The Atmospheric Infrared Sounder Version 6 Cloud Products” as well as the two papers: Susskind et al (2011), “Improved Temperature Sounding and Quality Control Methodology using AIRS/AMSU Data: The AIRS Science Team Version 5 Retrieval Algorithm”, and Susskind et al (2014), "Improved methodology for surface and atmospheric soundings, error estimates, and quality control procedures: the atmospheric infrared sounder science team version-6 retrieval algorithm."

19.2 Type of Product

The cloud formation products are level quantities, thus that the values are reported at discrete pressure levels.

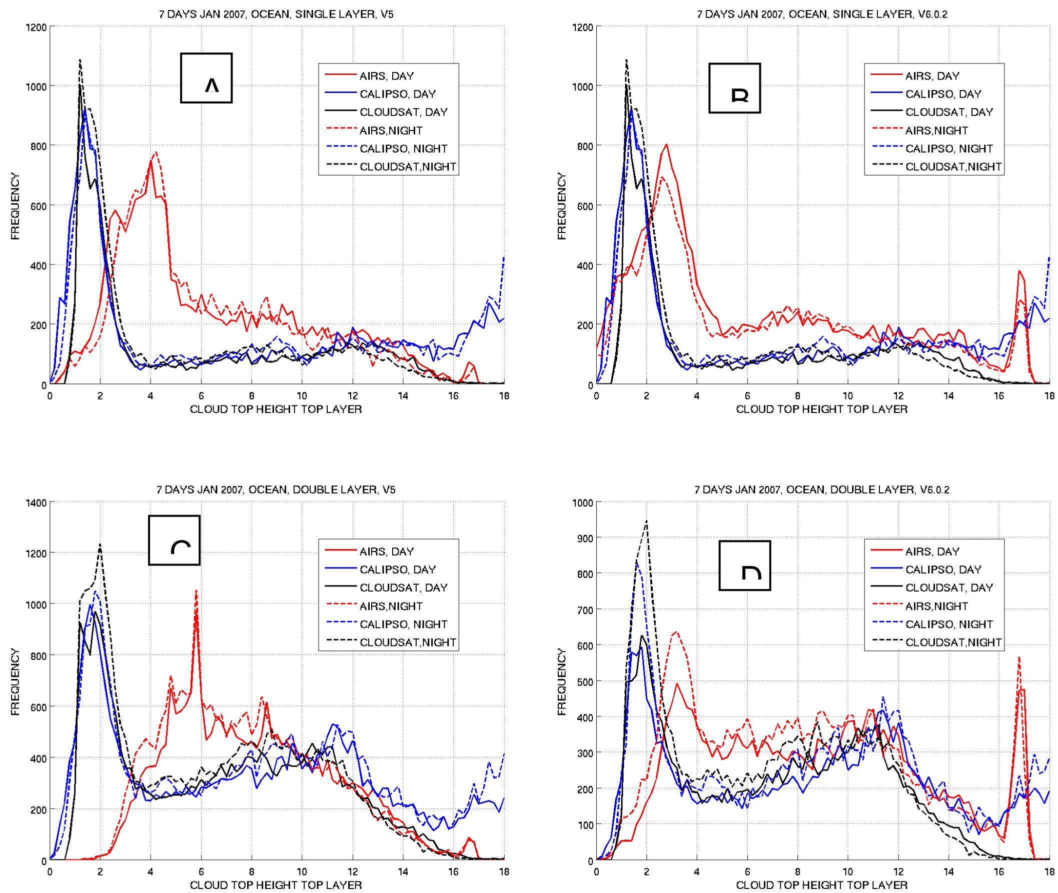

Figure 9: Comparison of AIRS V6 and V5 top cloud layer height with CALIPSO and CloudSat over ocean January 2007

Top Row: single cloud layer FOVs; Bottom Row: double cloud layer FOVs

19.3 Quality Indicators

The user is encouraged to read the QC and error estimation document and the cloud product section of the performance and test report:

V6_L2_Quality_Control_and_Error_Estimation.pdf
V6_L2_Performance _and_Test_Report.pdf

QC for cloud products is set as follows:

- If the final retrieval is accepted, Quality = 0
- If he final retrieval is accepted, but the final retrieved surface temperature differs from the neural net (prior) surface temperature by more than 5 K, the clouds are calculated from the retrieval with the neural net surface substituted, Quality = 1
- If the cloud retrieval does not complete, Quality = 2

19.4 Validation

A Validation Report for V6 data is currently under preparation and will be published after the V6 data products become publicly available. A V5 Validation Report, summarizing relevant publications, is also being prepared. Early V6 validation results are partially summarized in

V6_L2 Performance_and_Test_Report.pdf

19.5 Caveats

This section will be updated over time as V6 data products are analyzed and validated.

The user is cautioned that all reported cloud fraction values are actually "effective cloud fractions" calculated assuming opaque black clouds. If the actual emissivity is less than 1.0 or the cloud is partially transmissive, the actual cloud fraction is correspondingly larger than what we report, but radiatively equivalent.

The tendency for clouds to settle at round numbers has been corrected in V6. We now allow clouds to within 10 hPa of the surface.

It has been shown that the higher quality retrievals for **TAirStd** and **H2OMMRStd** do not correspond to higher quality retrievals of cloud fields [Kahn et al. 2007a], and in fact, may have opposite tendencies. This is not unexpected as a stronger cloud radiative signature is associated with a more accurate cloud temperature, pressure, and amount. Thus, scenes in which it is more difficult to retrieve **TAirStd** and **H2OMMRStd** contain more accurate cloud retrievals and are associated with smaller uncertainties [see Kahn et al. 2007a,b].

The cloud retrievals assume spectral unit emissivity and only two layers are considered in the retrieval. Recent work on the sensitivity of cloud fields to assumptions of $CH4_2$ show that spurious clouds arise from the treatment of $CH4_2$ in the AIRS algorithm [Hearty et al. 2006]. Furthermore, if a cloud top pressure is retrieved above the tropopause it is readjusted to the tropopause level. There are additional caveats, further discussed in Kahn et al. [2007a,b]. Validation efforts and scientific applications may be found in the references. Please refer to these publications for detailed discussion.

19.6 Suggestions for Researchers

This section will be updated over time as V6 data products are analyzed and validated.

Please refer to the publications below for validation and application of AIRS cloud fields in scientific analyses. In *Kahn et al*. [2007a] AIRS cloud top height (derived from cloud top pressure and TAirStd) is compared to Atmospheric Radiation Measurement (ARM) program millimeter-wave cloud radar and micropulse lidar observations of clouds coincident with EOS Aqua, as well as the Microwave Limb Sounder observations of thin tropopause-level cirrus clouds. *Kahn et al.* [2007b] comprehensively compare MODIS and AIRS operational cloud retrievals, including cloud top temperature and effective cloud fraction as a function of cloud and scene type. It is shown that AIRS is better able to capture thin cirrus clouds than the operational MODIS algorithm, although there are other instances in which MODIS may outperform AIRS.

Kahn et al. [2008a] validates the AIRS cloud fields as a function of cloud type as determined by CloudSat and CALIPSO. AIRS agrees somewhat better in these cases than with the ARM measurements, which highlights respective sensitivities to cloud tops between surface- and space-based measurements. In *Kahn et al*. [2008b] we demonstrate the application of AIRS cloud fields in deriving optical and microphysical properties of thin cirrus. The thin cirrus properties in turn are related to AIRS relative humidity fields and demonstrate the power of AIRS to observe multiple fields simultaneously. Lastly, the fast radiative transfer model used to derive cirrus properties from AIRS radiances is discussed in *Yue et al.* [2007]. Comparisons of these products are made with V6 in Kahn et al. (2014), and are used in studies of extratropical cyclones (Naud and Kahn, 2015), Arctic cloud trends (Devasthale et al., 2016), and the Southern Annular Mode (SAM) variations over Antarctica (Lubin et al., 2015).

Many other research efforts are ongoing, with publications in preparation, in peer review, or in press. The researcher is recommended to review these (and other) AIRS-related publications, and to contact any of the authors of these publications to answer further inquiries. Brian Kahn, who has headed the balance of the AIRS cloud validation efforts, can be contacted at **brian.h.kahn@jpl.nasa.gov**.

19.7 Recommended Papers

This section will be updated over time as research with V6 data products are published.

Chang, K.-W., T. S. L'Ecuyer, B. H. Kahn, and V. Natraj (2017), Information content of visible and midinfrared radiances for retrieving tropical ice cloud properties, Journal of Geophysical Research. Atmospheres, 122(9), 4944-4966. http://dx.doi.org/10.1002/2016JD026357

Devasthale, A., J. Sedlar, B. H. Kahn, M. Tjernström, E. J. Fetzer, B. Tian, J. Teixeira, and T. S. Pagano (2016), A decade of spaceborne observations of the Arctic atmosphere: Novel insights from NASA's AIRS instrument, Bull. Amer. Met. Soc., 97, 2163–2176, doi:10.1175/BAMS-D-14-00202.1.

Kahn, B.H., Irion, F.W., Dang, V.T., Manning, E.M., Nasiri, S.L., Naud, C.M., Blaisdell, J.M., Schreier, M.M., Yue, Q., Bowman, K.W. and Fetzer, E.J., (2014), The atmospheric infrared sounder version 6 cloud products. *Atmospheric Chemistry and Physics*, *14*(1), p.399

Aumann, H. H., and A. Ruzmaikin (2013), "Frequency of deep convective clouds in the tropical zone from 10 years of AIRS data." Atmospheric Chemistry and Physics 13, no. 21: 10795-10806.

Hearty, T.J., B.H. Kahn, and E. Fishbein (2006): Layer trends in Earth's cloud cover, Fall Meeting American Geophysical Union, Poster number 5337–A26.

Jin, Hongchun, and Shaima L. Nasiri. "Evaluation of AIRS cloud thermodynamic phase determination with CALIPSO." Journal of Applied Meteorology and Climatology 2013 (2013).

Kahn, B. H., Irion, F. W., Dang, V. T., Manning, E. M., Nasiri, S. L., Naud, C. M., Blaisdell, J. M., Schreier, M. M., Yue, Q., Bowman, K. W., Fetzer, E. J., Hulley, G. C., Liou, K. N., Lubin, D., Ou, S. C., Susskind, J., Takano, Y., Tian, B., and Worden, J. R. (2013): The Atmospheric Infrared Sounder Version 6 cloud products, Atmos. Chem. Phys. Discuss., 13, 14477-14543, doi:10.5194/acpd-13-14477-2013.

Kahn, B. H., Eldering, A., Braverman, A.J., Fetzer, E.J., Jiang, J.H., Fishbein, E., and Wu, D.L. (2007a): Toward the characterization of upper tropospheric clouds using Atmospheric Infrared Sounder and Microwave Limb Sounder observations, J. Geophys. Res., 112, D05202, doi:10.1029/2006JD007336.

Kahn, B. H., E. Fishbein, S. L. Nasiri, A. Eldering, E. J. Fetzer, M. J. Garay, and S.-Y. Lee (2007b), The radiative consistency of Atmospheric Infrared Sounder and Moderate Resolution Imaging Spectroradiometer cloud retrievals, J. Geophys. Res., 112, D09201, doi:10.1029/2006JD007486.

Kahn, B.H., Chahine, M.T., Stephens, G.L, Mace, G.C., Marhcand, R.T., Wang, Z., Barnet, C.D., Eldering, A., Holz, R.E., Kuehn, R.E., Vane, D.G. (2008a), Cloud type comparisons of AIRS, CloudSat and CALIPSO cloud height and amount Atmospheric Chemistry and Physics, 8, 5, 1231-1248

Kahn, B. H., Liang, C. K., Eldering, A., Gettelman, A., Yue, Q., and Liou, K. N., (2008b): Tropical thin cirrus and relative humidity observed by the Atmospheric Infrared Sounder, Atmos. Chem. Phys., 8, 1501-1518, 2008.

Kahn, B. H., F. W. Irion, V. T. Dang, E. M. Manning, S. L. Nasiri, C. M. Naud, J. M. Blaisdell et al. (2014), "The atmospheric infrared sounder version 6 cloud products." *Atmos. Chem. Phys* 14: 399-426.

Lubin, D., B. H. Kahn, M. A. Lazzara, P. Rowe, and V. P. Walden (2015), Variability in AIRS-retrieved cloud amount and thermodynamic phase over west versus east Antarctica influenced by the SAM, Geophys. Res. Lett., 42, doi:10.1002/2014GL062285.

Mace, G. G., R. Marchand, Q. Zhang, and G. Stephens (2007), Global hydrometeor occurrence as observed by CloudSat: Initial observations from summer 2006, Geophys. Res. Lett., 34, L09808, doi:10.1029/2006GL029017

NASA Technical Report GSFC/CR-1999-208643

McCoy, D. T., R. Eastman, D. L. Hartmann, and R. Wood (2017), The change in low cloud cover in a warmed climate inferred from AIRS, MODIS, and ERA-interim, Journal of Climate, 30(10), 3609-3620. https://dx.doi.org/10.1175/JCLI-D-15-0734.1.

Naud, C. M., and B. H. Kahn (2015), Thermodynamic phase and ice cloud properties in northern hemisphere winter extratropical cyclones observed by Aqua AIRS, J. Appl. Meteor. Climatol., 54, 2283–2303, doi:10.1175/JAMC-D-15-0045.1.

Naud, C. M., J. F. Booth, and A. D. Del Genio (2016), The Relationship between Boundary Layer Stability and Cloud Cover in the Post-Cold-Frontal Region, Journal of Climate, 29(22), 8129-8149. http://dx.doi.org/10.1175/jcli-d-15-0700.1

Ou, S. S. C., B. Kahn, K. Liou, Y. Takano, M. M. Schreier, and Q. Yue (2012), Retrieval of Cirrus Cloud Properties From the Atmospheric Infrared Sounder: The k-Coefficient Approach Using Cloud-Cleared Radiances as Input, IEEE Trans.

Geosci. Remote Sens., Article in Press, doi: http://dx.doi.org/10.1109/TGRS.2012.2205261

Protopapadaki, S. E., C. J. Stubenrauch, and A. G. Feofilov (2017), Upper tropospheric cloud systems derived from IR sounders: properties of cirrus anvils in the tropics, Atmospheric Chemistry and Physics, 17(6), 3845-3859. http://dx.doi.org/10.5194/acp-17-3845-2017.

Schreier, M. M., Kahn, B. H., Sušelj, K., Karlsson, J., Ou, S. C., Yue, Q., and Nasiri, S. L.: Atmospheric parameters in a subtropical cloud regime transition derived by AIRS and MODIS: observed statistical variability compared to ERA-Interim, Atmos. Chem. Phys., 14, 3573-3587, doi:10.5194/acp-14-3573-2014, 2014.

M. Schreier & K. Suselj (2016) Analysis of collocated AIRS and MODIS data: a global investigation of correlations between clouds and atmosphere in 2004–2012, International Journal of Remote Sensing, 37:11, 2524-2540, DOI: 10.1080/01431161.2016.1177244

Susskind, J., Blaisdell, J.M., Iredell, L., Keita, F.,Improved Temperature Sounding and Quality Control Methodology using AIRS/AMSU Data: The AIRS Science Team Version 5 Retrieval Algorithm, Geoscience and Remote Sensing, IEEE Transactions, March 2011, Volume 49, Issue 3, pages 883-907

Susskind, Joel, John M. Blaisdell, and Lena Iredell. "Improved methodology for surface and atmospheric soundings, error estimates, and quality control procedures: the atmospheric infrared sounder science team version-6 retrieval algorithm." Journal of Applied Remote Sensing 8, no. 1 (2014): 084994-084994.

Wang, Chenxi, Ping Yang, Steven Platnick, Andrew K. Heidinger, Bryan A. Baum, Thomas Greenwald, Zhibo Zhang, and Robert E. Holz. "Retrieval of Ice Cloud Properties from AIRS and MODIS Observations Based on a Fast High-Spectral-Resolution Radiative Transfer Model." Journal of Applied Meteorology & Climatology 52, no. 3 (2013).

Yue, Q., K.N. Liou, S.C. Ou, B.H. Kahn, P. Yang, and G.G. Mace, (2007), Interpretation of AIRS Data in Thin Cirrus Atmospheres Based on a Fast Radiative Transfer Model. J. Atmos. Sci., 64, 3827_x0013_3842.

Yue, Qing, Brian H. Kahn, Heng Xiao, Mathias M. Schreier, Eric J. Fetzer, João Teixeira, and Kay Sušelj, (2013), "Transitions of cloud-topped marine boundary layers characterized by AIRS, MODIS, and a large eddy simulation model." Journal of Geophysical Research: Atmospheres 118, no. 15: 8598-8611.

Yue, Q., B. H. Kahn, E. J. Fetzer, M. Schreier, S. Wong, X. Chen, and X. Huang (2016), Observation-based longwave cloud radiative kernels derived from the A-train, J. Climate, 29, 2023–2040, doi:10.1175/JCLI-D-15-0257.1

19.8 Recommended Supplemental User Documentation

V6_Data_Release_User_Guide.pdf

V6_Data_Disclaimer.pdf
V6_L2_Performance_and_Test_Report.pdf
V6_L2_Quality_Control_and_Error_Estimation.pdf
V6_Released_Processing_File_Description.pdf
V6_L2_Standard_Pressure_Levels.pdf
V6_L2_Support_Pressure_Levels.pdf
V6_L2_Levels_Layers_Trapezoids.pdf
V6_Retrieval_Channel_Sets.pdf
V6_Retrieval_Flow.pdf

20 Level 2 Physical Retrieval Ozone Retrievals

Standard product

Field Name	Dimension per FOV	Description
totO3Std	1	Retrieved Total Ozone Burden, (DU)
totO3StdErr	1	Error estimate, (DU)
totO3Std_QC	1	Quality flag (0,1,2)
O3VMRStd	StdPressureLay=28	Layer retrieved Ozone Volume Mixing Ratio Profile (vmr), (unitless)
O3VMRStdErr	StdPressureLay=28	Error estimate (vmr), (unitless)
O3VMRStd_QC	StdPressureLay=28	Quality flag array (0,1,2)
O3VMRLevStd	StdPressureLev=28	Level retrieved Ozone Volume Mixing Ratio Profile (vmr), (unitless)
O3VMRLevStdErr	StdPressureLev=28	Error estimate (vmr), (unitless)
O3VMRLevStd_QC	StdPressureLev=28	Quality flag array (0,1,2)
num_O3_Func	1	Number of valid entries in each dimension of O3_ave_kern
O3_verticality	O3Func=9	Sum of rows of O3_ave_kern, (unitless)
O3_dof	1	Degrees of freedom, measure of amount of information in O3 retrieval, (unitless)

Support Product

Field Name	Dimension per FOV	Description
O3CDSup	XtraPressureLay =100	Layer column ozone, (molecules/cm^2)
O3CDSup_QC	XtraPressureLay =100	Quality flag array (0,1,2)
O3CDSupErr	XtraPressureLay =100	Error estimate for O3CDSup, (molecules/cm^2)
O3VMRLevSup	XtraPressureLay =100	Ozone volume mixing ratio (vmr), (unitless)
O3VMRLevSup_QC	XtraPressureLay =100	Quality flag array (0,1,2)
O3VMRLevSupErr	XtraPressureLay =100	Error estimate for O3VMRLevSup
O3_VMR_eff	O3Func=9	Effective O3 volume mixing ratio for each trapezoid (vmr), (unitless)
O3_VMR_eff_err	O3Func=9	Error estimate (vmr), (unitless)
O3_VMR_eff_QC	O3Func=9	Quality flag (0,1,2)
O3VMRSurf	1	Ozone Volume Mixing Ratio at the surface (vmr), (unitless) DO NOT USE FOR RESEARCH. Retrieval has no sensitivity at surface. Value is from the initial guess
O3VMRSurfErr	1	Error estimate (vmr), (unitless)
O3VMRSurf_QC	1	Quality flag (0,1,2)
O3_eff_press	O3Func=9	Ozone effective pressure for the center of each trapezoid
O3_VMR_eff	O3Func=9	Effective ozone volume mixing ratio (vmr) for each trapezoid, (unitless)
O3_VMR_eff_QC	O3Func=9	Quality flag (0,1,2)
O3_VMR_eff_err	O3Func=9	Error estimate for O3_VMR_eff
O3_ave_kern	O3Func *O3Func =9x9	Averaging kernel for ozone retrieval, located in the support product
O3_Resid_Ratio	1	Internal retrieval quality indicator; residuals of O3 channels as compared to predicted uncertainty, located in support product (unitless)

20.1 Description

The AIRS ozone product is a product of the IR stage of the combined IR/MW retrieval. The **level** atmospheric ozone profile (**O3VMRLevStd**) is the retrieved mean volume mixing ratio at the pressure level upon which it is reported. For backward compatibility with V5, we also provide the **layer** atmospheric ozone profile (**O3VMRStd**), the retrieved mean volume mixing ratio (ratio of number of O_3 molecules to the number of molecules of air in a unit volume) between two **pressStd** levels and is reported on the lower altitude bounding pressure level bounding the layer. Standard pressure levels are arranged in order of decreasing pressure.

The ozone first guess is from the UARS climatology. It is provided for each of 17 latitude zones for each month and for the 100 pressure layers in the Level 2 Support Pressure array. The latitude zones are at 10° intervals from 80S to 80N.

Level quantities are calculated from layer quantities by the procedure described in the Algorithm Theoretical Document

AIRS_Layers_to_Levels_Theoretical_Basis_Document.pdf

The derivation of level quantities from layer quantities is essentially done by interpolation with smoothing kernels.

The ozone products are reported on all levels and layers above the surface. The **O3VMRStd** quoted on the lowest altitude pressure level above the surface (index = **nSurfStd**, which may be 1, 2, …, 15) is the mean volume mixing ratio in the layer bounded by the next higher level and the surface, i.e. the layer will be slightly thicker or thinner than the pressure on which it is quoted indicates and the lower bound pressure is actually **PSurfStd**.

totO3Std is the integrated column amount of O_3 from the top of the atmosphere (TOA = 0.005 hPa) to the surface. This quantity is computed by summing the 100 column density values, **O3CDSup,** contained in the AIRS Level 2 Support Products file with the appropriate weighting applied to the bottom layer which contains the surface. Layers below the surface are not included in this sum.

O3_dof provides a measure of the amount of information in the O_3 retrieval. It is computed by summing the diagonal elements of the 9x9 O_3 averaging kernel, **O3_avg_kern**, stored in the AIRS Support Product files.

O3_verticality is a 9 point vector computed by summing the columns of the 9x9 O_3 averaging kernel, **O3_avg_kern**, stored in the AIRS Level 2 Support Product. The associated 9 point pressure array is provided in **O3_eff_press**. The peak value of **O3_verticality** indicates the vertical location of the maximum sensitivity of the O_3 product and the width of this peaked function qualitatively describes the vertical resolution of the retrieval. The magnitudes of **O3_verticality** are a rough measure of the fraction of the retrieval determined from the data as opposed to the first guess. A value near unity indicates the retrieval is highly determined by the radiance measurements and thus has high information content. A smaller value indicates the retrieval contains a large fraction of the first guess. **O3_dof** is the number of degrees of freedom (a measure of the amount of information in the retrieval), and is the trace of **O3_avg_kern**.

NOTE: the problem with associating the verticality with a total column averaging kernel is that it neglects the fact that the retrieval can only move as superpositions of the trapezoids. Convolution using the verticality alone will not account for the possibility that the “independent O_3 profile” contains structure that the trapezoids cannot resolve.

O3CDSup provides the retrieved O_3 column density on 100 pressure levels used internally in the physical retrieval. **O3VMRLevSup** provides a smoothed version of this profile but in units of VMR and on 100 levels.

O3_VMR_eff is contained in the AIRS Level 2 Support Products file and is the retrieved volume mixing ratio (ratio of number of O_3 molecules to the number of molecules of air in a unit volume) for a layer defined by the faces of an O_3 trapezoidal retrieval function. The boundaries of faces of these layers are specified in **O3_trapezoid_layers** in which is an array of 1-based **pressSup** level indices. **O3_eff_press** provides the effective pressure for each trapezoid. There are 9 such trapezoidal layers corresponding to the 9 trapezoidal retrieval functions utilized for O_3.

NOTE: **num_O3_Func** provides the number of valid entries in each dimension of **O3_ave_kern**. Topography limits the number of valid O_3 averaging kernel trapezoids.

See:

V6_L2_Support_Pressure_Levels.pdf
V6_L2_Levels_Layers_Trapezoids.pdf

The ozone first guess is an observationally-based climatology developed for Version 8 TOMS and SBUV [McPeters et al., 2007], which is month-by-month on 10° latitude bins from 80S to 80N. The ozone first guess for V6 is unchanged from that used for V5, and is for the 100 pressure layers in the Level 2 Support Pressure array.

To make a look-up table suited to the AIRS retrieval software, ozone mixing ratios were interpolated by latitude and altitude and converted to slab columns on the AIRS 100-level support grid using the "Partial Column" approximation formula in Ziemke et al. [2001]. Where climatological data did not extend the highest or lowest pressure levels of the AIRS support grid, mixing ratio "endpoints" were assumed to extend to such regions.

A total of 41 channels are used in the retrieval channel and their selection includes the peak of the P-branch in the ozone 10 μm band. The "noise propagation threshold," DB_{max}, discussed in Susskind et al. [2003], has been effectively doubled, resulting in less damping of the final profile.

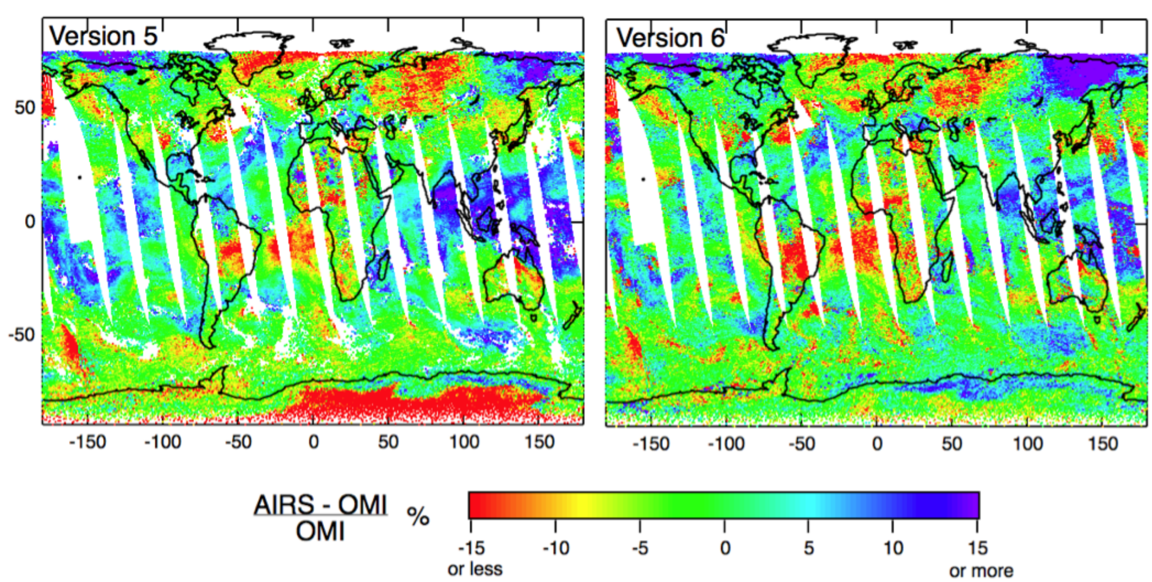

Figure 10: AIRS total column ozone retrievals from V5 (left panel) and V6 (right panel) relative to OMI for 24 February 2007 daytime.

The general pattern is similar in both versions. The large negative bias over the interior of Antarctica in V5 is greatly improved in V6.

20.2 Type of Product

O3VMRLevStd is a **level** quantity and so values represent the concentration at the pressure level upon which they are reported . **O3VMRStd** is a **layer** quantity, i.e. the values are reported on the fixed pressure levels but represent the layer bounded by the level on which they are reported and the next higher level (in altitude).

For more detail, see **V6_L2_Levels_Layers_Trapezoids.pdf** for a full discussion of level and layer quantities.

20.3 Quality Indicators

The user is encouraged to read the QC and error estimation document:

V6_L2_Quality_Control_and_Error_Estimation.pdf

If **PGood** = **PsurfStd**, then all ozone products are marked Quality = 0. Otherwise, all ozone products are marked Quality = 2.

Because the ozone channels are all sensitive to surface emission, we do not discriminate a "good" (Quality = 1) portion of the profile from a "best" (Quality = 0) portion of the profile; the entire profile is either Quality = 0 or Quality = 2.

20.4 Validation

A Validation Report for V6 data is currently under preparation and will be published after the V6 data products become publicly available. A V5 Validation Report, summarizing relevant publications, is also being prepared. Early V6 validation results are partially summarized in

V6_L2 Performance_and_Test_Report.pdf

20.5 Caveats

This section will be updated over time as V6 data products are analyzed and validated.

All **O3*_QC** flag are set to 0 if **Pgood**=**PSurfStd**. We do not distinguish portions of the ozone profile as being of different qualities because all ozone channels sense the surface as well atmospheric ozone and thus are sensitive to the entire profile's quality is compromised if the surface is not well characterized.

Errors in temperature profiles and water vapor mixing ratios will adversely affect the ozone retrieval. Significant biases (0 - 100%) may exist in the region between ~300 hPa and ~80 hPa; such biases currently being evaluated. Ozone mixing ratio data may not be reliable at pressures greater than 300 hPa or if the tropospheric mixing ratio is less 100 ppbv, however results may be qualitatively correct under conditions of high upper tropospheric ozone (such as in a tropopause fold). Mixing ratios and columns should not be considered reliable under conditions of very low skin temperatures (< 240 K).

The error fields, including **O3VMRLevStdErr**, **O3VMRStdErr, O3VMRLevSupErr, O3CDSupErr** and **totO3StdErr**, are fixed as a fraction of the ozone amount and should not be used.

The ozone first guess used to initialize the V5 retrieval is likely too high at pressures below ~0.5 hPa (altitudes above ~55 km) due to an error in extrapolation in its creation. This has a negligible effect on **totO3Std** and the portion of **O3VMRStd** profile at pressures greater than 0.5 hPa. At pressures lower than 0.5 hPa, biases in **O3VMRStd** are estimated to be between ~10% to ~50%. The extrapolation error occurs in the lowest 6 pressure levels of the support pressure level array (i.e., in the Level 2 Support Product **O3CDSup** array elements 1, 2, 3, 4, 5 and 6.

20.6 Suggestions for Researchers

This section will be updated over time as V6 data products are analyzed and validated.

V6 is a slight improvement over V5, but there are still problems when the surface skin temperature does not compare well to AMSR-E or the scene has a significant cloud amount.

20.7 Recommended Papers

This section will be updated over time as research with V6 data products are published.

Bian J., A. Gettelman, H. Chen, L. L. Pan (2007), Validation of satellite ozone profile retrievals using Beijing ozonesonde data, J. Geophys. Res., 112, D06305, doi:10.1029/2006JD007502.

Brasseur, G. P., Hauglustaine, D. A., Walters, S., Rasch, P. J., Muller, J. F., Granier, C. and Tie, X. X.: MOZART, a global chemical transport model for ozone and related chemical trac- ers 1. Model description, J. Geophys. Res.-Atmos., 103(D21), 28 265–28 289, 1998.

Chen, Francis, Miller (2002), Surface temperature of the Arctic: Comparison of TOVS satellite retrievals with surface observations, J. Climate, 15, 3698–3708. DOI: 10.1175/1520-0442(2002)015<3698:STOTAC>2.0.CH4;2

Divakarla, M., C. Barnet, M. Goldberg, E. Maddy, F. Irion, M. Newchurch, XP. Liu, W. Wolf, L. Flynn, G. Labow, XZ. Xiong, J. Wei, LH. Zhou, LH (2008), Evaluation of Atmospheric Infrared Sounder ozone profiles and total ozone retrievals with matched ozonesonde measurements, ECMWF ozone data, and Ozone Monitoring Instrument retrievals, J. Geophys. Res., 113, D15308 DOI:10.1029/2007JD009317.

Goldberg, M. D., Y. Qu, L. M. McMillin, W. Wolf, L. Zhou and M. Divakarla (2003), AIRS near-real-time products and algorithms in support of operational numerical weather prediction, IEEE. Trans. Geosci. Remote Sens., 41 (2), 379-389.

Kim, B., and S. Sarkar (2017), Impact of wildfires on some greenhouse gases over continental USA: A study based on satellite data, Remote Sensing of Environment, 188, 118-126. http://dx.doi.org/10.1016/j.rse.2016.10.047.

Levelt, P. F., et al. (2006), Science objectives of the Ozone Monitoring Instrument, IEEE Trans. Geosci. Remote Sens., 44, 1199-1208.

McPeters, R. D., J. A. Logan, G. J. Labow (2007), Ozone Climatological Profiles for Satellite Retrieval Algorithms, J. Geophys. Res., 112, D05308, 10.1029/2005JD006823

Morris G. A., et al. (2006), Alaskan and Canadian forest fires exacerbate ozone pollution over Houston, Texas, on 19 and 20 July 2004, J. Geophys. Res., 111, D24S03, doi:10.1029/2006JD007090.

Pittman, J. V., L. L. Pan, J. C. Wei, F. W. Irion, X. Liu, E. S. Maddy, C. D. Barnet, K. Chance, R. S. Gao (2009), Evaluation of AIRS, IASI, and OMI ozone profile retrievals in the extratropical tropopause region using in situ aircraft measurements, J. Geophys. Res., 114, D24109, 10.1029/2009JD012493.

Sitnov, S. A., and I. I. Mokhov (2016), Satellite-derived peculiarities of total ozone field under atmospheric blocking conditions over the European part of Russia in summer 2010, Russian Meteorology and Hydrology 41.1: 28-36. doi: http://dx.doi.org/10.3103/S1068373916010040.

Susskind, J., C. D. Barnet, and J. M. Blaisdell (2003), Retrieval of atmospheric and surface parameters from AIRS/AMSU/HSB data in the presence of clouds, IEEE Trans. Geosci. Remote Sens., 41 (2), 390 – 409.

Tian B., Y. L. Yung, D. E. Waliser, T. Tyranowski, L. Kuai, E. J. Fetzer, F. W. Irion (2007), Intraseasonal variations of the tropical total ozone and their connection to the Madden-Julian Oscillation, Geophys. Res. Lett., 34, L08704, doi:10.1029/2007GL029451.

Wang, H., X. Zou, G. Li, 2012: An Improved Quality Control for AIRS Total Column Ozone Observations within and around Hurricanes. J. Atmos. Oceanic Technol., 29, 417â€“432. doi: http://dx.doi.org/10.1175/JTECH-D-11-00108.1

Wei, Jennifer C., Laura L. Pan, Eric Maddy, Jasna V. Pittman, Murty Divarkarla, Xiaozhen Xiong, Chris Barnet, 2010: Ozone Profile Retrieval from an Advanced Infrared Sounder: Experiments with Tropopause-Based Climatology and Optimal Estimation Approach. J. Atmos. Oceanic Technol., 27, 1123â€“1139. doi: http://dx.doi.org/10.1175/2010JTECHA1384.1

Ziemke, J. R., S. Chandra, and P. K. Bhartia (2001), “Cloud slicing”: A new technique to derive upper tropospheric ozone from satellite measurements, J. Geophys. Res., 106 (D9), 9853-9867.

20.8 Recommended Supplemental User Documentation

V6_Data_Release_User_Guide.pdf

V6_Data_Disclaimer.pdf

V6_L2_Performance_and_Test_Report.pdf

V6_L2_Quality_Control_and_Error_Estimation.pdf

V6_Released_Processing_File_Description.pdf

V6_L2_Standard_Pressure_Levels.pdf

V6_L2_Support_Pressure_Levels.pdf

V6_L2_Levels_Layers_Trapezoids.pdf

V6_Retrieval_Channel_Sets.pdf

V6_Retrieval_Flow.pdf

21 Level 2 Physical Retrieval Carbon Monoxide Retrievals

A major change has been made in V6 to the first guess CO profile. Instead of a constant guess, we now use different guesses in the northern and southern hemispheres, smoothly varying across the tropics. This guess is based on monthly climatologies.

The peak sensitivity of the AIRS retrieval to CO occurs at 500 hPa. The AIRS retrieval is not sensitive to this atmospheric constituent near the surface. The total column value reported for CO is dominated by the initial guess and should not be used for research purposes. The total column CO will be moved to the Level 2 Support Product in the future V7 data product release.

Standard Product

Field Name	Dimension per FOV	Description
CO_total_column	1	Retrieved total column CO, (molecules/cm^2) DO NOT USE FOR RESEARCH
CO_total_column_QC	1	Quality flag (0,1,2)
COVMRLevStd	StdPressureLev =28	Level retrieved CO Volume Mixing Ratio Profile (vmr), (unitless)
COVMRLevStd_QC	StdPressureLev =28	Quality flag array (0,1,2)
COVMRLevStdErr	StdPressureLev =28	Error estimate for COVMRLevStd, Volume Mixing Ratio Profile (vmr), (unitless)
num_CO_Func	1	Number of valid entries in each dimension of CO_ave_kern
CO_verticality	COFunc =9	Sum of rows of CO_ave_kern, (unitless)
CO_dof	1	Degrees of freedom, measure of amount of information in CO retrieval, (unitless)

Support Product

Field Name	Dimension per FOV	Description
CO_trapezoid_layers	COFunc=9	1-based Index of **pressSup** array giving element defining lower altitude bound of trapezoid on which the CO variables are defined, located in support product (unitless)
CO_eff_press	COFunc=9	CO effective pressure for the center of each trapezoid, located in support product. These CO trapezoids were chosen to approximately match MOPITT standard levels, (hPa)
COCDSup	XtraPresureLev=100	Layer column carbon monoxide in molecules/cm^2 (climatology when bad_co ≠ 0)
COCDSup_QC	XtraPresureLev=100	Quality flag array (0,1,2)
COCDSup_Err	XtraPresureLev=100	Error estimate for COCDSup
COVMRLevSup	XtraPresureLev=100	CO Volume Mixing Ratio at support levels (vmr) (unitless)
COVMRLevSup_QC	XtraPresureLev=100	Quality flag array (0,1,2)
COVMRLevSupErr	XtraPresureLev=100	Error estimate for COVMRLevSup
COVMRSurf	1	CO Volume Mixing Ratio at the surface (vmr) (unitless) DO NOT USE FOR RESEARCH. Retrieval has no sensitivity at surface. Value is from the initial guess
COVMRSurf_QC	1	Quality flag array (0,1,2)
COVMRSurfErr	1	Error estimate for COVMRSurf
CO_VMR_eff	COFunc=9	Effective CO Volume Mixing Ratio Profile (vmr) for each trapezoid, located in support product (unitless)
CO_VMR_eff_QC	COFunc=9	Quality flag array (0,1,2)
CO_VMR_eff_err	COFunc=9	Error estimate (vmr), located in support product (unitless)
CO_ave_kern	COFunc*COFunc =9x9	Averaging kernel for CO retrieval, located in support product

21.1 Description

The AIRS carbon monoxide product is a product of the IR stage of the combined IR/MW retrieval. A volume mixing ratio profile on the 28 standard pressure levels, **pressStd**, is provided in the Level 2 Standard Product. Level and layer profiles on the 100 support pressure levels, **pressSup**, are provided in the Level 2 Support Product.

The first guess profiles for V6 CO retrieval are provided in the document:

V6_CO_Initial_Guess_Profiles.pdf

COVMRLevStd and **COVMRLevSup** are **level** quantities providing the retrieved carbon monoxide volume mixing ratio (ratio of number of CO molecules to the number of molecules of air in a unit volume) at the pressure levels upon which they are reported. The former is in the standard product and the latter is in the support product. Standard pressure levels are arranged in order of decreasing pressure and support pressure levels are arranged in order of increasing pressure.

COCDSup is a **layer** quantity in the support product providing the retrieved CO layer column density (number of CO molecules/cm^2) between two **pressSup** levels and is reported on the lower altitude pressure level bounding the layer.

Level quantities are calculated from layer quantities by the procedure described in the Algorithm Theoretical Document

AIRS_Layers_to_Levels_Theoretical_Basis_Document.pdf

The derivation of level quantities from layer quantities is essentially done by interpolation with smoothing kernels.

CO_eff_press is defined as the pressure weighted center of the trapezoid layers, i.e.,

$$\text{CO\_eff\_press} = \frac{\left[P_{bottom} - P_{top}\right]}{\log\left(P_{bottom}/P_{top}\right)}$$

where P_{bottom} is the bottom pressure of a trapezoid face and P_{top} is the top pressure. These trapezoid layers were chosen so that the **CO_eff_press** match as closely as possible to the standard pressure levels used by MOPITT and to optimize the AIRS CO retrieval.

CO_VMR_eff is a **layer** quantity contained in the support product providing the retrieved volume mixing ratio (ratio of number of CO molecules to the number of molecules of air in a unit volume) for a layer defined by the faces of an CH4 trapezoidal retrieval function. The boundaries of faces of these layers are specified in **CO_trapezoid_layers** in which is an array of 1-based **pressSup** level indices. There are 9 such trapezoidal layers corresponding to the 9 trapezoidal retrieval functions utilized for CO. **CO_VMR_eff** is reported at the effective trapezoid layer, **CO_eff_press**(**CO_trapezoid_layers**). It is computed from the integrated CO column density for the trapezoidal layer. **CO_eff_press** is defined as the pressure weighted center of the layer. Layers below the surface are filled with -9999. The value quoted on the lowest layer above the surface is the mean mixing ratio in the layer bounded by the next higher level and the surface. See

V6_L2_Support_Pressure_Levels.pdf
V6_L2_Levels_Layers_Trapezoids.pdf

COVMRSurf is a **level** quantity in the support product providing the retrieved CO volume mixing ratio at the surface.

CO_VMR_eff_err is the estimated error in CO mixing ratio due to the retrieved errors in temperature, water vapor and surface temperature as derived by Comer (2006) and McMillan(2011). This error is computed on the **pressSup** layers and then averaged to the CO trapezoids.

CO_total_column is the integrated column amount of CO from the top of the atmosphere (TOA = 0.005 hPa) to the surface. This quantity is computed by summing the 100 column density values, **COCDsup,** contained in the AIRS Level 2 Support Products file with the appropriate weighting applied to the bottom layer which contains the surface. Layers below the surface are not included in this sum. The reported total column is dominated by the initial guess and should not be used for research. This quantity will be moved to the Level 2 Support Product in the future V7 data product release.

CO_dof provides a measure of the amount of information in the CO retrieval. It is computed by summing the diagonal elements of the 9x9 CO averaging kernel, **CO_ave_kern**, stored in the AIRS Support Product files. V5 Validation and optimization studies (Comer, 2006) have shown **CO_dof** < 0.4 indicates little information in the retrieval comes from the measured radiances. Profiles for which 0.5 > **CO_dof** > 0.4 should be used with great caution.

CO_verticality is a 9 point vector computed by summing the columns of the 9x9 CO averaging kernel, **CO_ave_kern**, stored in the AIRS Level 2 Support Product. The associated 9 point pressure array is provided in **CO_eff_press**. The peak value of **CO_verticality** indicates the vertical location of the maximum sensitivity of the CO product and the width of this peaked function qualitatively describes the vertical resolution of the retrieval. The magnitudes of **CO_verticality** are a rough measure of the fraction of the retrieval determined from the data as opposed to the first guess. A value near unity indicates the retrieval is highly determined by the radiance measurements and thus has high information content. A smaller value indicates the retrieval contains a large fraction of the first guess. **CO_dof** is the number of degrees of freedom (a measure of the amount of information in the retrieval), and is the trace of **CO_avg_kern**.

NOTE: **num_CO_Func** provides the number of valid entries in each dimension of **CO_ave_kern**. Topography limits the number of valid CO averaging kernel trapezoids.

See the V5 and V6 CO first guess documentation:

V5_CO_Initial_Guess_Profile.pdf
V6_CO_Initial_Guess_Profiles.pdf

NOTE: the problem with associating the verticality with a total column averaging kernel is that it neglects the fact that the retrieval can only move as superpositions of the trapezoids. Convolution using the verticality alone will not account for the possibility that the “independent CO profile” contains structure that the trapezoids can or cannot resolve.

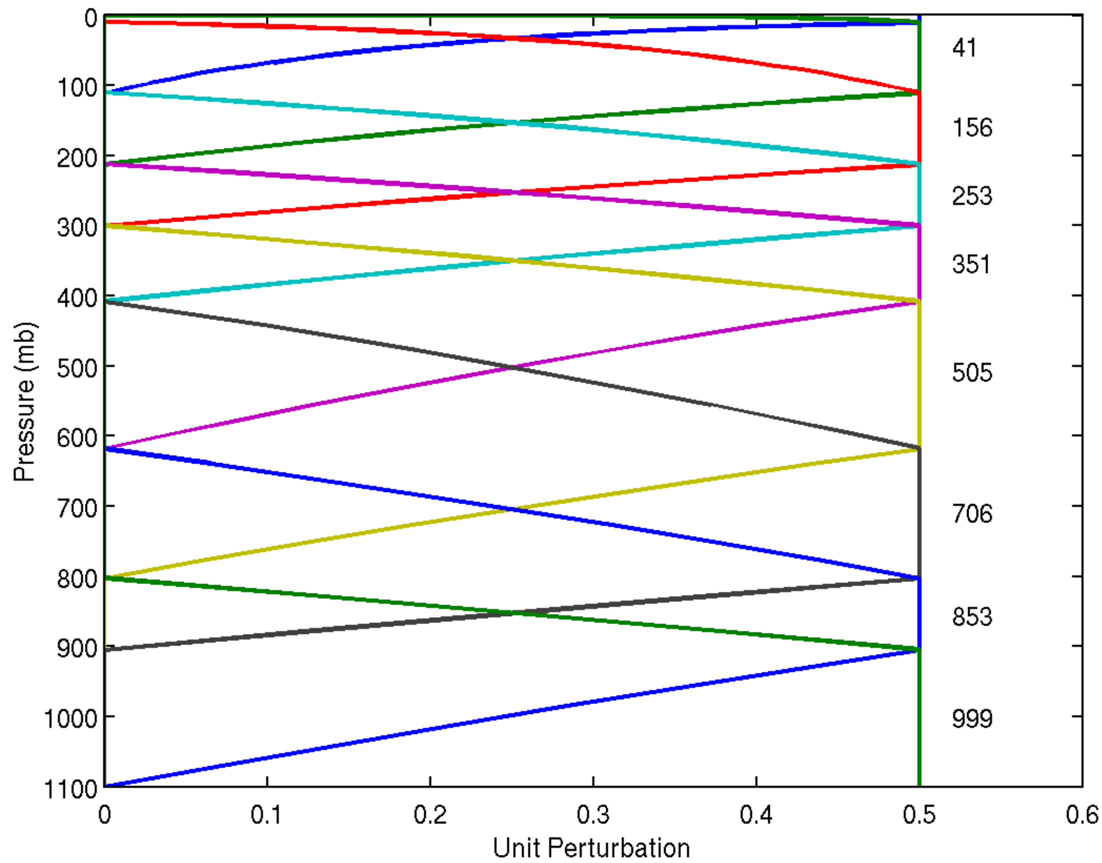

Figure 11: The 9 CO trapezoids.
Values at right are **CO_eff_press** for each. (Wallace McMillan)

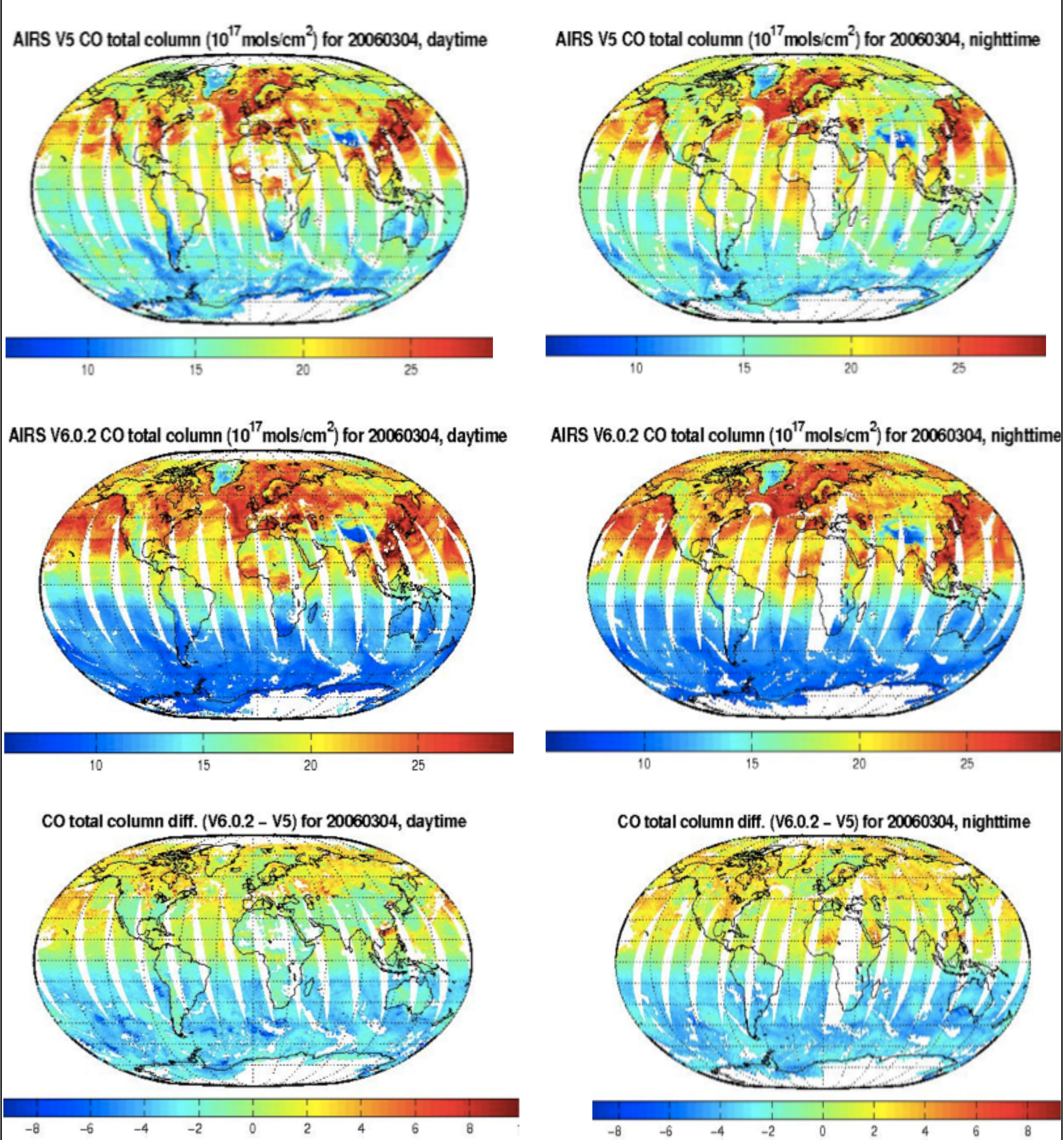

Figure 12: Comparison of V5 and V6 Global distribution of total CO burden on 4 March 2006 V5.0.7

Left Column: Daytime ; Right Column: Nighttime

Top Row: V5 ; Middle Row: V6 ; Bottom Row: V6-V5

21.2 Type of Product

The standard CO product profile is a level quantity, i.e. the values are reported on the pressure levels represent the volume mixing ratio at the pressure level on which they are reported.

21.3 Quality Indicators

The user is encouraged to read the QC and error estimation document:

V6_L2_Quality_Control_and_Error_Estimation.pdf

If **PGood = PSurfStd**, and **CO_dof** > 0.5, then all CO products are marked Quality = 0.

If **PGood = PSurfStd**, and 0.5 >= **CO_dof** > 0.4, then all CO products are marked Quality = 1.

Otherwise, all CO products are marked Quality = 2.

21.4 Validation

A Validation Report for V6 data is currently under preparation and will be published after the V6 data products become publicly available. A V5 Validation Report, summarizing relevant publications, is also being prepared. Early V6 validation results are partially summarized in

V6_L2 Performance_and_Test_Report.pdf

21.5 Caveats

This section will be updated over time as V6 data products are analyzed and validated.

The total column CO is dominated by the initial guess and thus should not be used for research.

Quality control is set to 0 if **PGood = PSurfStd** and the final IR retrieval is the atmospheric state of the reported products and **CO_dof** > 0.5.

21.6 Suggestions for Researchers

This section will be updated over time as V6 data products are analyzed and validated.

AIRS V6 CO retrievals are provisionally validated. We are still assessing the derived error fields for quality control, but have erred on the conservative side to provide the best possible data.

We recommend that researchers pre-filter retrievals by requiring
(**PsurfStd** – **PBest**) < 200 hPa
and then filtering further by requiring Quality control = 0.

We strongly urge caution in using any retrievals for which Quality control > 0. We suggest that trapezoids for which **CO_VMR_eff_err** is negative or greater than 50% of **CO_VMR_eff** should be excised.

21.7 Recommended Papers

This section will be updated over time as research with V6 data products are published.

Brasseur, G. P., Hauglustaine, D. A., Walters, S., Rasch, P. J., Muller, J. F., Granier, C. and Tie, X. X.(1998), MOZART, a global chemical transport model for ozone and related chemical tracers 1. Model description, J. Geophys. Res.-Atmos., 103(D21), 28 265–28 289.

Comer, M.M. (2006), Retrieving Carbon Monoxide Abundances from the Atmospheric Infrared Sound, PhD dissertation, Department of Physics, University of Maryland Baltimore County.

Devasthale, A., M. A. Thomas (2012), An investigation of statistical link between inversion strength and carbon monoxide over Scandinavia in winter using AIRS data, Atmos. Environ., 56, 109-114, http://dx.doi.org/10.1016/j.atmosenv.2012.03.042.

Fisher, J. A., D. J. Jacob, M. T. Purdy, M. Kopacz, P. Le Sager, C. Carouge, C. D. Holmes et al. (2010), "Source attribution and interannual variability of Arctic pollution in spring constrained by aircraft (ARCTAS, ARCPAC) and satellite (AIRS) observations of carbon monoxide." Atmospheric Chemistry & Physics 10, pp 977-996.

Freitas S. R., K. M. Longo, M. O. Andreae (2006), Impact of including the plume rise of vegetation fires in numerical simulations of associated atmospheric pollutants, Geophys. Res. Lett., 33, L17808, doi:10.1029/2006GL026608.

Kopacz, Monika, D. J. Jacob, J. A. Fisher, J. A. Logan, Lin Zhang, I. A. Megretskaia, R. M. Yantosca et al. (2010), "Global estimates of CO sources with high resolution by adjoint inversion of multiple satellite datasets (MOPITT, AIRS, SCIAMACHY, TES)." Atmos. Chem. Phys 10, no. 3, pp 855-876.

Huang, M., et al. (2017), Impact of intercontinental pollution transport on North American ozone air pollution: an HTAP phase 2 multi-model study, Atmospheric Chemistry and Physics, 17(9), 5721-5750. http://dx.doi.org/10.5194/acp-17-5721-2017

Kim, P. S., D. J. Jacob, X. Liu, J. X. Warner, K. Yang, K. Chance, V. Thouret, and P. Nedelec. "Global ozone–CO correlations from OMI and AIRS: constraints on tropospheric ozone sources." Atmospheric Chemistry and Physics 13, no. 18 (2013): 9321-9335.

Kim, B., and S. Sarkar (2017), Impact of wildfires on some greenhouse gases over continental USA: A study based on satellite data, Remote Sensing of Environment, 188, 118-126. http://dx.doi.org/10.1016/j.rse.2016.10.047.

Kumar, A., Wu, S., Weise, M. F., Honrath, R., Owen, R. C., Helmig, D., Kramer, L., Val Martin, M., and Li, Q.: Free-troposphere ozone and carbon monoxide over the North Atlantic for 2001–2011, Atmos. Chem. Phys., 13, 12537-12547, doi:10.5194/acp-13-12537-2013, 2013.

McMillan W. W., C. Barnet, L. Strow, M. T. Chahine, M. L. McCourt, J. X. Warner, P. C. Novelli, S. Korontzi, E. S. Maddy, S. Datta (2005), "Daily global maps of carbon monoxide from NASA's Atmospheric Infrared Sounder", Geophys. Res. Lett., 32, L11801, doi:10.1029/2004GL021821.

McMillan, W. W., R. B. Pierce, L. C. Sparling, G. Osterman, K. McCann, M. L. Fischer, B. Rappenglueck et al. (2010), "An observational and modeling strategy to investigate the impact of remote sources on local air quality: A Houston, Texas, case study from the Second Texas Air Quality Study (TexAQS II)." Journal of Geophysical Research 115, no. D1, pp D01301.

McMillan, W. W., Keith D. Evans, Christopher D. Barnet, Eric S. Maddy, Glen W. Sachse, and Glenn S. Diskin (2011), Validating the AIRS Version 5 CO Retrieval With DACOM *In Situ* Measurements During INTEX-A and –B, IEEE Trans. on Geosci. Remote Sensing, 10.1109/TGRS.2011.2106505, 2011

Nara,Hideki; Tanimoto,Hiroshi; Nojiri,Yukihiro; Mukai,Hitoshi; Zeng,Jiye; Tohjima,Yasunori; Machida,Toshinobu, Emissions from biomass burning in South-east Asia in the 2006 El Nino year: shipboard and AIRS satellite observations, Environmental Chemistry, 2011, 8, 2, 213-223 http://dx.doi.org/10.1071/EN10113

Sachse, G. W., Hill, G. F., Wade, L. O., and Perry, M. G.(1987), Fast-response, high-precision carbon monoxide sensor using a tunable diode laser absorption technique, J. Geophys. Res., 92, 2071–2081.

Singh, H. B., Brune, W. H., Crawford, J. H., Flocke, F., and Jacob, D. J.(2009), Chemistry and transport of pollution over the Gulf of Mexico and the Pacific: Spring 2006 INTEX-B Campaign overview and first results, Atmos. Chem. Phys. Discuss., 9, 363-409.

Thonat, T., C. Crevoisier, N. A. Scott, A. Chedin, T. Schuck, R. Armante, and L. Crepeau (2012), Retrieval of tropospheric CO column from hyperspectral infrared sounders - application to four years of Aqua/AIRS and MetOp-A/IASI, Atmospheric Measurement Techniques, 5(10), 2413-2429, http://dx.doi.org/10.5194/amt-5-2413-2012.

Warner, J., M. M. Comer, C. D. Barnet, W. W. McMillan, W. Wolf, E. Maddy, and G. Sachse (2007), A comparison of satellite tropospheric carbon monoxide measurements from AIRS and MOPITT during INTEX-A, J. Geophys. Res., 112, D12S17, doi:10.1029/2006JD007925

Warner, J. X., Wei, Z., Strow, L. L., Barnet, C. D., Sparling, L. C., Diskin, G., and Sachse, G., 2010 (2010), Improved Agreement of AIRS Tropospheric Carbon Monoxide Products with other EOS Sensors Using Optimal Estimation Retrievals, Atmos. Chem. Phys., 10, 9521-9533, doi:10.5194/acp-10-9521-2010.

Warner, J., F. Carminati, Z. Wei, W. Lahoz, and J-L. Attié. "Tropospheric carbon monoxide variability from AIRS and IASI under clear and cloudy conditions." Atmospheric Chemistry and Physics Discussions 13, no. 6 (2013): 16337-16366.

Warner, J. X., R. Yang, Z. Wei, F. Carminati, A. Tangborn, Z. Sun, W. Lahoz, J-L. Attié, L. El Amraoui, and B. Duncan. "Global carbon monoxide products from combined AIRS, TES and MLS measurements on A-train satellites." Atmospheric Chemistry and Physics 14, no. 1 (2014): 103-114.

Zhang, L., H. Jiang, X. Lu, and J. Jin (2016), Comparison analysis of global carbon monoxide concentration derived from SCIAMACHY, AIRS, and MOPITT, Int.J.Remote Sens., 37(21), 5155-5175. https://dx.doi.org/10.1080/01431161.2016.1230282

21.8 Recommended Supplemental User Documentation

V6_Data_Release_User_Guide.pdf

V6_Data_Disclaimer.pdf

V6_L2_Performance_and_Test_Report.pdf

V6_L2_Quality_Control_and_Error_Estimation.pdf

V6_Released_Processing_File_Description.pdf

V6_L2_Standard_Pressure_Levels.pdf

V6_L2_Support_Pressure_Levels.pdf

V6_L2_Levels_Layers_Trapezoids.pdf
V6_Retrieval_Channel_Sets.pdf
V6_Retrieval_Flow.pdf
V6_CO_Initial_Guess_Profiles.pdf

22 Level 2 Physical Retrieval Methane Retrievals

Significant changes have been made to the methane retrieval in V6.

- Modified first guess (see **V6_CH4_Initial_Guess_Profiles.pdf**)
- Retrieval functions have been increased from 7 to 10
- New tuning to the absorption coefficients in the peak CH_4 absorption channels
- Channel set and damping have been updated accordingly
- Quality control has been enhanced

Users should expect significant changes in the methane product.

The number of functions has been increased from 7 to 10, resulting in a better sensitivity to the lower atmosphere and a higher degree of freedom. This results in a dimension change in the output products. To ensure users are aware of this, the variables that were dimensioned 7 in V5 have been renamed to indicate the new dimension, 10.

The peak sensitivity of the AIRS retrieval to CH4 occurs at 300 hPa. The AIRS retrieval is not sensitive to this atmospheric constituent near the surface. The total column value reported for CH4 is dominated by the initial guess and should not be used for research purposes. The total column CH4 will be moved to the Level 2 Support Product in the future V7 data product release.

Standard Product

Field Name	Dimension per FOV	Description
CH4_total_column	1	Retrieved total column CH_4, (molecules/cm^2) DO NOT USE FOR RESEARCH
CH4_total_column_QC	1	Quality flag (0,1,2)
CH4VMRLevStd	StdPressureLev=28	Level retrieved CH_4 Volume Mixing Ratio Profile (vmr), (unitless)
CH4VMRLevStd_QC	StdPressureLev=28	Quality flag array (0,1,2)
CH4VMRLevStdErr	StdPressureLev=28	Error estimate for CH4VMRLevStd, Volume Mixing Ratio Profile (vmr),

Field Name	Dimension per FOV	Description
		(unitless)
num_CH4_Func	1	Number of valid entries in each dimension of CH4_ave_kern
CH4_verticality_10func	CH4Func=10	Sum of rows of CH4_ave_kern, (unitless)
CH4_dof	1	Degrees of freedom, amount of information in CH_4 retrieval, (unitless)

Support Product

Field Name	Dimension per FOV	Description
CH4_trapezoid_layers_10func	CH4Func=10	1-based Index of **pressSup** array giving element defining lower altitude bound of trapezoid on which the CH4 variables are defined, located in support product (unitless)
CH4_eff_press_10func	CH4Func=10	CH4 effective pressure for the center of each trapezoid, located in support product. These CH4 trapezoids were chosen to approximately match MOPITT standard levels, (hPa)
CH4CDSup	XtraPresureLev=100	Layer column methane in molecules/cm^2 (climatology when bad_co ≠ 0)
CH4CDSup_QC	XtraPresureLev=100	Quality flag array (0,1,2)
CH4CDSup_Err	XtraPresureLev=100	Error estimate for CH4CDSup
CH4VMRLevSup	XtraPresureLev=100	CH4 Volume Mixing Ratio at support levels (vmr) (unitless)

Field Name	Dimension per FOV	Description
CH4VMRLevSup_QC	XtraPresureLev=100	Quality flag array (0,1,2)
CH4VMRLevSupErr	XtraPresureLev=100	Error estimate for CH4VMRLevSup
CH4VMRSurf	1	CH4 Volume Mixing Ratio at the surface (vmr) (unitless) DO NOT USE FOR RESEARCH. Retrieval has no sensitivity at surface. Value is from the initial guess
CH4VMRSurf_QC	1	Quality flag array (0,1,2)
CH4VMRSurfErr	1	Error estimate for CH4VMRSurf
CH4_VMR_eff_10func	CH4Func=10	Effective CH4 Volume Mixing Ratio Profile (vmr) for each trapezoid, located in support product (unitless)
CH4_VMR_eff_10func_QC	CH4Func=10	Quality flag array (0,1,2)
CH4_VMR_eff_10func_err	CH4Func=10	Error estimate (vmr), located in support product (unitless)
CH4_ave_kern_10func	CH4Func*CH4Func =10x10	Averaging kernel for CH4 retrieval, located in support product

22.1 Description

The AIRS methane product is a product of the IR stage of the combined IR/MW retrieval. A volume mixing ratio profile on the 28 standard pressure levels, **pressStd**, is provided in the Level 2 Standard Product. Level and layer profiles on the 100 support pressure levels, **pressSup**, are provided in the Level 2 Support Product.

Level quantities are calculated from layer quantities by the procedure described in the Algorithm Theoretical Document

AIRS_Layers_to_Levels_Theoretical_Basis_Document.pdf

The derivation of level quantities from layer quantities is essentially done by interpolation with smoothing kernels.

The algorithm for computing first guess profiles for V6 CH_4 retrieval and some example profiles are provided in the document:

V6_CH4_Initial_Guess_Profiles.pdf

CH4VMRLevStd and **CH4VMRLevSup** are **level** quantities providing the retrieved carbon monoxide volume mixing ratio (ratio of number of CH4 molecules to the number of molecules of air in a unit volume) at the pressure levels upon which they are reported. The former is in the standard product and the latter is in the support product. Standard pressure levels are arranged in order of decreasing pressure and support pressure levels are arranged in order of increasing pressure.

CH4CDSup is a **layer** quantity in the support product providing the retrieved CH4 layer column density (number of CH4 molecules/cm^2) between two **pressSup** levels and is reported on the lower altitude pressure level bounding the layer.

CH4_eff_press_10func is defined as the pressure weighted center of the trapezoid layers, i.e.,

$$\mathrm{CH4\_eff\_10func\_press} = \frac{\left[P_{bottom} - P_{top}\right]}{\log\left(P_{bottom} / P_{top}\right)}$$

where P_{bottom} is the bottom pressure of a trapezoid face and P_{top} is the top pressure.

CH4_VMR_eff_10func is a **layer** quantity contained in the support product providing the retrieved volume mixing ratio (ratio of number of CH4 molecules to the number of molecules of air in a unit volume) for a layer defined by the faces of an CH4 trapezoidal retrieval function. The boundaries of faces of these layers are specified in **CH4_trapezoid_layers_10func** in which is an array of 1-based **pressSup** level indices. There are 10 such trapezoidal layers corresponding to the 10 trapezoidal retrieval functions utilized for CH4. **CH4_VMR_eff_10func** is reported at the effective trapezoid layer, **CH4_eff_press_10func**. It is computed from the integrated CH4 column density for the trapezoidal layer. **CH4_eff_press_10func** is defined as the pressure weighted center of the layer. Layers below the surface are filled with -9999. The value quoted on the lowest layer above the surface is the mean mixing ratio in the layer bounded by the next higher level and the surface. See

V6_L2_Support_Pressure_Levels.pdf
V6_L2_Levels_Layers_Trapezoids.pdf

CH4_VMR_eff_10func_err is the estimated error in CH_4 mixing ratio. This error is computed on the **pressSup** layers and then averaged to the CH_4 trapezoids.

CH4VMRSurf is a **level** quantity in the support product providing the retrieved CH4 volume mixing ratio at the surface.

CH4_total_column is the integrated column amount of CH4 from the top of the atmosphere (TOA = 0.005 hPa) to the surface. This quantity is computed by summing the 100 column density values, **CH4CDSup,** contained in the AIRS Level 2 Support Products file with the appropriate weighting applied to the bottom layer which contains the surface. Layers below the surface are not included in this sum. The reported total column is dominated by the initial guess and should not be used for research. This quantity will be moved to the Level 2 Support Product in the future V7 data product release.

CH4_dof provides a measure of the amount of information in the CH4 retrieval. It is computed by summing the diagonal elements of the 10x10 CH4 averaging kernel, **CH4_ave_kern**, stored in the AIRS Support Product files.

CH4_verticality is a 10 point vector computed by summing the columns of the 10x10 CH_4 averaging kernel, **CH4_ave_kern**, stored in the AIRS Level 2 Support Product. The associated 10 point pressure array is provided in **CH4_eff_press**. The peak value of **CH4_verticality** indicates the vertical location of the maximum sensitivity of the CH_4 product and the width of this peaked function qualitatively describes the vertical resolution of the retrieval. The magnitudes of **CH4_verticality** are a rough measure of the fraction of the retrieval determined from the data as opposed to the first guess. A value near unity indicates the retrieval is highly determined by the radiance measurements and thus has high information content. A smaller value indicates the retrieval contains a large fraction of the first guess. **CH4_dof** is the number of degrees of freedom (a measure of the amount of information in the retrieval), and is the trace of **CH4_avg_kern**. See the V5 and V6 CH4 first guess documentation:

V5_CH4_Initial_Guess_Profile.pdf
V6_CH4_Initial_Guess_Profiles.pdf

NOTE: **num_CH4_Func** provides the number of valid entries in each dimension of **CH4_ave_kern**. Topography limits the number of valid CH_4 averaging kernel trapezoids.

NOTE: the problem with associating the verticality with a total column averaging kernel is that it neglects the fact that the retrieval can only move as superpositions of the trapezoids. Convolution using the verticality alone will not account for the possibility that the “independent CH_4 profile” contains structure that the trapezoids can or cannot resolve.

22.2 Type of Product

The standard CH_4 product profile is a level quantity, i.e. the values are reported on the standard pressure levels and provide the volume mixing ratios at the level on which they are reported.

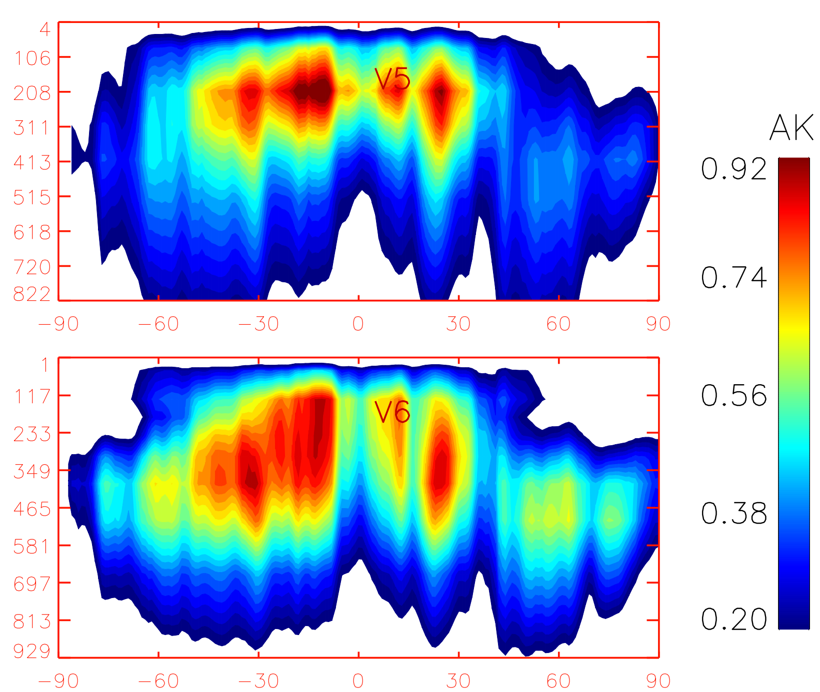

Figure 13: Comparison of AIRS V5 and V6 CH4 averaging kernels on 27 March 2010.
Top Row: V5 ; Bottom Row: V6

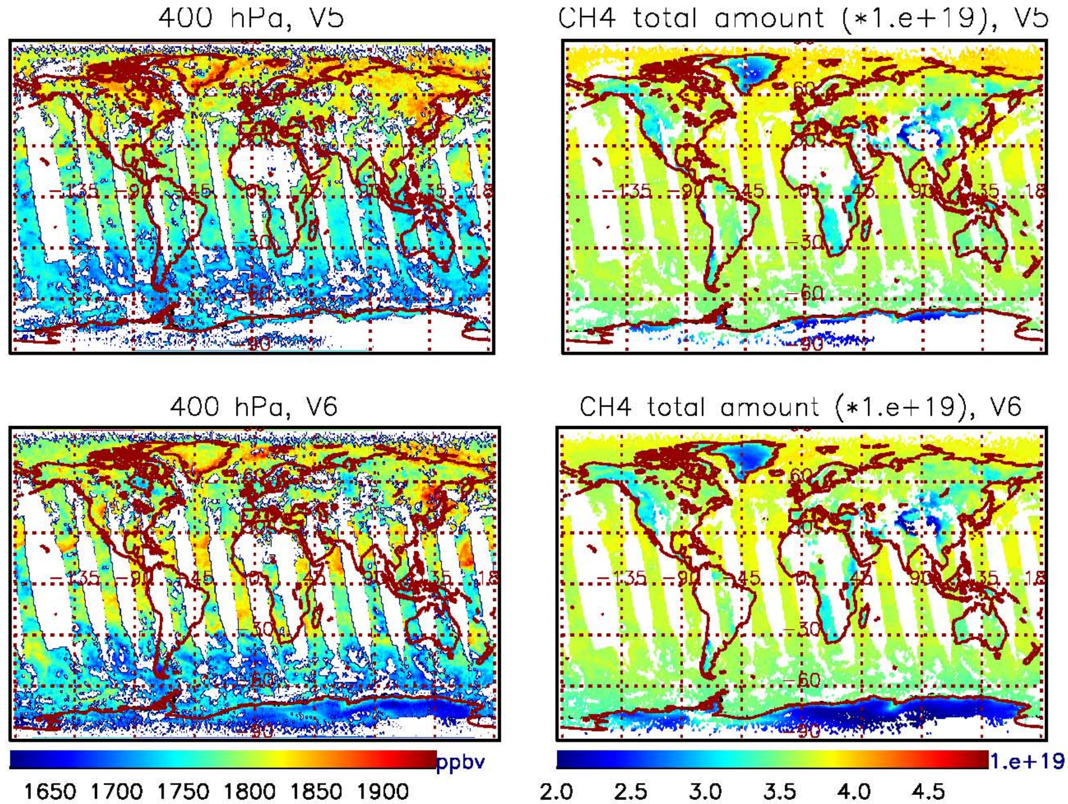

Figure 14: Comparison of AIRS V5 and V6 CH4 total column and CH4 @ 400 hPa on 27 March 2010.

Top Row: V5 ; Bottom Row: V6
Left Column: vmr @ 400 hPa (ppbv) ; Right Column: Total column (mole/cm^2)

22.3 Quality Indicators

The user is encouraged to read the QC and error estimation document:

V6_L2_Quality_Control_and_Error_Estimation.pdf

If **PGood = PSurfStd** and **CH4_Resid_Ratio** < 1.5 and **CH4_dof** > 0.5,
then all CH4 products are marked Quality = 0.

If **PGood = PSurfStd** and **CH4_Resid_Ratio** < 1.5 and 0.5 >= **CH4_dof** > 0.4,
then all CH4 products are marked Quality = 1.

Otherwise, all CH4 products are marked Quality = 2,
and additional tests are then applied to lower the Quality if appropriate.

V6 employs stricter QC flags than V5. The CH4 absorption band is within the water vapor absorption band near 7.6 mm, and thus the quality of the moisture product impacts that of the CH4 product. Therefore, if **totH2OStd_QC** = 1, we set all CH_4 quality flags to 1 if:

- **CH4_Resid_Ratio** ≥ 1.0, or
- **PGood** ≤ 610 hPa

We found the contamination of CH_4 retrievals is mainly from low water clouds. Under the condition of **totH2OStd_QC** = 1, we set all CH_4 quality flags to 2 when the cloud fraction among the 9 AIRS spots within a retrieval FOV are mainly water clouds or they are very different. The test for water clouds uses **cloud_phase_3x3** (located in the Level 2 Support Product).

We recognize there remains a scan angle dependence of retrieved CH_4 at altitudes above the 200 hPa level in the tropics. To minimize its impact upon research, we set Quality=2 for the two most extreme san angle retrievals at the beginning and end of each scan set (i.e., retrieval FOVs 1, 2, 29 and 30) whenever **PTropopause** ≤ 100 hPa.

With the new QC flags plus V6, the distribution of CH_4 mixing ratio is more uniform than V5. After applying the new QC flags, the yield drops by 8-10% but is still greater than 60%.

22.4 Validation

A Validation Report for V6 data is currently under preparation and will be published after the V6 data products become publicly available. A V5 Validation Report, summarizing relevant publications, is also being prepared. Early V6 validation results are partially summarized in

V6_L2 Performance_and_Test_Report.pdf

The validation of the AIRS V6 CH_4 product will be made using the profiles from aircraft measurements obtained from different campaigns after the official V6 products become available. In addition to the aircraft data used in V5 CH4 validation more recent data from the HIAPER Pole-to-Pole Observations (HIPPO) project will be used.

22.5 Caveats

This section will be updated over time as V6 data products are analyzed and validated.

The total column CH4 is dominated by the initial guess and thus should not be used for research.

Due to the uncertainty in CH_4 absorption spectrum, tuning of CH4 channels in the Q-branch requires additional investigation. Current tuning for V6 is based on HIPPO-1,-2,-3 data, but is still limited due to the lack of aircraft data in the summer season.

22.6 Suggestions for Researchers

This section will be updated over time as V6 data products are analyzed and validated.

We caution researchers to consider the V6 CH_4 profile products to be a provisional release.

22.7 Recommended Papers

This section will be updated over time as research with V6 data products are published.

Kim, B., and S. Sarkar (2017), Impact of wildfires on some greenhouse gases over continental USA: A study based on satellite data, Remote Sensing of Environment, 188, 118-126. http://dx.doi.org/10.1016/j.rse.2016.10.047.

Peters, C. N., R. Bennartz, and G. M. Hornberger (2017), Satellite-derived methane emissions from inundation in Bangladesh, J. Geophys. Res. Biogeosci., 122, 1137–1155, doi:10.1002/2016JG003740.

Mahmood, I., M. F. Iqbal, M. I. Shahzad, A. Waqas, and L. Atique (2016), Spatiotemporal Monitoring of CO2 and CH4 over Pakistan Using Atmospheric Infrared Sounder (AIRS), Int. Lett. Nat. Sci., 58, 35-41. https://dx.doi.org/10.18052/www.scipress.com/ILNS.58.35.

Rajab, J.M., M.Z. MatJafri, H.S. Lim (2012), Methane Interannual Distribution over Peninsular Malaysia from Atmospheric Infrared Sounder Data: 2003-2009, *Aerosol and Air Quality Research*, **12**, 1459-1466, doi: 10.4209/aaqr.2012.02.0039

Streets, David G., Timothy Canty, Gregory R. Carmichael, Benjamin de Foy, Russell R. Dickerson, Bryan N. Duncan, David P. Edwards et al. "Emissions estimation from satellite retrievals: A review of current capability." Atmospheric Environment 77 (2013): 1011-1042.

Xiong, X., C. Barnet, E. Maddy, C. Sweeney, X. Liu, L. Zhou, and M. Goldberg, (2008), Characterization and validation of methane products from the Atmospheric Infrared Sounder (AIRS), *J. Geophys Res.,* **113**, G00A01, doi:10.1029/2007JG000500.

Xiong, X., C. Barnet, J. Wei, and E. Maddy. "Information-based mid-upper tropospheric methane derived from Atmospheric Infrared Sounder (AIRS) and its validation." Atmospheric Chemistry and Physics Discussions 9, no. 4 (2009): 16331-16360.

Xiong, X., S. Houweling, J. Wei, E. Maddy, F. Sun, C. D. Barnet (2009), Methane Plume over South Asia during the Monsoon Season: Satellite Observation and Model Simulation, *Atmos. Chem. Phys*., **9**, 783-794, 2009.

Xiong, X., Barnet, C. D., Maddy, E. , Wei, J., Liu, X., Thomas.S.Pagano (2010), Seven Years' Observation of Mid-Upper Tropospheric Methane from Atmospheric Infrared Sounder, *Remote Sensing*, **2**, 2509-2530; doi:10.3390/rs2112509

Xiong, X., Barnet, C.; Zhuang, Q.; Machida, T.; Sweeney, C.; Patra, P.K. (2010),Mid-upper Tropospheric Methane in the High Northern Hemisphere: Space-borne Observations by AIRS, Aircraft Measurements and Model Simulations, *J. Geophys. Res*., **115**, D19309, doi:10.1029/2009JD013796.

Xiong, X. Z., Y. Han, Q. H. Liu, and F. Z. Weng (2016), Comparison of Atmospheric Methane Retrievals From AIRS and IASI, IEEE Journal of Selected Topics in Applied Earth Observations and Remote Sensing, 9(7), 3297-3303. http://dx.doi.org/10.1109/jstars.2016.2588279.

Xu, Y., J. Wang, J. Sun, Y. Xu, and W. Harris (2012), Spatial and Temporal Variations of Lower Tropospheric Methane During 2010-2011 in China, IEEE Journal of Selected Topics in Applied Earth Observations and Remote Sensing, 5(5), 1464-1473, http://dx.doi.org/10.1109/JSTARS.2012.2195640.

Zhang,XingYing, Bai,WenGuang, Zhang,Peng, Wang,WeiHe,(2011), Spatiotemporal variations in mid-upper tropospheric methane over China from satellite observations, Chin.Sci.Bull., 56, 31, 3321-3327

Zhang, Y., Chen, L., Tao, J., Su, L., Yu, C., and Fan, M., 2012, Retrieval of methane profiles from spaceborne hyperspectral infrared observations: Journal of Remote Sensing, v. 16, no. 2, p. 232-247

Zhang, Y., X. Xiong, J. Tao, C. Yu, M. Zou, L. Su, and L. Chen (2014), Methane retrieval from Atmospheric Infrared Sounder using EOF-based regression algorithm and its validation, Chinese Science Bulletin, 59(14), 1508-1518, doi:http://dx.doi.org/10.1007/s11434-014-0232-7.

Zou, M., Xiong, X., Saitoh, N., Warner, J., Zhang, Y., Chen, L., Weng, F., and Fan, M.: Satellite observation of atmospheric methane: intercomparison between AIRS and GOSAT TANSO-FTS retrievals, Atmos. Meas. Tech., 9, 3567-3576, doi:10.5194/amt-9-3567-2016, 2016

22.8 Recommended Supplemental User Documentation

V6_Data_Release_User_Guide.pdf
V6_Data_Disclaimer.pdf
V6_L2_Performance_and_Test_Report.pdf
V6_L2_Quality_Control_and_Error_Estimation.pdf
V6_Released_Processing_File_Description.pdf
V6_L2_Standard_Pressure_Levels.pdf
V6_L2_Support_Pressure_Levels.pdf
V6_L2_Levels_Layers_Trapezoids.pdf
V6_Retrieval_Channel_Sets.pdf
V6_Retrieval_Flow.pdf
V6_CH4_Initial_Guess_Profiles.pdf

23 Level 2 Physical Retrieval Outgoing Longwave Radiation Retrievals

Standard Product

Field Name	Dimension per FOV	Description
olr	1	Outgoing longwave radiation flux integrated over 2 to 2800 cm^{-1}, (W/m^2)
olr_err	1	Error estimate for olr, (W/m^2)
olr_QC	1	Quality flag (0,1,2)
olr3x3	AIRSTrack *AIRSXTrack =3x3	Outgoing longwave radiation flux integrated over 2 to 2800 cm^{-1}, per 15km AIRS FOV (W/m^2)
olr3x3_QC	AIRSTrack *AIRSXTrack =3x3	Quality flag array (0,1,2)
clrolr	1	Clear sky outgoing longwave radiation flux integrated over 2 to 2800 cm^{-1}, (W/m^2)
clrolr_err	1	Error estimate for clrolr, (W/m^2)
clrolr_QC	1	Quality flag (0,1,2)

Support Product

Field Name	Dimension per FOV	Description
spectralolr	OLRBand=16	Outgoing Longwave Radiation Flux integrated over 16 frequency bands (per 45 km AMSU-A FOV) ($Watts/m^2$)
spectralolr_QC	OLRBand=16	Quality flag (0,1,2)
spectralclrolr		Clear-sky Outgoing Longwave Radiation Flux integrated over 16 frequency bands (per 45 km AMSU-A

Field Name	Dimension per FOV	Description
		FOV) (Watts/m^2)
spectralclrolr_QC		Quality flag (0,1,2)

23.1 Description

Outgoing longwave radiation (OLR) is the total longwave radiative flux (W/m^2) going to space, emitted by the earth-atmosphere system integrated over all angles and over all frequencies. OLR (**olr**) is not directly measured but is calculated from the retrieved state using an OLR RTA (the "AER" algorithm) due to Iacono et al. (2008). OLR at a given location is affected primarily by the earth's skin surface temperature, skin surface spectral emissivity, atmospheric vertical temperature and water vapor profile, as well as the heights, amounts, and spectral emissivities of multiple layers of cloud cover. OLR also depends on the vertical distributions of trace gases. V5 computed OLR according to Mehta and Susskind (1999) at the AMSU FOV resolution. V6 computes OLR according to Iacono et al (2008) at the AIRS spot resolution. Clear-sky outgoing longwave radiation (**clrolr**) is calculated using the same algorithm, setting the cloud fraction equal to zero.

The Iacono et al (2008) algorithm computes spectral components of OLR in sixteen spectral bands covering the entire spectral range from 100 cm^{-1} to 3260 cm^{-1} and sums these up to give the total OLR. Because the OLR is computed from the retrieved solution, it is possible to compute the contribution from spectral regions not directly observed by AIRS. The contributions from each of the sixteen bands are output in the support product.

23.2 Type of Product

The OLR products are integrated values for the radiances that would be observed at the TOA.

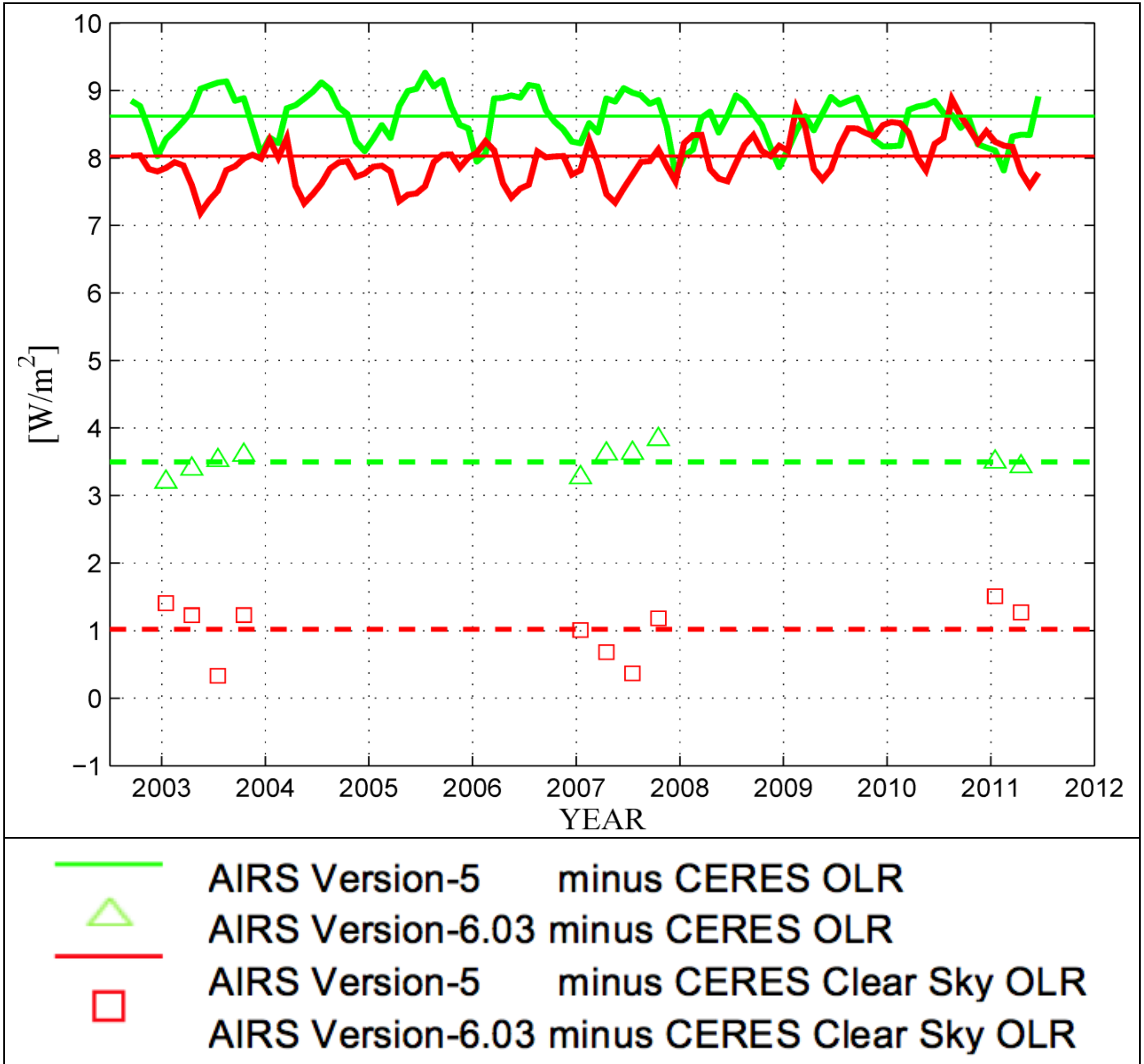

Figure 15: Time series of difference between AIRS and CERES global and clear sky OLR

23.3 Quality Indicators

The user is encouraged to read the QC and error estimation document and the cloud product section of the performance and test report:

V6_L2_Quality_Control_and_Error_Estimation.pdf

V6_L2_Performance _and_Test_Report.pdf

Quality of OLR (except for **clrolr**) are flagged as follows:

If we accept a final retrieval, Quality = 0.

If we accept a final retrieval, but the final retrieved surface temperature differs from the neural net surface temperature by > 5 K, the OLR is calculated from the neural net surface temperature, and Quality = 1.

In the event that the cloud retrieval is not completed, Quality = 2.

The clear sky OLR products require an accurate retrieval to the surface, so their QC are set as follows. If the profile quality is good to the surface (**PGood = PSurfStd**), **clrolr_QC** (in the standard product) and **spectralclrolr_QC** (in the support product) are set to 0; otherwise they are both set to 2.

23.4 Validation

A Validation Report for V6 data is currently under preparation and will be published after the V6 data products become publicly available. A V5 Validation Report, summarizing relevant publications, is also being prepared. Extensive V5 OLR validation is reportedin Susskind et al (2012). Early V6 validation results are partially summarized in

V6_L2 Performance_and_Test_Report.pdf

23.5 Caveats

This section will be updated over time as V6 data products are analyzed and validated.

23.6 Suggestions for Researchers

This section will be updated over time as V6 data products are analyzed and validated.

OLR has been widely used as a proxy for convective activity in the tropics. Susskind et al (2012) have used AIRS data to explain changes in OLR observed over the past decade in terms of the effects of El Niño/ La Niña oscillations over the time period on the distributions of tropical water vapor and cloud cover.

23.7 Recommended Papers

This section will be updated over time as research with V6 data products are published.

Aumann, Hartmut H., Alexander Ruzmaikin, Ali Behrangi, 2012: On the Surface Temperature Sensitivity of the Reflected Shortwave, Outgoing Longwave, and Net Incident Radiation. J. Climate, 25, 6585â€“6593. doi: http://dx.doi.org/10.1175/JCLI-D-11-00607.1

Chen, Xiuhong, Xianglei Huang, Norman G. Loeb, Heli Wei (2013), Comparisons of Clear-Sky Outgoing Far-IR Flux Inferred from Satellite Observations and Computed from the Three Most Recent Reanalysis Products. J. Climate, 26, 478–494, doi: 10.1175/JCLI-D-12-00212.1

Dessler, A. E., P. Yang, J. Lee, J. Solbrig, Z. Zhang, and K. Minschwaner (2008), An analysis of the dependence of clear-sky top-of-atmosphere outgoing longwave radiation on atmospheric temperature and water vapor, J. Geophys. Res., 113, D17102, doi:10.1029/2008JD010137.

Huang, X., N. G. Loeb, and W. Yang (2010), Spectrally resolved fluxes derived from collocated AIRS and CERES measurements and their application in model evaluation: 2. Cloudy sky and band?by?band cloud radiative forcing over the tropical oceans, J. Geophys. Res., 115, D21101, doi:10.1029/2010JD013932.

Huang, Xianglei, Jason N. S. Cole, Fei He, Gerald L. Potter, Lazaros Oreopoulos, Dongmin Lee, Max Suarez, Norman G. Loeb, 2013: Longwave Band-By-Band Cloud Radiative Effect and Its Application in GCM Evaluation. J. Climate, 26, 450–467,doi: 10.1175/JCLI-D-12-00112.1

Iacono, M.J., J.S. Delamere, E.J. Mlawer, M.W. Shephard, S.A. Clough, and W.D. Collins (2008), Radiative forcing by long-lived greenhouse gases, Calculations with the AER radiative transfer models, *J. Geophys*. Res., **113**, D13103, doi:10.1029/2008JD009944.

Kahn, B. H., X. Huang, G. L. Stephens, W. D. Collins, D. R. Feldman, H. Su, S. Wong, and Q. Yue (2016), ENSO regulation of far- and mid-infrared contributions to clear-sky OLR, Geophys. Res. Lett., 43, doi:10.1002/2016GL070263.

Loeb, N. G., S. Kato, W. Su, T. Wong, F. G. Rose, D. R. Doelling, J. R. Norris, and X. Huang (2012), Advances in Understanding Top-of-Atmosphere Radiation Variability from Satellite Observations, Surveys in Geophysics, 33(3-4), 359-385, doi:http://dx.doi.org/10.1007/s10712-012-9175-1

Metha, A and J. Susskind (1999), Outgoing longwave radiation from the TOVS Pathfinder Path A data set, *J. Geophys. Res.*, **104**, 12193 doi:10.1029/1999JD900059.

Moy, L. A., R. O. Knuteson, D. C. Tobin, H. E. Revercomb, L. A. Borg, and J. Susskind (2010), Comparison of measured and modeled outgoing longwave radiation for clear-sky ocean and land scenes using coincident CERES and AIRS observations, *J. Geophys. Res.*, **115**, D15110, doi:10.1029/2009JD012758

Sedlar, J., and Devasthale, A., 2012, Clear-sky thermodynamic and radiative anomalies over a sea ice sensitive region of the Arctic: Journal of Geophysical Research-Atmospheres, v. 117, p. D19111. http://dx.doi.org/10.1029/2012JD017754

Stephens, G. L., B. H. Kahn, and M. Richardson (2016), The super greenhouse effect in a changing climate, J. Climate, 29, 5469–5482, doi:10.1175/JCLI-D-15-0234.1.

Sun, F., M. D. Goldberg, X. Liu, and J. J. Bates (2010), Estimation of outgoing longwave radiation from Atmospheric Infrared Sounder radiance measurements, J. Geophys. Res., 115, D09103, doi:10.1029/2009JD012799

Susskind, J., G. Molnar, L. Iredell, N. Loeb (2012), Interannual Variability of OLR as Observed by AIRS and CERES, *J. Geophys Res.*, **117**, D23107, doi:10.1029/2012JD017997

23.8 Recommended Supplemental User Documentation

V6_Data_Release_User_Guide.pdf
V6_Data_Disclaimer.pdf
V6_L2_Performance_and_Test_Report.pdf
V6_L2_Quality_Control_and_Error_Estimation.pdf
V6_Released_Processing_File_Description.pdf
V6_L2_Standard_Pressure_Levels.pdf
V6_L2_Support_Pressure_Levels.pdf
V6_L2_Levels_Layers_Trapezoids.pdf
V6_Retrieval_Channel_Sets.pdf
V6_Retrieval_Flow.pdf

24 Level 2 Physical Retrieval SurfClass, Dust Flag, SO2 Flag and Cloud Phase Flag

Standard Product

Field Name	Dimension per FOV	Description
SurfClass	1	Surface class used in physical retrieval, from microwave (MW) and/or infrared (IR). Identical to MWSurfClass when MW is used; 0 for coastline (Liquid water covers 50-99% of area); 1 for land (Liquid water covers < 50% of area); 2 for ocean (Liquid water covers > 99% of area); 3 for sea ice (Indicates high MW emissivity when MW information is used); 4 for sea ice (Indicates low MW emissivity. This value is only produced when MW information is used.); 5 for snow (Indicates higher-frequency MW scattering when MW information is used); 6 for glacier/snow (Indicates very low-frequency MW scattering. This value is only produced when MW information is used.); 7 for snow (Indicates lower-frequency MW scattering. This value is only produced when MW information is used.); -1 for unknown
dust_flag	AIRSTrack *AIRSXTrack =3x3	Flag indicating whether dust was detected in this scene; 1: Dust detected; 0: Dust not detected; -1: Dust test not valid because of land; -2: Dust test not valid because of high latitude; -3: Dust test not valid because of suspected cloud; -4: Dust test not valid because of bad input data

Support Product

Field Name	Dimension per FOV	Description
dust_score	AIRSTrack *AIRSXTrack =3x3	Each bit results from a different test comparing radiances. Higher scores indicate more certainty of dust present. Dust probable when dust_score>380. Not valid if dust_flag is negative.
BT_diff_SO2	AIRSTrack *AIRSXTrack =3x3	Tb(1433.06 cm-1) used as an indicator of SO2 release from volcanoes. Values under -6 K have likely volcanic SO2. (K)
Cloud_Resid_Ratio3x3	AIRSTrack *AIRSXTrack =3x3	Internal retrieval quality indicator, ratio of residual of cloud channels to predicted uncertainty, per AIRS FOV. Located in Support Product. (unitless)
cloud_phase_3x3	AIRSTrack *AIRSXTrack =3x3	Flag indicating whether clouds are ice or liquid water; -9999: No cloud phase retrieval was possible; -2: Liquid water (high confidence); -1: Liquid water (low confidence); 0: Unknown; 1: Ice (low confidence); 2: Ice (higher confidence); 3: Ice (very high confidence); 4: Ice (very high confidence)
cloud_phase_bits	AIRSXTrack=3	Bit 0: (LSB, 0x0001, value 1) One or more tests could not be performed

24.1 Description

SurfClass – Surface classification derived from MW and/or IR radiance tests, present in the Level 2 Standard Product as well as the Level 2 Support Product. It is identical to **MWSurfClass** when MW radiances are used. In the case of the AIRS-Only retrieval, only **landFrac** and **tsurf_forecast** are available and are used to determine if the surface is land or ocean and frozen or not.

dust_flag – flag for each of the 3x3 AIRS spots in an AMSU FOV indicating whether dust was detected in the spot. Values are

1 = dust detected

0 = dust not detected

-1 = dust test not valid because of land

-2 = dust test not valid because of high latitude

-3 = dust test not valid because of suspected cloud

-4 = dust test not valid because of bad input data

The flag is set based on **dust_score**, an array in the Level 2 Support Product that is dimensioned (1350,3,3) to provide information for each AIRS field of regard.

SO_2 detection - The detection of the presence of dust or volcanic SO_2 is made by comparison of radiances, and the flags originate in the AIRS Level 1B Product. They are propagated to the Level 2 Standard and Support Products. Each granule of Level 2 Standard Product has an attribute, **NumSO2FOVs**, which provides the number of retrieval FOVs (out of a nominal 1350 for a granule) with a significant SO2 concentration based on the value of **BT_diff_SO2**. The support product also has a quality factor, **BT_diff_SO2_QC**. These arrays are of dimension (1350,3,3), since they provide the information for each AIRS spot.

Data indicating which AMSU FOVs and which AIRS spots within the AMSU FOVs indicate the presence of excessive SO_2 are located in the AIRS Level 2 Support Product. The entry is **BT_diff_SO2** and it is a 3x3 array of brightness temperature differences for each AMSU FOV. The temperature difference tested is:

$$\Delta T_b = T_b\left(1361.44\ cm^{-1}\right) - T_b\left(1433.06\ cm^{-1}\right)$$

If $\Delta T_b < -6\ K$ the presence of volcanic SO_2 is highly likely.

cloud_phase_3x3 – flag for each of the 3x3 AIR spots in an AMSU FOV indicating the phase (liquid or ice) of the moisture in a cloud.

The tests by which **dust_flag**, **BT_diff_SO2** and **cloud_phase_3x3** are set are described in

V6_Retrieval_Channel_Set.pdf

24.2 Type of Product

The AIRS V6 SO_2 and Dust products are flags indicating the present or absence of a detection of these constituents. The algorithm is unchanged from V5.

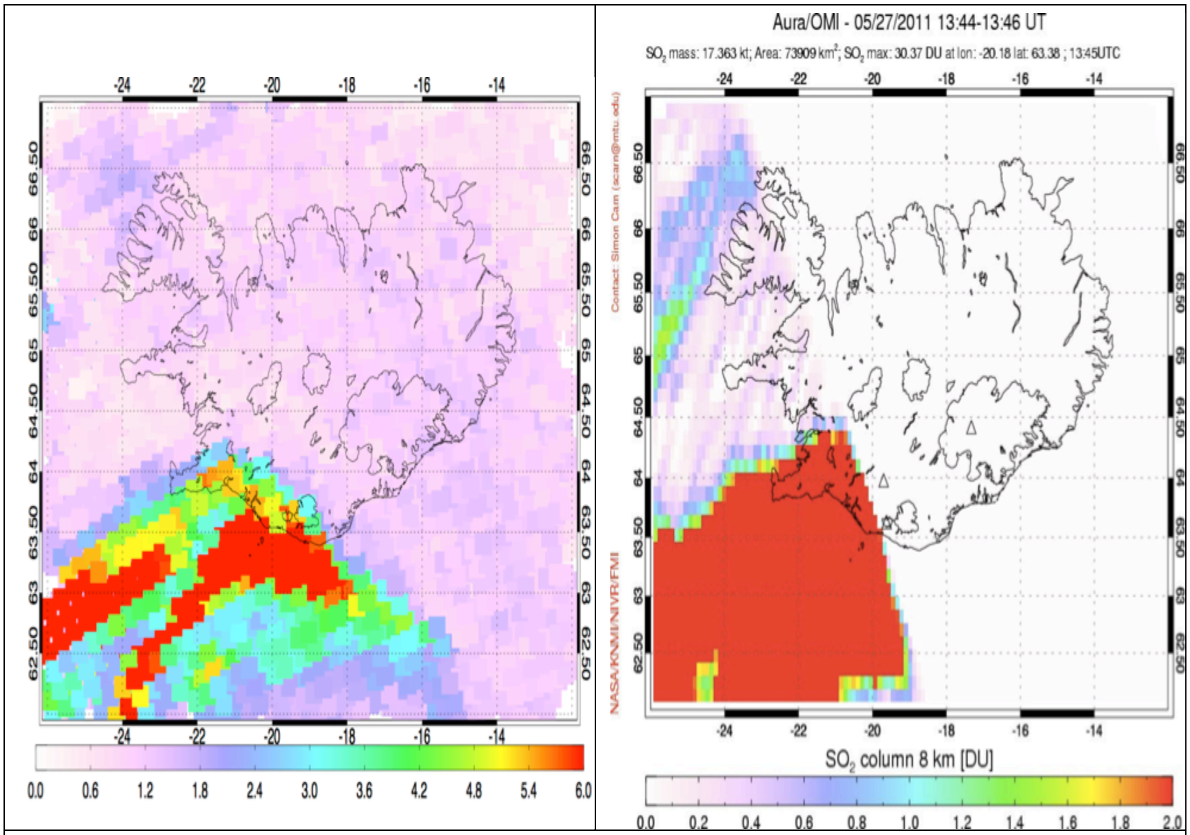

Figure 16: AIRS V6 SO_2 flags compared with Aura/OMI SO_2 total column on 27 May 2011

Left panel: AIRS V6 SO_2 flags color coded by ΔT_b

Right panel: Aura/OMI SO_2 total column (DU)

24.3 Quality Indicators

The user is encouraged to read the QC and error estimation document:

V6_L2_Quality_Control_and_Error_Estimation.pdf

BT_diff_SO2 is a simple difference between two Level 1B radiances so it will be good unless one of the detectors involved becomes bad.
If it is bad it will be -9999.0.

Dust_flag and **dust_score** are derived parameters and therefore do not have QC fields. Negative values of **dust_flag** indicate when both are not trustworthy.

Cloud_phase_3x3 is a derived parameter, rather than a retrieved parameter and therefore does not have a _QC field associated with it. Instead, whenever the cloud phase cannot be determined the value of cloud_phase_3x3 is set to -9999 and the low bit of **cloud_phase_bits** is set. These are cases where QC indicates that required inputs were of low quality.
Reasons for cloud_phase_3x3 to be set to -9999 are:

1) QC=2 for surface emissivity
2) QC=2 for cloud fraction
3) All radiances = -9999 for all channels in any band.

24.4 Validation

A Validation Report for V6 data is currently under preparation and will be published after the V6 data products become publicly available. A V5 Validation Report, summarizing relevant publications, is also being prepared. Early V6 validation results are partially summarized in

V6_L2 Performance_and_Test_Report.pdf

There is a paper in preparation (Kahn et al, 2013) which explains the new cloud retrievals and provides some initial validation results.

24.5 Caveats

This section will be updated over time as V6 data products are analyzed and validated.

The dust flag is valid **ONLY OVER OCEAN** and fails if thin cirrus or other clouds are present ABOVE the dust.

Physical retrievals can be seriously compromised if the AIRS field of regard is contaminated by dust and/or volcanic ash. Most dust-contaminated scenes are already marked as Quality = 2. However, cautious users should include the **dust_flag** and **dust_score** in their quality control filtering of data. Despite being valid only over ocean the dust detection algorithm should be useful for filtering data contaminated by dust in the Saharan Air Layer (SAL). **We recommend that users filtering to select high quality data over oceans should avoid AIRS Level 2 retrievals for which *dust_score ≥ 380 or dust_flag = 1, regardless of the values of other QA indicators*.**

Physical retrievals can be seriously compromised if the AIRS field of regard is contaminated by dust volcanic ash. **We recommend that users filtering to select high quality data should also avoid AIRS Level 2 retrievals for which BT_dif_SO2 ≤ 6 K. Those retrievals may be contaminated by volcanic ash**.

24.6 Suggestions for Researchers

This section will be updated over time as V6 data products are analyzed and validated.

24.7 Recommended Papers

This section will be updated over time as research with V6 data products are published.

Brenot, H., Theys, N., Clarisse, L., van Geffen, J., van Gent, J., Van Roozendael, M., van der A, R., Hurtmans, D., Coheur, P.-F., Clerbaux, C., Valks, P., Hedelt, P., Prata, F., Rasson, O., Sievers, K., and Zehner, C.: Support to Aviation Control Service (SACS): an online service for near-real-time satellite monitoring of volcanic plumes, Nat. Hazards Earth Syst. Sci., 14, 1099-1123, doi:10.5194/nhess-14-1099-2014, 2014.

Carboni, E., Thomas, G.E., Sayer, A.M., Siddans, R., Poulsen, C.A., Grainger, R.G., Ahn, C., Antoine, D., Bevan, S., Braak, R., Brindley, H., DeSouza-Machado, S., Deuze, J.L., Diner, D., Ducos, F., Grey, W., Hsu, C., Kalashnikova, O.V., Kahn, R., North, P.R.J., Salustro, C., Smith, A., Tanre, D., Torres, O., and Veihelmann, B., 2012, Intercomparison of desert dust optical depth from satellite measurements: Atmospheric Measurement Techniques, v. 5, no. 8, p. 1973-2002. http://dx.doi.org/10.5194/amt-5-1973-2012

Carn S. A., L. L. Strow, S. de Souza-Machado, Y. Edmonds, S. Hannon (2005), Quantifying tropospheric volcanic emissions with AIRS: The 2002 eruption of Mt. Etna (Italy), Geophys. Res. Lett., 32, L02301, doi:10.1029/2004GL021034.

Carn, S. A., Arlin J. Krueger, Nickolay A. Krotkov, Kai Yang, and Keith Evans (2008), Tracking volcanic sulfur dioxide clouds for aviation hazard mitigation, Nat. Hazards, doi:10.1007/s11069-008-9228-4

Carn, Simon A., John S. Pallister, Luis Lara, John W. Ewert, Sebastian Watt, Alfred J. Prata, Ronald J. Thomas, and Gustavo Villarosa. "The unexpected awakening of Chaitén volcano, Chile." Eos, Transactions American Geophysical Union 90, no. 24 (2009): 205-206.

Corradini, S., L. Merucci, A. J. Prata, and A. Piscini (2010), Volcanic ash and SO2 in the 2008 Kasatochi eruption: Retrievals comparison from different IR satellite sensors, J. Geophys. Res., 115, D00L21, doi:10.1029/2009JD013634.

Davidi, A., A. B. Kostinski, I. Koren, and Y. Lehahn (2012), Observational bounds on atmospheric heating by aerosol absorption: Radiative signature of transatlantic dust, Geophys. Res. Lett., 39, L04803, doi:10.1029/2011GL050358

DeSouza-Machado, S. G., L. L. Strow, S. E. Hannon, and H. E. Motteler (2006), Infrared dust spectral signatures from AIRS, Geophys. Res. Lett., 33, L03801, doi:10.1029/2005GL024364.

DeSouza-Machado, S. G., et al. (2010), Infrared retrievals of dust using AIRS: Comparisons of optical depths and heights derived for a North African dust storm to other collocated EOS A-Train and surface observations, J. Geophys. Res., 115, D15201, doi:10.1029/2009JD012842.

Eckhardt, S., Prata, A. J., Seibert, P., Stebel, K., and Stohl, A.: Estimation of the vertical profile of sulfur dioxide injection into the atmosphere by a volcanic eruption using satellite column measurements and inverse transport modeling, Atmos. Chem. Phys., 8, 3881-3897, 2008.

Goldberg M. D., Y. Qu, L. McMillin, W. Wolf, L. Zhou, and M. Divakarla (2003), AIRS near-real-time products and algorithms in support of operational numerical weather prediction. IEEE Trans. Geosci. Remote Sens., 41(2), 379–399.

Griessbach, S., Hoffmann, L., Spang, R., von Hobe, M., Müller, R., and Riese, M.: Infrared limb emission measurements of aerosol in the troposphere and stratosphere, Atmos. Meas. Tech., 9, 4399-4423, doi:10.5194/amt-9-4399-2016, 2016.

Heng, Y., Hoffmann, L., Griessbach, S., Rößler, T., and Stein, O.: Inverse transport modeling of volcanic sulfur dioxide emissions using large-scale simulations, Geosci. Model Dev., 9, 1627-1645, doi:10.5194/gmd-9-1627-2016, 2016.

Hoffmann, L., T. Rößler, S. Griessbach, Y. Heng, and O. Stein (2016), Lagrangian transport simulations of volcanic sulfur dioxide emissions: Impact of meteoro- logical data products, J. Geophys. Res. Atmos., 121, 4651–4673, doi:10.1002/2015JD023749.

Hsu, N. C., C. Li, N. A. Krotkov, Q. Liang, K. Yang, and S.-C. Tsay (2012), Rapid transpacific transport in autumn observed by the A-train satellites, J. Geophys. Res., 117, D06312, doi:10.1029/2011JD016626.

Kahn, B.H., F. W. Irion, V. T. Dang, E. M. Manning, S. L. Nasiri, C. M. Naud, J. Blaisdell, H. Jin, M. M. Schreier, Q. Yue, K. W. Bowman, E. J. Fetzer, R. E. Holz, G. Hulley, K. N. Liou, D. Lubin, S. C. Ou, J. Susskind, B. Tian, Y. Takano, and J.

Krotkov, N.A., S.A. Carn, A.J. Krueger, P.K. Bhartia, and K. Yang (2006). Band residual difference algorithm for retrieval of SO2 from the Aura Ozone Monitoring Instrument (OMI). IEEE Trans.Geosci. Remote Sensing, AURA special issue, 44(5), 1259-1266, doi:10.1109/TGRS.2005.861932, 2006.

Maddy, E. S., et al. (2012), On the effect of dust aerosols on AIRS and IASI operational level 2 products, Geophys. Res. Lett., 39, L10809, doi:10.1029/2012GL052070

Mielonen, T., H. Portin, M. Komppula, A. Leskinen, J. Tamminen, I. Ialongo, J. Hakkarainen, K. E. J. Lehtinen, and A. Arola (2012), Biomass burning aerosols observed in Eastern Finland during the Russian wildfires in summer 2010 - Part 2: Remote sensing Atmospheric Environment, 47, 279-287, doi:http://dx.doi.org/10.1016/j.atmosenv.2011.07.016.

Nalli N. R., et al. (2005), Profile observations of the Saharan air layer during AEROSE 2004, Geophys. Res. Lett., 32, L05815, doi:10.1029/2004GL022028.

Nalli N. R., et al. (2006), Ship-based measurements for infrared sensor validation during Aerosol and Ocean Science Expedition 2004, J. Geophys. Res., 111, D09S04, doi:10.1029/2005JD006385.

Pierangelo C., M. Mishchenko, Y. Balkanski, A. Chédin (2005), Retrieving the effective radius of Saharan dust coarse mode from AIRS, Geophys. Res. Lett., 32, L20813, doi:10.1029/2005GL023425.

Pan,Weiyu; Wu,Liguang; Shie,Chung-Lin, Influence of the Saharan Air Layer on Atlantic Tropical Cyclone Formation during the Period 1-12 September 2003, Adv.Atmos.Sci., 2011, 28, 1, 16-32,

Prata, A.J., Bernardo, C., Retrieval of volcanic SO2 column abundance from atmospheric infrared sounder data, Journal of Geophysical Research Atmospheres, 2007, 112, D20, D20204

Prata, A. J., G. Gangale, L. Clarisse, and F. Karagulian (2010), Ash and sulfur dioxide in the 2008 eruptions of Okmok and Kasatochi: Insights from high spectral resolution satellite measurements, J. Geophys. Res., 115, D00L18, doi:10.1029/2009JD013556.

Prata, A. J., and A. T. Prata (2012), EyjafjallajÃ¶kull volcanic ash concentrations determined using Spin Enhanced Visible and Infrared Imager measurements, J. Geophys. Res., 117, D00U23, doi:10.1029/2011JD016800.

Thomas, Helen E., I. Matthew Watson, Simon A. Carn, Alfredo J. Prata, and Vincent J. Realmuto. "A comparison of AIRS, MODIS and OMI sulphur dioxide retrievals in volcanic clouds." Geomatics, Natural Hazards and Risk 2, no. 3 (2011): 217-232.

Realmuto, V.J., Berk, A., Plume Tracker: Interactive mapping of volcanic sulfur dioxide emissions with high-performance radiative transfer modeling, J. Volcanol. Geotherm. Res. (2016), http://dx.doi.org/10.1016/j.jvolgeores.2016.07.001

Torres, O., C. Ahn, and Z. Chen. "Improvements to the OMI near-UV aerosol algorithm using A-train CALIOP and AIRS observations." Atmospheric Measurement Techniques 6, no. 11 (2013): 3257-3270.

Wong S., P. R. Colarco, A. E. Dessler (2006), Principal component analysis of the evolution of the Saharan air layer and dust transport: Comparisons between a model simulation and MODIS and AIRS retrievals, J. Geophys. Res., 111, D20109, doi:10.1029/2006JD007093.

Wright,R., Carn,S. A., Flynn,L. P. (2005), A satellite chronology of the May-June 2003 eruption of Anatahan volcano, Journal of Volcanology and Geothermal Research, 146, 102-116. doi: 10.1016/j.jvolgeores.2004.10.021

Yao, Z., J. Li, H. Han, A. Huang, B. J. Sohn, and P. Zhang (2012), Asian dust height and infrared optical depth retrievals over land from hyperspectral longwave infrared radiances, Journal of Geophysical Research-Atmospheres, 117, D19202, doi:http://dx.doi.org/10.1029/2012JD017799.

24.8 Recommended Supplemental User Documentation

V6_Data_Release_User_Guide.pdf

V6_Data_Disclaimer.pdf

V6_L2_Performance_and_Test_Report.pdf

V6_L2_Quality_Control_and_Error_Estimation.pdf

V6_Released_Processing_File_Description.pdf

V6_L2_Standard_Pressure_Levels.pdf

V6_L2_Support_Pressure_Levels.pdf

V6_L2_Levels_Layers_Trapezoids.pdf

V6_Retrieval_Channel_Sets.pdf

V6_Retrieval_Flow.pdf